Effects of confinement on material behaviour at the nanometre size scale

2005 J. Phys.: Condens. Matter 17 R461

(http://iopscience.iop.org/0953-8984/17/15/R01)

INSTITUTE OF PHYSICS PUBLISHING JOURNAL OF PHYSICS: CONDENSED MATTER

J. Phys.: Condens. Matter **17** (2005) R461–R524 doi:10.1088/0953-8984/17/15/R01

TOPICAL REVIEW

Effects of confinement on material behaviour at the nanometre size scale

Mataz Alcoutlabi and Gregory B McKenna[1]

Department of Chemical Engineering, Texas Tech University, Lubbock, TX 79409-3121, USA

E-mail: greg.mckenna@ttu.edu

Received 15 December 2004, in final form 28 January 2005
Published 1 April 2005

Abstract

In this article, the effects of size and confinement at the nanometre size scale on both the melting temperature, T_m, and the glass transition temperature, T_g, are reviewed. Although there is an accepted thermodynamic model (the Gibbs–Thomson equation) for explaining the shift in the first-order transition, T_m, for confined materials, the depression of the melting point is still not fully understood and clearly requires further investigation. However, the main thrust of the work is a review of the field of confinement and size effects on the glass transition temperature. We present in detail the dynamic, thermodynamic and pseudo-thermodynamic measurements reported for the glass transition in confined geometries for both small molecules confined in nanopores and for ultrathin polymer films. We survey the observations that show that the glass transition temperature decreases, increases, remains the same or even disappears depending upon details of the experimental (or molecular simulation) conditions. Indeed, different behaviours have been observed for the same material depending on the experimental methods used. It seems that the existing theories of T_g are unable to explain the range of behaviours seen at the nanometre size scale, in part because the glass transition phenomenon itself is not fully understood. Importantly, here we conclude that the vast majority of the experiments have been carried out carefully and the results are reproducible. What is currently lacking appears to be an overall view, which accounts for the range of observations. The field seems to be experimentally and empirically driven rather than responding to major theoretical developments.

Contents

---

[1] Author to whom any correspondence should be addressed.

0953-8984/05/150461+64$30.00

1. Introduction

The 1991 paper of Jackson and McKenna [1] initiated a coming plethora of work on the dynamics of glass forming liquids at the nanoscale or in nanoconfinement, probably because the work was the first to recognize the importance of observing a reduced glass transition temperature T_g due simply to size effects. The importance of the Jackson and McKenna work [1] was the recognition that a depression in T_g at small size scales is not readily explained by conventional theory. In fact, subsequent work has proven this to be the case, as T_g is found to increase, decrease, remain the same and even disappear depending upon details of the experimental (or even molecular simulation) conditions. Importantly, this work was actually presaged by observations where a change in T_g was reported in block copolymers [2–8], in the amorphous phases between crystalline lamellae in semicrystalline polymers [9–12] and in glass forming microemulsions [13–15].

Among the results reported on the T_g change at the nanoscale are those observed in ultrathin polymer films where a very large decrease in T_g has been observed for free standing thin polystyrene films [16–18] whereas a smaller decrease and even increases in T_g have been reported for supported polymer thin films [19–21]. It appears that interactions between the substrate and the constrained thin films contribute to the contradictory results found in thin polymer films. In addition, results reported for molecular simulations for both small molecules confined in nanopores and thin polymer films [22–24] also indicate that the interaction between the wall and confined liquid can play an important role in determining the sign of the shift in T_g of the confined liquid compared with the bulk.

The purpose of the present article is to review the nanoscale confinement effects on the glass transition for both small molecules in nanopores and for thin polymer films. This paper is organized as follows. We first examine first-order thermodynamics in confined geometries where an existing theory (the Gibbs–Thomson equation) has been thought to account reasonably for the shift in the melting point T_m observed at the nanometre size scale. We then focus on the results reported in the literature for T_g for both small molecules confined in nanopores and polymers in the form of ultrathin films. This is followed by a discussion of both the experimental methods and the molecular simulations used to investigate confinement

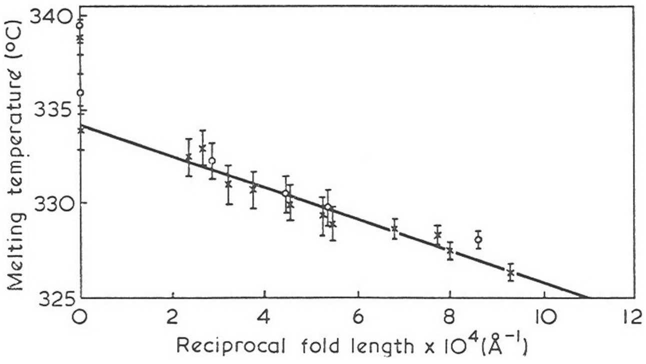

Figure 1. Melting point as a function of reciprocal of the crystal thickness for PTFE (cross symbols) and Fluon CD1 (open circle) along with the prediction from the Gibbs–Thomson relationship. After Bassett and Davitt [36] with permission.

effects on T_g. The thermodynamic, pseudo-thermodynamic (defined subsequently) and dynamic measurements of the glass transition of confined systems are examined in detail by focusing on the different methods used to perform the experiments, the materials used and the interpretations of the results. Finally, we propose suggestions for future research followed by a summary and conclusions.

1.1. Thermodynamic first-order transition in confined geometries

A definition of a thermodynamic first-order transition is that the free energy as a function of any given state variable is a continuous function, but first partial derivatives of the free energy with respect to the relevant state variable are discontinuous [25]. Although not exhaustively, it has been established that the first-order transition, i.e., melting point, for a bulk material differs from that of the same material when it is confined in porous systems [26–30]. Size effects on T_m have been studied for organic small molecules [26–33], metal particles [34, 35], finely dispersed non-porous powders [26] and polymer lamellae of different thicknesses [12, 36]. These results show a depression of the melting point, T_m, of small crystals as a function of crystal size. Figure 1 shows a plot of the melting temperature as a function of the crystal size for poly(tetrafluoroethylene) PTFE [36] and a linear relationship between T_m and the inverse of crystal thickness is observed. It is shown in the figure that the T_m depression for small crystals of PTFE compares well with that calculated from the Gibbs–Thomson thermodynamic relationship [37–39]. This relationship is frequently used to describe the shift in melting temperature for small crystals in nanopores [26–33] where the contact angle at the solid–liquid interface for small crystal melting was assumed to be 180°. The magnitude of the melting point depression of a small crystal having cylindrical shape, ΔT_m, as described by the Gibbs–Thomson equation is given by [37–39]

$$\Delta T_m = T_m - T_m(d) = \frac{4\sigma_{sl} T_m}{(d \Delta H_f \rho_s)} \tag{1}$$

where σ_{sl} is the surface energy (tension) of the solid–liquid interface, T_m is the bulk melting point, $T_m(d)$ is the melting point of crystals within a constant pore diameter of size d, ΔH_f is the bulk enthalpy of fusion and ρ_s is the density of the solid. Equation (1) is also used to describe the melting point depression for small crystals having different shapes (e.g., nanoparticles of spherical shape). There are several assumptions underlying this thermodynamic relationship.

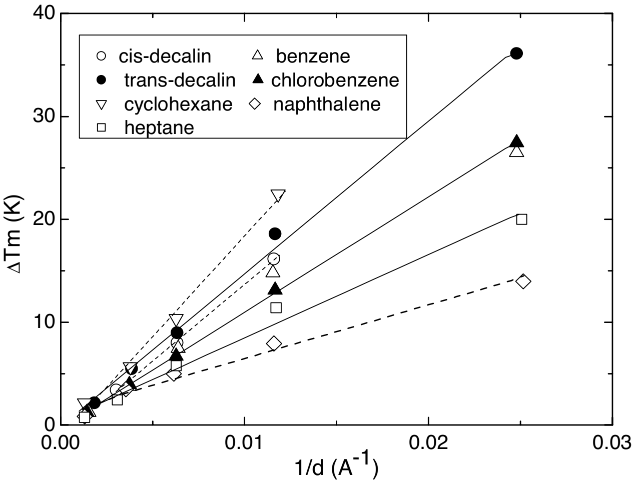

Figure 2. Melting temperature depression as a function of pore diameter for small molecules confined in nanopores. After Jackson and McKenna [26].

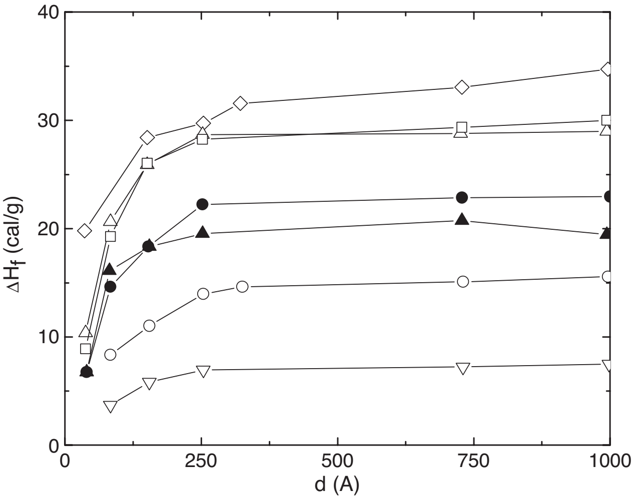

Figure 3. Enthalpy of fusion ΔH_f versus pore diameter for liquids confined in nanopores as reported by Jackson and McKenna [26]. The symbols are the same as in figure 2.

Among these are that the surface tension is isotropic and that the material retains its bulk properties for ΔH_f and ρ_s as size decreases. In figure 2, we show the melting point depression, ΔT_m, as a function of $1/d$ for different small molecules confined in nanopores of diameter d [26]. The results show a linear relationship between ΔT_m and $1/d$, which is consistent with the Gibbs–Thomson equation. The surface energy, σ_{sl}, was calculated from the slope of ΔT_m versus $1/d$. Figure 3 shows the Jackson and McKenna results for the effect of pore diameter on the enthalpy of fusion, ΔH_f [26]. This figure shows that ΔH_f for small molecules confined in controlled pore glasses (CPGs) decreases with decreasing pore diameter d. We remark here that in spite of the linear relationship shown in figure 2 between T_m and $1/d$, the enthalpy of fusion in nanopores is not constant. In addition, not all confined molecules in nanopores behave in the same way to that observed in figure 2 [26, 28]. For example, Alba-Simionesco and co-workers [28] have observed a deviation from the Gibbs–Thomson relationship for ΔT_m of benzene confined in nanopores having diameters less than 4.7 nm.

In addition to the Gibbs–Thomson equation, other models have been developed to explain the effects of particle size on the melting point on the basis of different melting

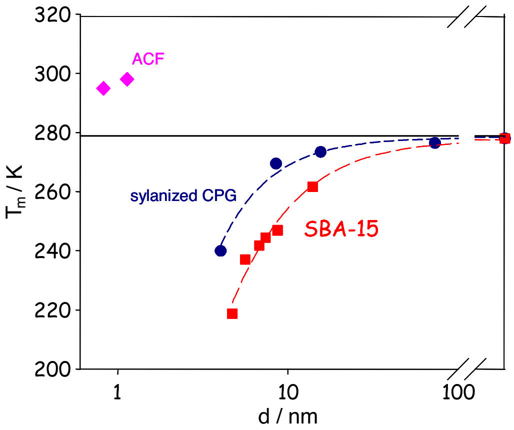

Figure 4. The melting temperature of benzene confined in different pores: in activated carbon fibres (ACF, diamonds), in controlled pore glasses (CPG circles), grafted at the surface with trimethylsilyl groups (in SBA-15 squares) without treatment. After Alba-Simionesco *et al* [28] with permission.

(This figure is in colour only in the electronic version)

mechanisms [34, 40–48]. The homogeneous melting model assumes the simultaneous existence of solid and liquid particles and equates the chemical potentials of the three phases [34, 40, 45]. The liquid skin melting model assumes that there is a liquid layer at the surface of the solid particle [34, 41–48]. The liquid nucleation and growth model assumes that the liquid layer is unstable [46, 47]. Although these models represent different proposed mechanisms of melting of the small particles, they predict essentially the same relationship as shown in equation (1), except that the surface tension of the liquid in contact with solid, σ_{sl}, is replaced by α which has been shown to differ slightly among the models [45, 46]. More recently, additional models have emerged considering the shape and environment of the nanocrystals including a unified model, which is free of any adjustable parameters [49, 50] and a liquid drop model [51]. For particles with relatively free surfaces, the melting point depends not only on the size, but also on the shape of the particle [49, 51]; for particles embedded in a matrix, the melting point can either be higher or lower than the bulk value [49, 51] and this depends on the difference between the surface energies of the embedded particles and the matrix. For example, an increase in the melting point T_{m} for indium and lead nanoparticles having higher surface energy than a surrounding aluminium matrix has been observed [51]. More recently, the melting of nanostructured organic materials (drugs) embedded into a matrix has been investigated by Colombo *et al* [52]. In that work, a depression of 33 K in the melting temperature compared to the bulk material was observed.

It now seems that the melting of confined liquids is not fully understood and many questions have still to be addressed. Among the assumptions that are made in the Gibbs–Thomson relationship are that the values of σ_{sl}, ΔH_{f} and ρ_{s} are independent of the crystal size. For example, the existence of a monolayer that remains unfrozen on the surface of the crystal can affect the value of ΔH_{f} and this would result in a change of the apparent thermodynamic parameters when equation (1) is used to describe the data. The surface roughness and the transport between the bulk and the pores can also have a considerable effect on the predictions of the Gibbs–Thompson equation [37–39].

Alba-Simionesco and co-workers have reported results on the melting behaviour of confined benzene for different types of porous confinement [28]. Their results are shown in figure 4 as the melting temperature versus pore diameter for benzene confined in different nanopores [28]. This figure shows that no crystallization is observed below a pore size of 4.7 nm, which corresponds roughly to 10 molecular diameters. Also, in the work of Jackson and McKenna [26], no melting endotherms were observed in 4 nm diameter pores for cyclohexane and *cis*-decalin in controlled pore glasses. Does the pore shape affect the melting behaviour of confined liquids? Monte Carlo and molecular dynamics simulation results show that the departure of the melting and freezing temperatures from the bulk values for cylindrical pores is always lower than for slit pores with the same pore properties [28, 53, 54]. Results reported in the literature for the melting of benzene confined in slit pores also show that melting occurs for pore diameters of 0.7 nm [53] whereas in the case of cylindrical pores the melting occurs above 4.7 nm [28]. In the work of Jackson and McKenna the melting of confined benzene in nanopores was observed in 4 nm pores and a broadening of the melting endotherm was observed [26].

Considerations that have not been incorporated in the Gibbs–Thomson equation are the confined fluid–fluid and fluid–solid interactions (pore). The interaction between the confined molecules and the solid (pore) has been used by Gubbins and co-workers as a parameter in molecular simulations to investigate the freezing behaviour of liquids confined in nanopores [55]. The strength of the interaction of the fluid–solid relative to the fluid–fluid interaction was found to play an important role in determining the sign of the shift in the freezing point [55]. For example, an increase in the freezing point was predicted for strong interactions between the confined fluid and the pore (silica and graphite) whereas a decrease in the freezing point was reported for weak interactions [55]. The simulations reported for the freezing point [54] were in agreement with the experiments reported on the freezing of CCl_4 confined in activated carbon fibres where an increase of 57 K in the melting point was observed [56, 57]. Phase transitions and dynamics of liquid crystals confined in nanopores were investigated by Decressain and co-workers using an NMR technique [58–60]. In that work, a depression of the phase transition in nanopores was reported. A topical review [61] gives further details concerning confinement effects on freezing and melting of fluids. Remark that, freezing, however, is not a thermodynamic condition due to possible supercooling of the liquid [27] and the thermodynamic relationships discussed here should be applied strictly to melting only.

As indicated above, the surface energy can play an important role in the T_m shift in nanopores. Does the surface energy, σ_{sl}, (equation (1)) affect the behaviour of small crystals at the nanoscale? Recently, Sun and Simon [62] performed experiments using differential scanning calorimetry (DSC) to investigate the melting behaviour of aluminium particles having an aluminium oxide layer. The weight-average aluminium core size studied ranged between 8 and 50 nm. As depicted in figure 5, the melting point of the nanoparticles decreases with decreasing particle size and this behaviour is consistent with the Gibbs–Thomson relationship [37–39]. Figure 6 shows the effect of particle size on the normalized heat of fusion of the aluminium nanoparticles [62]. Such a heat of fusion depression can also be represented in the Gibbs–Thomson context. The most important conclusion reported by Sun and Simon [62] is that the solid–liquid interfacial energy calculated from the slope of the depression ΔH_f versus $1/r$ (figure 6) is higher by one order of magnitude than that calculated from the ΔT_m versus $1/r$ plot (figure 5). This is a very interesting and important result because it suggests that the conditions in which the Gibbs–Thomson equation is used need to be reconsidered.

Clearly even the first-order transitions at the nanoscale require further investigation. For another view on this topic, see references concerning the thermodynamics of small systems [63–66].

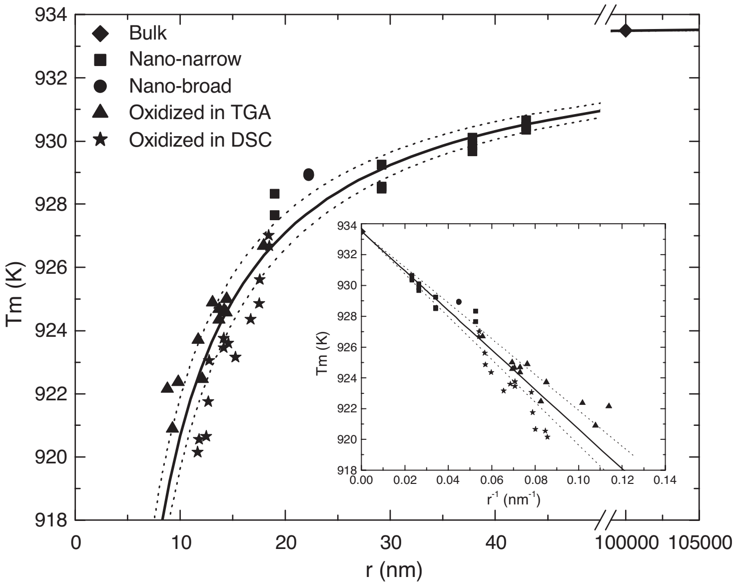

Figure 5. Melting point depression for aluminium nanoparticles as a function of the weight-average aluminium core radius r. The inset shows the plot of T_m against the reciprocal of r to show the linear relationship. After Sun and Simon with permission [62].

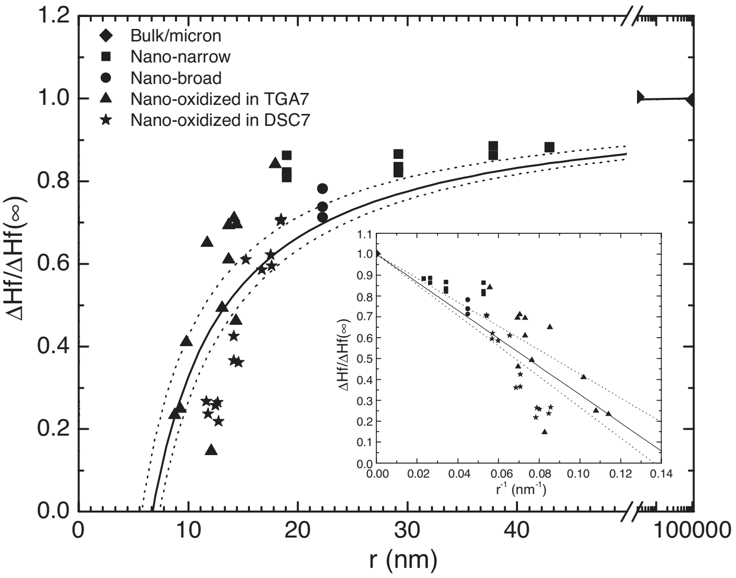

Figure 6. Normalized heat of fusion as a function of weight-average aluminium core radius. The inset shows the data plotted against the reciprocal of r. After Sun and Simon with permission [62].

1.2. The thermodynamic second-order transition in confined geometries

We now turn to size effects on the glass transition—a transition that has aspects of a second-order thermodynamic transition, but is only observed kinetically in the laboratory. As mentioned above, the glass transition temperature, T_g, for materials confined to small size geometries was reported to be different from that of the bulk [1, 16–21, 67]. One of the most surprising results reported on glass formers at the nanometre length scale is the depression of T_g, which is not readily explained in the framework of our understanding of the glass transition. In fact, simple consideration of the configurational entropy theory of the glass transition [68, 69] implies that T_g should increase for supported thin films and for materials confined to nanopores. This is because the confinement is expected to decrease the entropy and, therefore, an increase in T_g would result. On the other hand, both the entropy [68, 69] and the free volume [25, 70–72] theories of the glass transition predict that a decrease in the density of the confined liquid (e.g., due to hydrostatic tension) could cause a decrease in T_g, though smaller in magnitude than what is observed [1, 27]. Hence, the observation of a T_g reduction at the nanometre size scale provides the possibility of a better understanding of the glass transition phenomenon itself. This is discussed subsequently.

Although thermodynamic models, such as the Gibbs–Thomson relationship (under certain assumptions), can describe the melting point depression of small crystals, a similarly successful explanation of the cause of the reduction in the glass transition temperature at the nanolength scale remains unachieved. We keep in mind that the bulk glass transition itself is not fully understood and it is not clear whether or not T_g is a real thermodynamic second-order transition or a kinetic transition [25, 73, 74]. Note that there may be an intrinsic size effect on T_g similar to that reported for the melting point for crystalline materials [26]. If this is the case, it might be expected that the glass transition depression in nanogeometries would be proportional to the inverse of the confinement dimensions (pore size or film thickness).

The impact of confinement on T_g for both small molecules and polymer thin films has been widely investigated using both experimental measurements and computer simulations. The experimental study of size effects on the glass temperature of glass forming materials consists of two major types of measurements: thermodynamic-type measurements of the glass transition and dynamic-type measurements of the alpha relaxation associated with T_g or the molecular mobility.

The thermodynamic measurement is defined as a direct measurement of a thermodynamic property such as heat capacity or volume versus temperature. In this measurement, a break or jump in the thermodynamic property is seen at the transition temperature. We also include in this class of experiments the pseudo-thermodynamic measurement that is defined as a measurement of property other than a thermodynamic one as a function of temperature. These are properties—such as the film thickness, Brillouin frequency, lateral force microscopy response (if only one frequency is considered), fluorescence probe intensity etc—that vary with temperature so that the plots look like they would for thermodynamic measurements in that they show a break at the glass transition temperature. However, the property itself is related to the thermodynamic property (e.g., volume, entropy, enthalpy) or structural state of the glass or liquid. We will consider thermodynamic and pseudo-thermodynamic as, essentially, equivalent. However, we note that those that are conventionally thermodynamic can be used more readily to compare with other aspects of bulk behaviour, e.g., enthalpy recovery is more straightforward to study than ‘thickness’ recovery.

In dynamic measurements, the properties to be investigated are the viscosity, the relaxation times etc as a function of temperature where the classical non-Arrhenius behaviour of the dynamics of glass forming systems is studied.

The thermodynamic-type measurements of T_g for small molecules in nanopores have frequently been made using calorimetric techniques [1, 27, 28, 67, 75]. The dynamic-type measurements in nanopores are performed using dielectric spectroscopy [76, 79], NMR [80], solvation dynamics [81–84] as well as thermally stimulated depolarization current measurements (TSDC) [85, 86]. Remark here that in the TSDC measurement, vitrification and devitrification of the confined liquid can occur (vitrification measurement versus devitrification). For ultrathin films, pseudo-thermodynamic measurements of T_g are performed using different techniques; among these are the Brillouin light scattering [16–18, 87–90], x-ray reflectivity [20, 91–93], neutron reflectivity [94, 95], ellipsometry [19, 96–98], positron annihilation spectroscopy [99, 100], local thermal analysis [101], fluorescence probe intensity [102–104] and lateral force microscopy [105] approaches. In addition, thermodynamic measurements on ultrathin films have been recently performed using differential scanning nanocalorimetry [106]. The relaxation in thin polymer films can be directly investigated using dynamic measurements such as dielectric spectroscopy [107–112] and second-harmonic generation ones [113]. In addition, the rheological behaviour of thin polymer films can be investigated using different techniques such as hole growth [114–117], dewetting dynamics [117–120] and nanobubble inflation [121].

As indicated above, the results reported concerning the glass transition at the nanometre length scale show increasing, decreasing or no effect depending on the experimental method, material studied and group of researchers. However, there are many issues to be considered here. Among these are size effects, interfacial effects and macroscopic confinement effects and how these can be related or separated in discussing the behaviour of materials in confined geometries. These effects are discussed below. Importantly, here we emphasize that the vast majority of the experiments have been carried out carefully and the results are correct and reproducible. What is currently lacking appears to be an overall view, which synthesizes the observed range of results. Hence, the field seems to be experimentally empirically driven [122] rather than responding to major theoretical developments. In the following sections, we present in detail the thermodynamic and dynamic measurements reported on the glass transition for both small organic molecules in nanopores and thin polymer films.

2. Glass forming liquids confined in nanoporous media

In this section we discuss the results reported in the literature concerning the change of the glass transition for small molecules confined in nanopores. In considering the behaviour of glass forming liquids in confinement, we caution the reader to keep in mind that the type of confinement or the nature of the pore system used to perform the experiment may have an impact on the observations made and their interpretations, though any systematic effects have not been demonstrated. Most of the experiments reported in the literature were performed using controlled pore glasses (CPGs) [123, 124] or Vycor [125, 126] as a confining medium. These porous systems have a fairly narrow size distribution, but the pores themselves can be irregular due to the shape of the interconnected (bicontinuous) cavities that result from the spinodal decomposition involved in their production. The porous systems that have been investigated also include the sol–gel glasses that are fractal in nature [127, 128] and, hence, have a pore geometry that is different from that of the CPGs. The pore size distribution is also broader. An example of this is provided by silica aerogel that is obtained by a sol–gel condensation process. Both the CPGs and sol–gel systems consist of interconnected networks. In addition, the regular porous silicates (MCM-41 and SBA-15) have been used to investigate the glass transition in nanopores [28, 53]. MCM-41 and SBA-15 are formed of parallel cylindrical porous channels arranged in a hexagonal lattice where there are no pore channel intersections. The well defined channels that form the confinement of the MCM-41 can be considered as a two-dimensional (2D) confinement [53]. For liquids confined in Vycors and CPGs, the confinement is considered to be between 2D and three-dimensional confining geometry. We note here that for small molecules confined in nanopores, the confinement is considered as a hard confinement, whereas, for spheres or nanodroplets suspended in a fluid environment [15], the confinement is considered to be soft and 3D. For polymers confined to

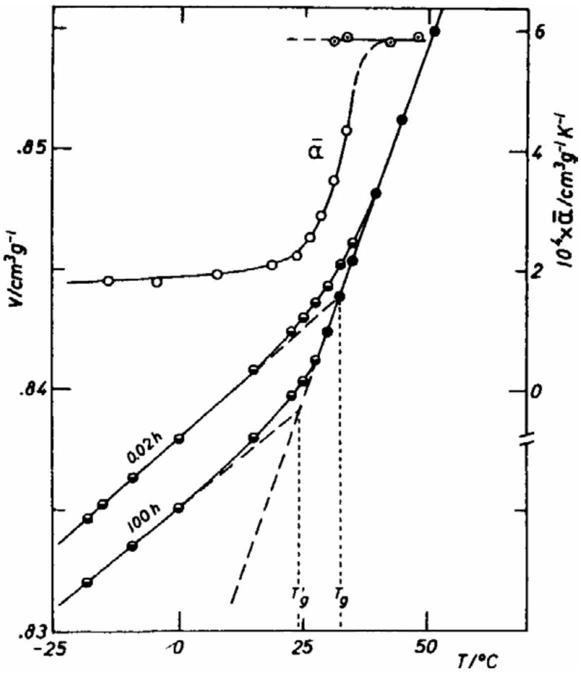

Figure 7. Specific volume versus temperature for poly(vinyl acetate). Also depicted is the thermal expansion coefficient α as a function of temperature showing a jump in α at the glass transition. After Kovacs [129].

thin films, the confinement is classified as a 2D confinement where one dimension (the film thickness) is confined to the nanometre size scale. The confinement of polymer films can be considered hard or soft. The confinement and size effects on T_g for ultrathin polymer films are discussed in detail in a subsequent section. Because the full set of results described below is not completely reconciled, the different sorts of confinement should be kept in mind when the results are compared, although there has not been significant effort to establish whether the pore geometry is or is not a major factor in determining the impact of confinement on dynamics and T_g behaviours at the nanometre size scale.

2.1. Thermodynamic measurements of the glass transition

The glass transition describes the transition from the supercooled liquid state to a glassy one as a material is cooled. The thermodynamic measurements of the glass transition are done by measuring the property P (such as volume, enthalpy or entropy and their derivatives) as a function of temperature [129]. The signature of the glass transition is observed as a break in the property (volume or enthalpy) or from a sudden change of its derivative (heat capacity or the coefficient of the thermal expansion) at the transition temperature [25, 65, 130–134]. The volumetric glass transition temperature T_g, as shown in figure 7, depends on the thermal history of the sample (e.g., cooling rate) [135]. It is accepted that the measured T_g is not a true thermodynamic transition but is a kinetic phenomenon (time dependent). Figure 7 also shows the jump in the coefficient of thermal expansion that gives the T_g the aspect of a second-order thermodynamic transition [25]. Upon cooling a liquid from above to below T_g, the molecular mobility slows down and a dramatic reduction in the mobility occurs in the glassy state far below the glass transition. The reduced mobility (or the slowing of the dynamics) manifests

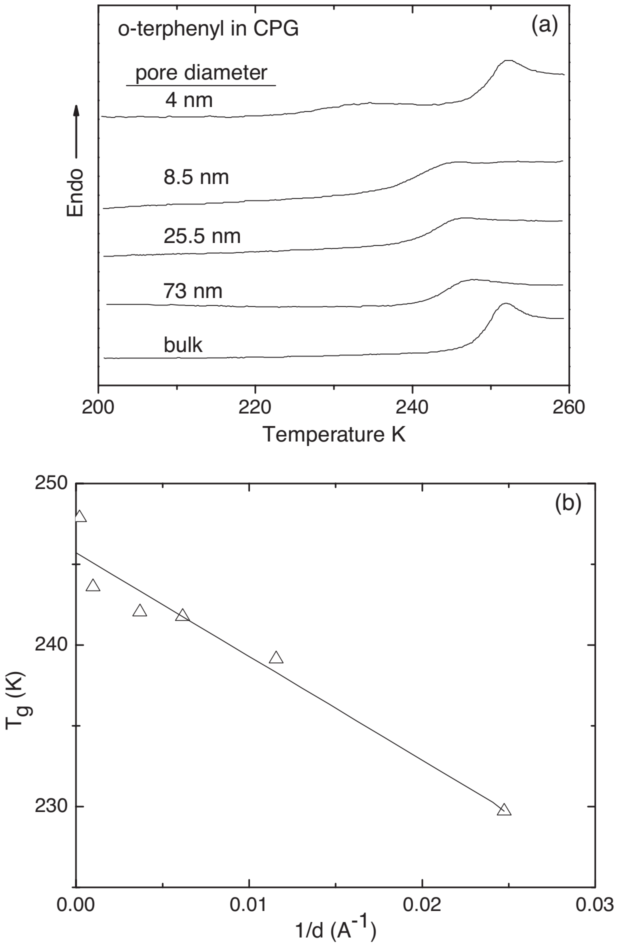

Figure 8. (a) The original data of Jackson and McKenna for the behaviour of *o*-terphenyl in nanopores. The figure shows the DSC traces versus temperature for *o*-terphenyl in controlled pore glass. The behaviour of the bulk *o*-TP is shown as well. (b) A plot showing reduction of T_g with decreasing pore diameter (increasing $1/d$) for the *o*-TP in CPG. After Jackson and McKenna [1].

itself in dramatic increases of the viscosity and the relaxation times. In the following section we discuss the results reported on the thermodynamic measurements of the glass transition for small molecules confined in nanopores.

2.1.1. Calorimetric measurements of T_g. As noted previously, the cause of the glass transition depression at the nanometre scale size is unknown despite the fact that considerable effort has been made to gain insight into this topic. Among the techniques that have been used to investigate the size effect on the thermodynamic properties of small molecules confined in nanopores is differential scanning calorimetry (DSC). The first results reported on reduced glass transition temperatures for materials constrained in nanopores are those of Jackson and McKenna [1]. The results are shown in figures 8(a) and (b) where figure 8(a) shows the DSC traces for *ortho*-terphenyl (*o*-TP) confined in nanopores of different diameters. Figure 8(b) shows the glass transition as a function of the inverse of pore diameter $1/d$. We see in the

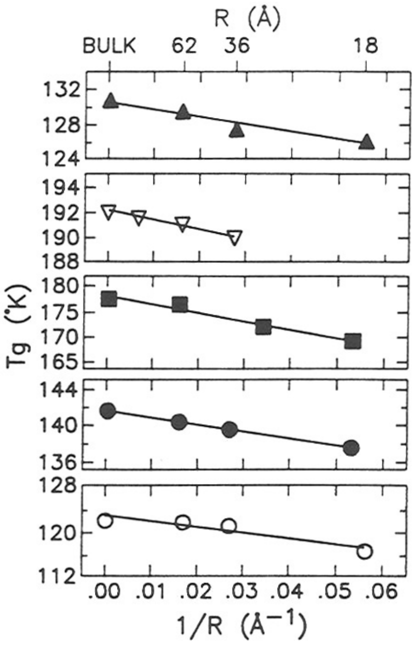

Figure 9. T_g versus inverse pore diameter for small molecules confined in nanopores. The T_g values for bulk liquids are also given ($1/R = 0$): solid triangle, isopropylbenzene; open triangle, glycerol; solid square, di-*n*-butyl phthalate; solid circle, tert-butylbenzene; open circle, b-butyl acetate. After Zhang, Liu and Jonas [67] with permission.

figures that a decrease in T_g for *ortho*-terphenyl (*o*-TP) in controlled pore glasses (CPG) is observed with decreasing pore size [1]. If we look at figure 8(b), the glass transition temperature is plotted as a function of $1/d$ and the authors fitted the data with a straight line in order to compare this result with their previous results on T_m [26] where the Gibbs–Thomson relationship was used to fit the T_m depression. The experimental data, however, do not show a strictly linear relationship between T_g and $1/d$ over the range of pore diameters investigated. Using calorimetric measurements, similar magnitude reductions in T_g were independently confirmed by Zhang, Liu and Jonas with a wider range of small molecule glass forming liquids [67]. The results are shown in figure 9 where a depression in T_g for small organic molecules confined in sol–gel silica glasses is observed. In this case, a linear relationship between T_g and $1/d$ was observed. We remark that the magnitude of the depression of the glass transition relative to T_g itself ($\Delta T/T_g$) is relatively small compared to the magnitude of the melting point depression relative to T_m ($\Delta T/T_m$) [1, 27].

Jonas and co-workers [67] suggested that the depression of T_g for small molecules in nanopores was observed because of the development of negative hydrostatic pressure that resulted from the constraint of the liquid by the pore wall. This is not in agreement with the interpretation in the original work of Jackson and McKenna [1] that suggested that too large a pressure change was required to cause the observed depression in T_g. (We remark that similar observations of the reduction of the glass temperature in block copolymers have been attributed to negative hydrostatic pressures [2, 3].) For example, the pressure dependence of T_g for *o*-terphenyl was measured to be 0.26 K MPa^{-1} [135, 136]; a reduction in T_g of 15 K requires a negative pressure of 58 MPa. The development of such large a negative pressure seems implausible because it requires too large a temperature change from above to below the glass transition, i.e., from the stress free state (where constraints due to the pore walls begin

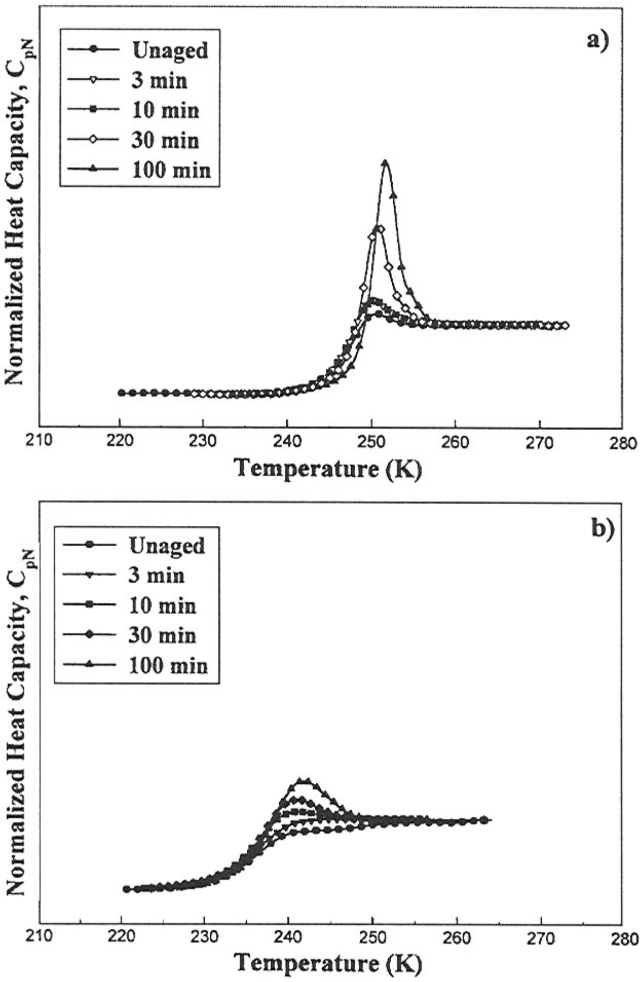

Figure 10. Heat flow versus temperature during DSC scans showing the development of the enthalpy overshoot as a function of time for *o*-terphenyl (a) in bulk and (b) in 11.6 nm pores. The ageing temperature was T_g—11 K. After Simon *et al* [138].

to induce stresses due to the coefficient of thermal expansion mismatches, $\Delta\alpha$, between the liquid and the porous glass matrix) and the reduced glass transition temperature. We note that the pressure that results in the pore is the result of the thermal pressure coefficient of the glass, $\alpha_g K_g$ [137], where α_g is the thermal expansion coefficient of the glass and K_g is the glassy bulk modulus of the material.

Related to this are more recent results of Simon *et al* [138] in which the structural recovery of *o*-TP confined in nanopores was investigated with the specific aim of considering the hydrostatic tension effects on behaviour. They used the TNM-KAHR models [133, 139–141] extended to the case of the constrained or isochoric liquid. Their results [138] on bulk and confined organic liquids are shown in figures 10(a) and (b). These figures show the build-up of the enthalpy recovery overshoot measured by differential scanning calorimetry (DSC) after ageing for various times below T_g of the bulk and constrained *o*-TP. It is clear that a reduction in T_g of the confined material (figure 10(b)) is observed. In addition, the development of the enthalpy overshoot for the confined material is less than that for the bulk material.

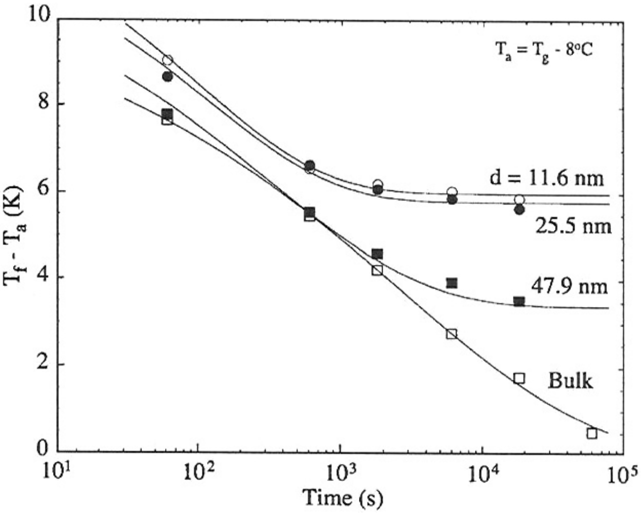

Figure 11. Structural recovery of *o*-terphenyl in the bulk and in nanometre pores of the size indicated as measured by $T_f - T_a$. The test temperature is at $T_g - T_a = 8$ K. After Simon *et al* [147].

The results shown in figure 10 were analysed to obtain the difference between the fictive and ageing temperatures $T_f - T_a$. Figure 11 shows the value of $T_f - T_a$ versus the ageing time for the bulk *o*-TP and the *o*-TP confined in different pore diameters. The interesting point in this figure is that the bulk material reaches the equilibrium state at a value of $T_f - T_a = 0$ whereas the confined material recovers to higher values of $T_f - T_a$. In addition, the time for reaching this different equilibrium state for the confined material is shorter than that for the bulk [138]. The non-zero values of $T_f - T_a$ observed in the ageing of the confined materials indicated that the material in the nanopore is constrained and vitrifies under isochoric conditions (constant volume) [142]. This suggested that the equilibrium state (sub-glass transition temperature and negative pressure) of the confined material at the ageing temperature is different from that of the bulk, i.e., it has a different specific volume. However, the equilibrium conditions (V_g, T_g, P_g) for bulk materials created under isobaric and isochoric conditions are the same as reported by Colucci *et al* [142]. The modelling of the structural recovery by Simon *et al* [138] gave results that were consistent with the formation of an isochoric glass in the nanopores, i.e., there are negative hydrostatic pressures on the glass formed in the pores. The modelling results also provided evidence that the cause of the reduction in T_g was an intrinsic size effect and was not the negative pressure induced by the vitrification under the confining conditions. As mentioned above, if the negative pressure were the cause of the observed depression in T_g, the temperature at which the isochoric conditions are imposed would have to be large, i.e., 20–40 K above T_g [138]. This is not consistent with the results of Simon *et al* [138] where the confinement was found from the modelling to be induced within 3 K of the reduced T_g of the material in the pore.

An interesting result reported by Park and McKenna [75] on the calorimetric glass transition in nanopores was that there are two different glass transitions for *o*-terphenyl (*o*-TP) and polystyrene/*o*-terphenyl (*o*-TP/PS) solutions confined in controlled pore glasses. The first T_g was lower than the bulk T_g and the other was higher than $T_{g(\mathrm{bulk})}$. The lower T_g was found to decrease with decreasing pore diameter which was in agreement with prior observations on reduced T_g in nanopores [1, 67]. The observation of higher T_g was attributed to the interaction between layers of the confined molecules and the pore surface [75]. While the thermodynamic

Table 1. Typical results for the glass transition behaviour when two transitions are observed in liquids confined to porous media. (See the text for a discussion.)

Reference	T_g surface	T_g core	Method
[75] (weak interactions), non-H bonding	$T_g > T_g$ (bulk)	$T_g < T_g$ (bulk)	DSC (calorimetry)
[144] (weak interactions), non-H bonding	$T_g > T_g$ (bulk)	$T_g < T_g$ (bulk)	Dielectric
[143] (strong interactions), H bonding	$T_g \uparrow$	$T_g = T_g$ (bulk)	Dielectric
[146] (weak interactions)	$T_g \downarrow$	$T_g = T_g$ (bulk)	Simulation
[146] (strong interactions)	$T_g \uparrow$	$T_g = T_g$ (bulk)	Simulation

measurements on nanopores have indicated a depression of the glass transition for small molecules in nanopores, the Park and McKenna results raise an important question about the existence of two glass transitions in confined geometries. Both increased and decreased transitions have been observed in dielectric spectroscopy (two relaxations at lower frequencies for confined liquids in nanopores were observed) [77–79, 143, 144] and in NMR relaxation experiments [145].

Scheidler *et al* [24, 146], using molecular simulations, observed two glass transitions for liquids confined in nanopores. In that work, the glass transition was found to depend on the interaction between the wall of the pore and the confined liquid. In the case of a strong interaction, the first T_g is found to be higher than that for the bulk T_g whereas the second one was equal to the T_g in the bulk. For a weak interaction, the first T_g was lower than that of the bulk and the second one was the same as that of the bulk T_g [24, 146]. These simulation results suggest the existence of multiple glass transitions and this is similar to experimental observations. However, the molecular simulations do not predict at the same time an increase and decrease of the glass transition as observed experimentally in nanopores [143, 144]. Table 1 provides some comparisons from experiment and simulation concerning the existence of two different T_gs for liquids confined in nanopores.

Alba-Simionesco and co-workers [28, 147] performed measurements using an adiabatic calorimeter to investigate confinement effects on small molecules in nanopores. In that work, the glass transition of benzene and toluene confined in cylindrical pores of synthesized silicates was measured [28, 147]. Figure 12 shows the glass transition of toluene confined in nanopores as a function of pore diameter d. This figure shows that T_g decreases and then increases with decreasing pore diameter. Alba-Simionesco and co-workers suggested that competing effects took place in the confined geometries [28, 147]. The large increase in T_g of toluene (37 K) in very small pore diameters (2.4 nm) was attributed to a surface effect due to the interaction between the confined molecules and the pore. The reduced T_g observed in the larger pore diameters was attributed to an intrinsic size effect where a decrease in the surface to volume ratio occurs [28, 147]. The authors suggested that the surface effect can be stronger if one takes into account the difference in density between the bulk and confined liquid where the glass transition of the bulk with the same density as the confined liquid would be lower than $T_g\infty$ (the dotted line in figure 12). The non-monotonic variation of T_g observed in figure 12 is similar to that observed by Schonhals and co-workers [148, 149] in dielectric experiments for propylene

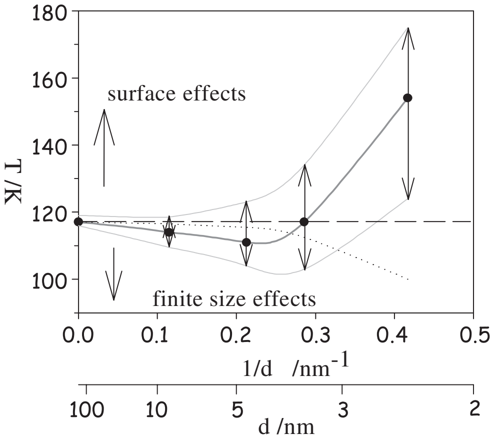

Figure 12. Glass transition versus pore diameter for toluene confined in nanopores. After Alba-Simionesco *et al* [28, 147] with permission.

glycol of low molecular weight (PPG) confined in CPGs where the dielectric glass transition was found to decrease and then increase with decreasing pore diameter. Alba-Simionesco and co-workers proposed that the non-monotonic variation of T_g is only observed in the case of confined fragile liquids such as toluene and benzene [28]. The results reported on the adiabatic calorimetric measurements of benzene (strong liquid) showed a monotonic increase in the glass transition with decreasing pore diameter (2.5–20 nm). The authors attributed the increase in T_g for benzene to the inhomogeneous distribution of the relaxation times in the pore [28]. More experiments using different small molecules in nanopores should be carried out to confirm the results reported by Alba-Simionesco and co-workers [28, 147]. We recall here that Jonas and co-workers performed experiments by means of NMR and reported the first result on the confinement effects on the molecular dynamics of liquid toluene in porous sol–gel glasses [80]. In addition, Jonas and co-workers did look at the behaviours of different materials confined to nanopores [67, 80, 145]. Note that the result reported by Alba-Simionesco and co-workers [28, 147] on the increase of T_g in benzene is the only thermodynamic result available in the literature on confined liquids in nanopores where T_g increases. However, Alba-Simionesco and co-workers have not observed two T_gs for the confined benzene and toluene, which differs from the observation of Park and McKenna for *o*-TP in controlled pore glass-type nanopores [75]. Hence, a comparison between adiabatic calorimetric and DSC measurements for *o*-TP confined in similar nanopores would be interesting. Further, the difference in confining media should be considered.

Using neutron scattering [150, 151], Alba-Simionesco and co-workers [28, 147] reported the first measurement of the density for glass forming liquids in well defined pores. In that work, the measurements were performed using toluene confined in mesoporous silicates (MCM-41 and SBA-15). These are made up of parallel cylindrical pores of diameters from 2.4 nm to 14 nm with a narrow pore size distribution [147]. In figure 13, we show the results of the density measurements for the bulk and toluene confined in 2.4, 3.5 and 4.7 nm nanopores [147]. This figure shows that the density at room temperature of the confined toluene is approximately the same as for the bulk material. In this case, no change in the glass transition of the toluene in 3.5 and 4.7 nm pores was observed. However, for the toluene confined in the 2.4 nm pores, a decrease in the density is observed and an increase of 30 K in T_g occurred. We note here that a free volume model would predict that the decrease in density observed in the confined toluene

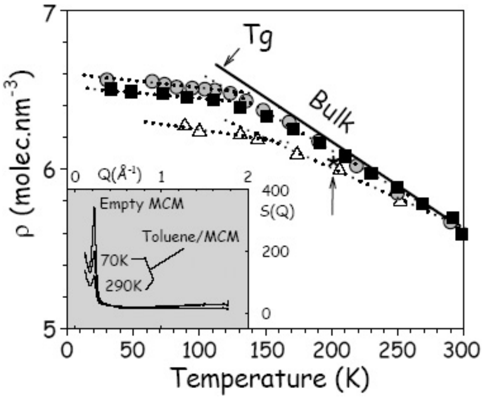

Figure 13. The temperature dependence of the number density of bulk and confined toluene. After Alba-Simionesco *et al* [147] with permission.

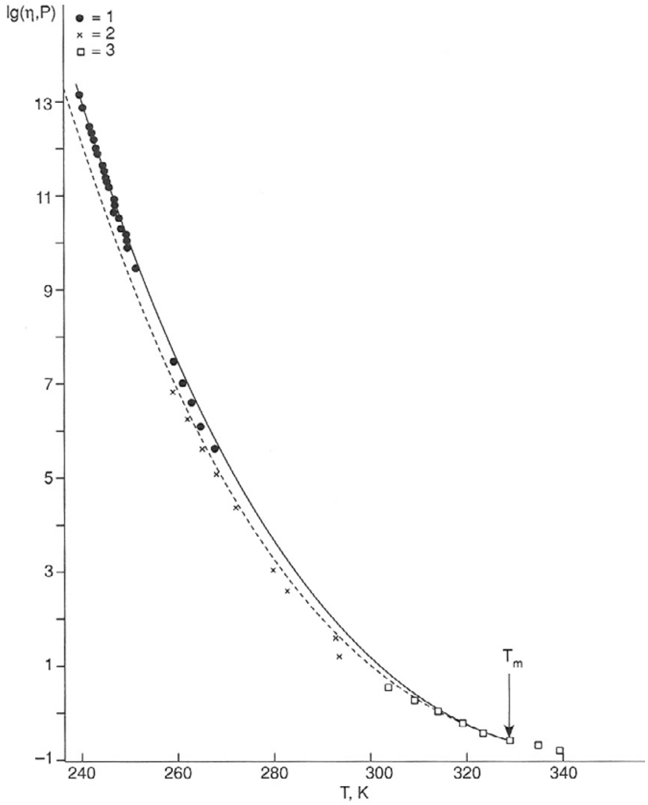

Figure 14. Viscosity for *o*-terphenyl as a function of temperature. The figure is from Nemilov [152] with permission.

would result in a decrease in the glass transition, which is the opposite of what was observed by Alba-Simionesco and co-workers [147].

2.2. Dynamic measurements of glass forming materials confined in nanopores

In this section we review the results reported in the literature for the dynamic behaviour of small molecules confined in nanopores. In dynamic measurements, the property examined is the material relaxation time and how this relaxation is affected by the confinement. In figure 14 we show a typical plot that illustrates the dynamics of a glass forming liquid as the glass transition is approached [152, and references therein]. This figure shows the temperature dependence of the viscosity for *o*-terphenyl upon cooling from above to near the glass transition [152]. In this plot, the glass transition is defined as the temperature at which the equilibrium liquid has a viscosity of 10^{12} Pa s, or as the temperature at which the average relaxation time in the equilibrium liquid is 100 s. It is known that below T_g the viscosity η and the relaxation times τ would increase by several orders of magnitude where the non-Arrhenius (fragile liquid) behaviour observed extrapolated to below T_g whereas a return to Arrhenius behaviour is observed at higher temperature. The concept of fragility was originally proposed by Angell to classify the behaviour of glass forming liquids where the temperature dependence is non-Arrhenius [73].

The variation of the average relaxation time with temperature T generally obeys the empirical Vogel–Fulcher–Tammann (VFT) relationship [153–155]:

$$\tau_{\text{avg}} = \tau_0 \exp\left(\frac{B}{T - T_0}\right) \tag{2}$$

where the parameter τ_0 is a microscopic relaxation time, B is the activation parameter which is related to the fragility of the glass former [73, 156, 157] and T_0 for polymers is generally approximately equal to T_g—50 K. The relaxation behaviour for bulk polymers (α relaxation) is well described by equations (2) and (3). A change in temperature dependence of the dynamics in confined molecules or thin polymer films may indicate changes in the glass transition. Therefore, it is important to understand the origins of the change in dynamics of glass forming materials in confined geometries. Many attempts have been made to understand the dynamic behaviour at the nanometre size scale by using the VFT equation where, in some cases, changes in the B and T_0 parameters compared to their values in the bulk were observed [76–79, 107–110, 143, 144]. Differences in the relaxation behaviour between bulk and thin polymer films (or confined liquid) samples, such as changes in the VFT B parameter or the $T_g - T_0$ value may indicate finite size effects as the sample size approaches the cooperativity length, ξ [158], in the glass forming system [88, 159, 160]. If only negligible deviations from bulk behaviour are observed, then explanations not involving cooperativity may be favoured. However, if there is a change in activation energy or the VFT B parameter, then depending on distance from T_g one may interpret the results differently (increase or decrease in T_g) if care is not taken in the analysis of the data.

Another aspect of dynamics is the distribution of relaxation times or non-exponentiality of decay. One way of treating this behaviour is by using the stretched exponential function or Kohlrausch–Williams–Watts (KWW) [161, 162] function:

$$\phi(t) = \phi_0 \exp\left(\frac{t}{\tau}\right)^{\beta} \tag{3}$$

where the parameter β describes the shape of the distribution of relaxation times. For $\beta = 1$, the relaxation function is a simple exponential where the relaxation behaviour is described by only one relaxation time. For $\beta = 0$, this function is constant and there is no relaxation. Therefore, smaller values of the β parameter (between 0 and 1) indicate a broadening of the distribution of relaxation times.

At the nanometre size scale, the relaxation behaviour of glass forming materials has been reported to be different from that observed for bulk behaviour in the same material.

Measurements of dynamics of small molecules confined in nanopores have been extensive [76–86, 143–145, 148, 149, 163–184]. As mentioned above, the dynamic measurements for materials confined in nanopores can be carried out using different techniques such as the dielectric spectroscopy, NMR, dynamic light scattering, solvation dynamics and thermally stimulated depolarization current (TSDC) methods. In the following sections we discuss the experimental results obtained using these techniques.

2.2.1. Dielectric measurements for glass forming liquids confined in nanopores. The first dielectric experiments to investigate the α relaxation associated with the glass transition of confined glass forming liquids were reported by Pissis *et al* [85] who used Vycor glass as the pore system. The Vycor-type glasses and the CPGs are similar in having a nanoporous structure that is characterized by a narrow distribution of pore diameters. Figure 15 depicts the Pissis *et al* [85] results as the normalized dielectric loss versus frequency for glycerol confined in pores and for the unconstrained bulk glycerol. The results show a broadening of the dielectric loss that is due to the confinement. Pissis *et al* [85] attributed their observations on the change in the relaxation behaviour in the confined fluid to the change in the cooperativity length ξ taken from the concepts originally developed by Adam and Gibbs [158]. ξ increases with decreasing temperature towards T_g and becomes comparable to the dimensions of confinement. Richert and co-workers [143] reported results from dielectric measurements on propylene glycol (PG) and two poly(propylene glycol)s (PPGs) of different molecular weight confined in controlled pore glasses (CPGs). (CPGs have pores that are cylindrical in shape, similar to the Vycor ones. They come in powder form and consist of particles 30–60 μm in diameter with a pore volume of 0.4–0.8 cm^3 per g of glass [123, 124].) These were cleaned and dried under vacuum, i.e., the CPGs were not chemically treated. The dielectric measurements were performed in a frequency range of 10^{-2}–10^6 Hz. Richert and co-workers [143] used the VFT relationship to analyse the dielectric results that showed retardation and broadening of the α relaxation process, an increase in T_0 and a decrease in the fragility of the liquid (decrease in the B parameter of the VFT equation) and the appearance of an additional relaxation process below the α relaxation frequency (at higher temperatures). Consequently, an increase in the glass transition T_g for the PG and PPG liquids in nanopores was observed. The existence of an additional relaxation was attributed to the interaction of a few layers (hydrogen bonding effect) of the confined liquid with the pore. This result was the first to report an increase in the T_g in nanopores, which is consistent with a simple explanation based on the configurational entropy concept of Gibbs and DiMarzio [68, 69].

In a subsequent paper, Schuller *et al* [144] measured the dielectric responses of N-methyl-ε-caprolactam (NMEC) confined to mesopores of a controlled pore glass (CPG). Schuller *et al* [144], used CPGs having a mean pore diameter of 10.2 nm. In that work, native and treated controlled pore glasses were used to investigate the surface effects on the relaxations at the nanometre size scale. The CPG surface was treated by replacing the polar OH groups on the pore surface with a less polar group, which resulted in a more hydrophobic surface. Figure 16 shows the dielectric responses at two temperatures for the bulk and confined NMEC in a native CPG [144]. The figure shows that the α relaxation (I) of the confined NMEC at 183 K shifts to higher frequencies. In addition, broadening of the α relaxation of the confined NMEC is observed. Also, the additional relaxation peaks (II and III) for the NMEC confined in native controlled pore glasses were detected at the higher temperature of 227 K [144]. Figure 17 shows the temperature dependence of the peak dielectric relaxation times τ_m for the bulk and confined NMEC. The figure shows that a shift in the relaxation times τ_m for the loss peak (I) towards lower temperatures is observed. This indicates an increase in T_g for the confined liquid compared to the bulk.

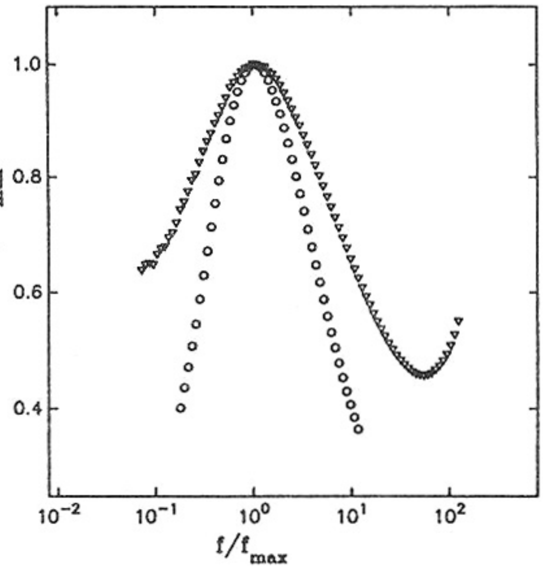

Figure 15. Normalized plot of dielectric loss as a function of frequency for bulk (open circle) and confined glycerol (open triangle) at 233 K. After Pissis *et al* [85] with permission.

The additional relaxations (II and III) that disappeared for materials confined in the silanized surfaces were attributed to the CPG surface; Schuller *et al* interpreted the results as implying that the liquid formed an interfacial layer near to the surface of the pore [144]. They showed that the dynamic properties of this interfacial layer are dominated by the number of hydroxyl groups per molecule due to the specific interaction with the silanol (one hydroxy group) groups on the surface of the porous glass [143, 144]. In dielectric spectroscopy, the interfacial layer can be detected as a separate relaxation peak for molecules with only one hydroxyl group per molecule (e.g., salol, propanol). The surface to volume ratio and its effect on the α relaxation in pores was discussed in Schuller *et al* [143, 144].

Richert and co-workers [171], extended their previous dielectric results [143, 144] to study the molecular mobility of propylene glycol (PG) and poly(propylene glycol)s confined to a 10 nm diameter CPG in order to investigate size effects on the dynamics of hydrogen bonded liquids of different molecular weights but identical chemical composition. The authors used dielectric and neutron spectroscopy to investigate the low and high frequency features as a function of temperature [171]. The CPG was treated to replace the polar OH groups on the glass surface with the less polar trimethylsilyl groups resulting in a more hydrophobic surface. In their work, Richert and co-workers [171] observed an increase in T_g for all liquids, which has been attributed to the interactions at the liquid–solid interface, such as the hydrogen bonding with silanol groups of the pore surface. This effect was reduced by increasing the molecular weight of the confined liquids or by decreasing the amount of hydrogen bonding. We note here that in the Park and McKenna work [75], two calorimetric glass transitions were observed for *o*-TP molecules and for concentrated *o*-TP/PS solutions both confined in treated controlled pore glasses with hexamethyldisilazane. Hence, when the pore surfaces are treated, the observation of an additional loss relaxation peak at lower frequencies [143, 171] and that of two calorimetric glass transitions [75] suggest that interactions between the pore surface and the confined liquid are important to understanding confinement effects.

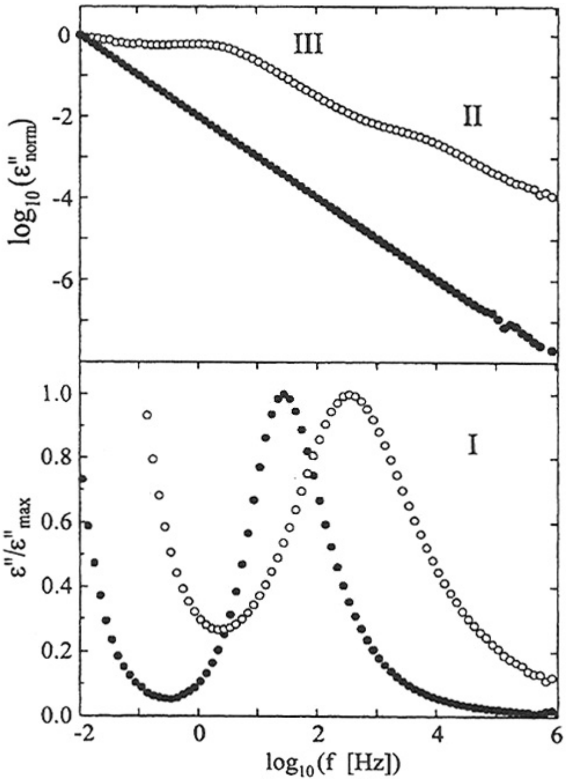

Figure 16. Normalized dielectric loss spectra $\varepsilon''(\omega)$ of bulk (solid circles) and confined (open circles) NMEC for two different temperatures. Upper panel: $T = 227$ K showing peaks II and III; lower panel: $T = 183$ K showing peak I. After Richert and co-workers [144] with permission.

Kremer and co-workers [79] studied the effects of confinement on the dynamic properties of low molecular weight H bonded organic small molecules using broadband dielectric spectroscopy over a wide frequency range between 10^{-2} and 10^{9} Hz. The materials used in that work form a homologous series of molecules having two H bonds but different molecular sizes (propylene glycol (PG), butylene glycol (BG) and pentylene glycol (PeG)) confined to porous sol–gel glasses with pore sizes of 7.5, 5.0 and 2.2 nm. The results reported by Kremer and co-workers [79] showed no effect of the confinement on the relaxation rates of PG and BG in 7.5 and 5 nm pores whereas for the PeG the α relaxation in 7.5 and 5 nm pores became slightly faster compared to the bulk at low temperature (T_g decreases). For all the confined liquids in 2.5 nm pores the peak relaxation rate is slower than that for the bulk (T_g increases). The authors suggested that the increase in T_g for the confined liquids in small pores was due to the existence of a fraction of glass-like molecules at the pore wall. The stiffness of this layer was caused by strong H bonding to the surface of the pore wall. Therefore, the interaction between the wall and the molecules can affect the relaxation mechanism in nanopores; strong interactions cause T_g to increase whereas weak interactions result in a reduced T_g. A three-layer model was proposed by Kremer and co-workers [79] in order to explain the relaxation mechanism (or the increasing molecular mobility towards the pore centre) of small molecules in nanopores observed in their work. This model consists of three layers: an interface layer contacting the substrate (solid-like), a surface layer (bulk-like) and an interfacial layer between both surface layers [79]. The relaxation time distribution $h(\tau)$ can be estimated using this model where

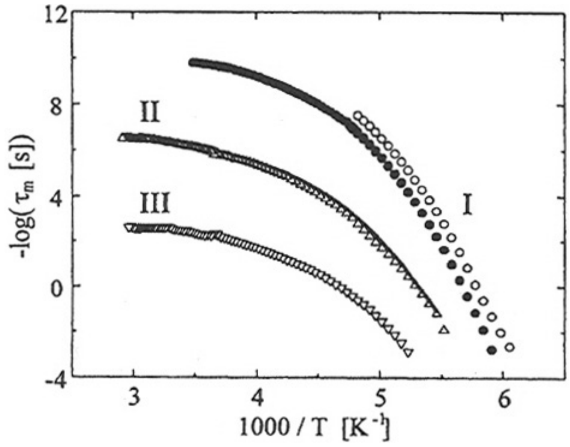

Figure 17. Temperature dependence of the peak dielectric relaxation times τ_m for bulk (solid circles) and confined (peak I, open circles; peak II, open up-pointing triangles; peak III, open down-pointing triangles). After Richert and co-workers [144] with permission.

the magnitude of τ depends on the distance of the molecules from the wall. The authors assumed that the dielectric strength is proportional to the number of molecules participating in the relaxation process. In their work, a decrease and increase in the glass transition were reported. In addition, two relaxation processes were observed at lower frequencies for PG confined in nanopores [79].

Arndt *et al* [77] have also reported results from broadband dielectric spectroscopy on the relaxation behaviour of glass forming materials confined in controlled pore glasses. The materials used were salol (one hydroxyl group), pentylene glycol (two hydroxyl groups) and glycerol (three hydroxyl groups). In that work, the authors reported that for liquids with one hydroxyl group (salol) two separate loss processes were detected in all pore sizes and these were assigned to the relaxation of an interfacial layer and the relaxation of bulk-like molecules in the centre of the pores. Liquids with two (PG) or three hydroxyl groups (PeG) showed only the α relaxation associated with T_g. The authors interpreted their results using a two-state model in which there is a dynamic exchange between a bulk-like phase in the pore volume and an interfacial phase close to the pore wall. In general, the results reported in this paper are similar to those reported by Schuller *et al* [144], except that the decrease in T_g was more pronounced. In other dielectric spectroscopic experiments, Arndt *et al* [78] studied confinement effects on the low molecular weight glass forming liquid salol (phenyl salicylate) confined to CPG. The CPGs were chemically treated to replace the –OH groups on the glass with trimethylsilyl groups. In the case where the liquid is confined to the native CPG, the results showed a broadening of the relaxation time distribution compared to that for the bulk. In addition, two additional relaxations at lower frequencies appeared [78]. However, these additional relaxations disappeared when the molecules were confined in treated CPGs. In this case, a depression in T_g was reported [78].

Schonhals and Stauga [169, 170] also performed dielectric spectroscopy experiments using poly(propylene glycol), PPG, of different molecular weights confined to native CPG. The relaxation spectra for the confined PPG showed two relaxation processes, the α relaxation associated with T_g and an additional relaxation process at lower frequencies [169, 170]. This result is similar to that reported on the dynamic glass transition of small molecules in nanopores [78, 163, 171].

Moreover, dielectric and temperature modulated DSC measurements reported by Schonhals *et al* [149] for PPG of different molecular weights confined to nanopores showed a non-monotonic variation of the glass transition with decreasing pore size. For larger pore size (>3 nm), T_g was observed to decrease, while for small confining dimensions (<3 nm) T_g increased with decreasing pore size. These results were different from those obtained for the monomeric PG where an increase of T_g with decreasing pore size was found by Gorbatschow *et al* [79]. The difference in results was discussed in terms of reduced number of OH groups for the polymeric PPG whereas in the case of the PG monomer, the OH groups can form H bonds with each other and with the surface.

Petychakis *et al* [183] studied the dielectric properties of polyisoprene (PI) with different molecular weights, between 2000 and 108 000 g mol^{-1}, in a treated controlled porous glass with diameter of 10.2 nm. The entanglement molecular weight of polyisoprene, M_e, is approximately 5000 g mol^{-1} [131] and the end-to-end vectors of the polymer molecules were between 3.6 and 8.6 nm. The dielectric spectra of the bulk PI showed three relaxation processes, a fast segmental relaxation followed by an intermediate mode and a much slower process. There was also a pronounced effect of the confinement on the dynamics, which was found to depend on the molecular weight. For example, the PI confined in native CPG with molecular weight of 2000, which is less than the entanglement molecular weight ($M_e = 5000$), the relaxation times of the α relaxation were found to shift to longer times [183]. For the higher molecular weight polyisoprene (with $M_w > M_e$) confined in the untreated CPG, it was found that the relaxation times shift to shorter times (the higher the molecular weight the shorter the relaxation times). In the case where the highest molecular weight PI was confined in the treated CPG, broadening of the normal modes and a shift in the relaxation times to lower frequencies (longer times) were observed [183]. Hence, T_g could increase or decrease depending on details of molecular weight, pore size and pore surface treatment.

2.2.2. Solvation dynamics and inelastic neutron scattering techniques. Richert and co-workers [82–84] have investigated confinement effects on the dynamics of glass forming liquids of different polarities in nanopores using a solvation dynamics technique, which is an optical technique. In this technique, a chromophore is a local probe for the orientational relaxation of permanent dipoles. This is similar to the local dielectric relaxation in polar liquids [82–84]. The materials used in one of those studies [82] were quinoxaline (QX) in 2-methyltetrahydrofuran (MTHF) and in 3-methylpentane (3 MP) solvents. The solutions of QX in MTHF and 3MP were confined to treated and native Gelsil glasses made by a sol/gel process and having the form of a monolithic cylinder. The pore geometry resulting from the sol/gel process is different from the bicontinuous channels in the CPGs. The results reported on QX/MTHF confined in untreated Gelsil glasses showed an increase in the glass transition compared to the bulk case and a broadening in the distribution of relaxation times. In the case of QX/MTHF confined to silanized pores, the authors observed that the dynamics of the liquid remained unchanged; this includes the relaxation times, the apparent activation energy and the amplitude of the response in the solvation dynamics experiment. This was different from what was observed in native pores. Richert and co-workers [81] also performed solvation dynamics measurements using 2-methyltetrahydrofuran confined in nanopores of sol–gel glasses. The α relaxation of the confined liquid was faster than that for the bulk, indicating a decrease in T_g. This was accompanied by a decrease in the KWW β parameter indicating a broadening of the relaxation time distribution.

Recent measurements reported by Zorn *et al* [176, 177] on the glassy dynamics of glass forming liquids confined in microporous silica glass (Gelsil) using inelastic neutron scattering showed a reduced glass transition compared to the bulk case. In addition, a broadening of

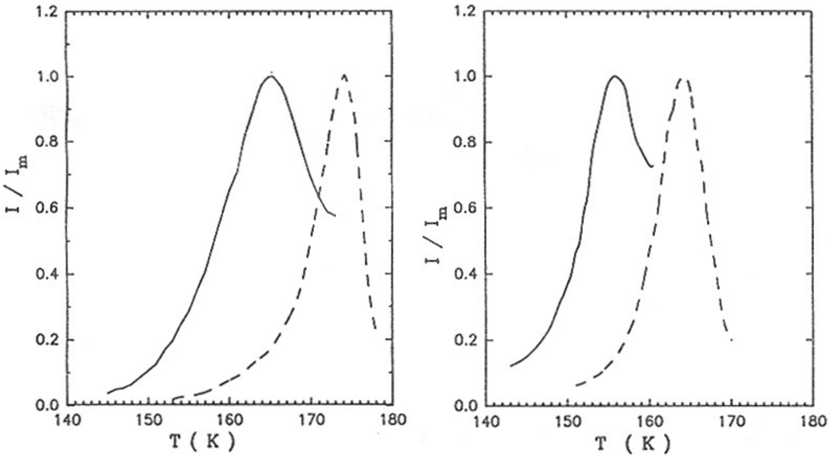

Figure 18. The thermally stimulated depolarization current results reported for bulk (dashed curve) and confined (solid curve) propylene and propylene carbonate. After Pissis *et al* [85] with permission.

the relaxation spectra for the confined liquids was observed which was consistent with the dielectric results discussed above.

Schonhals and co-workers [148, 149] and Zorn *et al* [176, 177] have discussed the confinement of glass forming materials in nanopores in terms of the cooperativity length scale ξ [158–160]. Because ξ cannot become larger than the confining dimensions, nanoporous materials are an obvious template in which to study cooperativity length aspects of the glass transition event and associated dynamics. According to these groups, this effect leads to an acceleration of the molecular dynamics compared to the bulk. On the other hand, the dynamics of the confined liquid is affected by the interaction with the surface (surface interaction effects). This surface effect (adsorption) should increase with the surface-to-volume ratio of the pores. The dielectric spectroscopy, temperature modulated DSC and neutron scattering experiments on confined PPG and PDMS were interpreted as implying that an inherent length scale is relevant for glassy dynamics. Schonhals and co-workers [148] observed a speeding up of the dynamics (confinement effects) for both PPG and PDMS. The confinement effect in the case of PDMS was more pronounced than that for PPG because the PDMS is more hydrophobic than the PPG. A non-monotonic variation of T_g with pore diameter was observed for the confined PPG whereas a monotonic decrease of T_g was reported for PMDS. We remark that a contrary view of length scale effects can be put forward [122]. If glassiness occurs because of a growing cooperativity length as T_g is approached from above, as proposed by Adam and Gibbs [158], then one would expect this length to represent the amount of material that must move cooperatively or motion will not occur. If one puts a material into a pore that inhibits cooperativity by not letting sufficient material be available to move, then we think that this should lead to decreased mobility and the T_g should go up. Issues of jamming may also be important in this context [185].

2.2.3. *Thermally stimulated depolarization current technique (TSDC).*

Another dynamic-type measurement of the glass transition in confined geometries is the thermally stimulated depolarization current (TSDC) experiment performed by Pissis *et al* [85, 86, 163]. This technique was developed to investigate the structures of water in different systems over a wide range of temperature [186]. The TSDC method requires the application of an electric field to the sample (the sample is polarized) and the polarization is subsequently frozen in (vitrification) by cooling the sample to temperature sufficiently low to prevent depolarization by thermal energy. The field is then switched off and the sample is heated (devitrification) at a constant rate, while the depolarization current, as the dipoles relax, is detected with an electrometer [186].

This is a dynamic measurement of the glass transition but it has an aspect of a pseudo-thermodynamic measurement. In fact, some issues of interpretation can arise during the experiments due to the vitrification and the devitrification (thermal history effects [25] of the confined liquid upon cooling and heating, respectively). Figure 18 shows the normalized TSDC plot, measured for bulk and confined propylene glycol [85]. The TSDC peaks represent the α relaxation. The results indicate that the relaxation mechanisms of the bulk and confined propylene glycol are different where the relaxation times of the confined liquid are changed under confinement. Pissis and co-workers indicated that the temperature of the α peak maximum (TSDC peak) is close to the calorimetric glass transition temperature and a reduced glass transition of propylene glycol in Vycor glass was reported by TSDC [85]. The shift in T_g to lower temperature observed was interpreted by the authors [85] in terms of the cooperativity length scale [158–160] where the dynamics of glass formers under confinement become faster than for the bulk [78, 187–189]. It was mentioned above that according to this concept, the mobility of small molecules in confined geometries increases because the decrease of the size of the system causes a decrease in the number of molecules rearranging collectively.

2.2.4. Discussion of the behaviour of small molecules in nanopores. The thermodynamic and dynamic measurements of small molecules confined in nanopores reported above showed behaviours that differed from that of the bulk material. This may be a good indication of the existence of a different T_g in confining geometries. For example, the results reported from dielectric measurements [76–79, 143, 144] and NMR relaxation experiments [145] on the existence of two relaxation processes in liquids confined in nanopores are consistent with the observation of two glass transitions in nanopores reported from thermodynamic measurements [75]. Moreover, the adiabatic calorimetric experiments that have shown a non-monotonic glass transition for toluene in nanopores [28, 147] are similar to those observed in dielectric experiments for PPG in nanopores [148, 149] where an estimated glass transition at 10^{-2} Hz was calculated from the VFT equation. However, the glass transition for PG in nanopores showed a monotonic increase as pore diameters decreased.

The relevant question to ask here in order to understand the behaviour of confined liquids concerns the finite size effects: are these intrinsic? There are two size effects to consider in discussing this topic. The first is the size of the constrained system. As mentioned in the first section of this paper, thermodynamic models such as the Gibbs–Thomson relationship [38–40] provide a reasonable description of the melting point depression (first-order transition) to sizes of 4–10 nm. Thus, it is expected that there would also be a size effect on T_g for confined liquids similar to the T_m depression but, perhaps, of smaller magnitude. Therefore, it is important to perform experiments in which at least one dimension is reduced to the range 2–100 nm. For this, different constraining systems such as controlled pore glass or glasses can be used, varying the size between 2 and 100 nm to clarify this effect.

The second size effect is that of the size of the confined molecules relative to the size of the constrained system. We expect then that there would be a molecular weight effect on the depression of T_g in confined geometries. There have been few systematic studies on small molecule glass formers confined in pores that address this issue. Therefore, further investigation of the molecular size effects on confined liquids in nanopores could be used to investigate the relationship between confinement and the molecular structure. In addition, the shape and the dimensionality of the confining medium could have an effect on the change in T_g in confined geometries [122] and this requires further investigation. We do note that results reported on thin polymer films supported on substrates showed a minor effect of molecular weight on T_g [17, 97] whereas recent results showed a large effect of the molecular weight on T_g for free standing thin PS films as observed by Dutcher and co-workers [16–18, 90] and this is discussed in the following sections on thin polymer films.

Another important aspect of the behaviour at the nanometre length scale is the interaction between the confined liquid and the walls of the confinement. The nature of the wall, for example whether it is hydrophobic or hydrophilic, can have an important effect on the change of T_g in nanopores. Hence, a quantitative estimate of wall/surface interactions is required. Is the surface tension, as in the Gibbs–Thompson equation, the most important parameter? Or the strength of specific interactions that cause the grafting of the material to the surface or wall? It is clear then that more experiments have to be done to systematically examine the interface effect on the dynamics in confinement geometries. In order to do this, the surface treatment in the pore glasses has to be changed to modify the surface interaction between the confined liquid and the pore.

One explanation of the observed results in dielectric experiments is the –OH bonding between the confined molecules and the pore surface. This could be affected by the pore surface/pore volume ratio. As discussed above, this might not be the case because in some of the dielectric work, an additional relaxation at lower frequencies for small molecules in treated pores was reported [76–79, 143, 144, 170, 171]. In addition, no significant change in the calorimetric T_g was found for small molecules confined in treated and untreated controlled pore glasses as reported by Jackson and McKenna [27]. However, it is still difficult to understand the exact cause of the observation of different material behaviour at the nanometre size scale. Is there evidence of confinement, interface and intrinsic size effects?

Finally, the presence of a confining matrix or surface can lead to confinement effects that would occur under similar conditions in macroscopic materials. One effect arises because the glass transition is kinetic in nature and can be strongly path dependent [25, 130–133]. For example, confinement of liquids in nanopores can lead to the transition of a glass under isochoric (constant volume) rather than isobaric (constant pressure) conditions [138], which leads to the presence of a negative hydrostatic pressure in the confined material and, as noted above, the hydrostatic pressure can affect the glass transition. Hence, it is important to understand the 'macroscopic' confinement effect on the material behaviour in order to separate the size and confinement effects at the nanometre scale. To separate the size effects from the effects of hard constraint, systematic studies should be performed that can vary the type of confinement from hard to soft confinement [122, 190–192].

3. The glass transition temperature in thin polymer films

As mentioned above, the glass transition in thin polymer films has been widely examined using different experimental techniques [16–21, 87–121, 193–272]. The results reported have shown disagreement among laboratories and among different experimental methods about the behaviour of ultrathin polymer films relative to their behaviour in the bulk. Remark here that the chain conformation in the bulk material is different from that in 2D thin films where the chains retain unperturbed Gaussian conformations in the direction parallel to the surfaces. This was observed experimentally by Russell and co-workers [93, 242, 273, 274]. Hence, the relaxation dynamics in 2D thin films is different from that observed in 3D bulk materials.

The early work reported on thin polymer films was performed primarily using a pseudo-thermodynamic mode. More recently dynamic measurements and measurements of the rheological responses have been performed. What we mean here by a pseudo-thermodynamic measurement is, as mentioned previously, that the glass transition temperature is determined from a change in the slope of a property of the film, such as thickness and Brillouin frequency, with temperature. In figures 19(a) and (b), we show an example of pseudo-thermodynamic measurement results for thin polystyrene (PS) films as reported by Keddie *et al* [97] using ellipsometry. Figure 19 shows the thickness of PS on a silicon substrate as a function of temperature for different thermal histories. The linear thermal expansion coefficient of the film is calculated and the glass transition of the thin PS films can be determined. This is a relative measurement of the thermal expansion of the material, which is different from that of the volumetric thermal expansion of the materials: the expansion of the thin film is only observed in (one dimension) the thickness of the film, whereas no expansions occur in the other dimensions because of the interaction and biaxial constraint of the substrate. In the following sections, we discuss the results reported on ultrathin polymer films using pseudo-thermodynamic methods as well as for other techniques used to study the thermodynamic, dynamic and rheological properties in ultrathin polymer films.

3.1. Sample preparation issues for ultrathin polymer films

Before discussing the details of the experimental results on thin polymer films, we first discuss how they are prepared. The important point that we think needs to be considered here is that a nanometre thick polymer film is not an inherently equilibrium structure. In fact, one anticipates surface tensions to be sufficient to drive the thin films into droplets given sufficient time. Hence, the fact that polymers can be made into such non-equilibrium structures is due to the process of entanglement that led to high viscosities and long relaxation times, thereby stabilizing the films. The price we pay is the non-equilibrium state of the material that may play a role in the experimental findings obtained at the nanoscale. There are other issues and these are also discussed below.

There are several methods used to prepare ultrathin polymer films that are supported on substrates. The spin coating process has frequently been used to create thin polymer films constrained for example to SiO_2 surfaces [97, 101]. Measurements are performed directly on the supported thin films and sometimes on free standing thin films created by floating the film from the substrate onto which it was originally formed [16–18]. In the spin coating process, the film is created by evaporating the solvent from concentrated solution where the material vitrifies. The resulting film is in a non-equilibrium state due to the evaporation of the solvent and to the constraint of the surface. Hence, the material created by spin coating can undergo approximately 14% volume change in the glassy state after the evaporation of the solvent [131, 190], which would be equivalent to a very large temperature jump. In addition to the solvent effect, the strain resulting from the biaxial constraint of the substrate can possibly lead to yielding of the material. The resulting yielded material can be considered to be in a thermodynamic state different from that of the undeformed material [190]. This post-yield state has been postulated McKenna [275] to be a deformation induced polyamorphism [276]. In the experiments performed on spin cast polymer thin films, first the cast material is annealed above the glass transition of the bulk material to allow it to reach the equilibrium state. In early work, the measurements were carried out from below to above T_g, i.e., during devitrification. However, experimentalists now pay more attention to performing experiments on cooling (during vitrification) after annealing the material above T_g. We note here that the spin coating process could also affect the liquid state of the spin cast film. Recent experiments performed

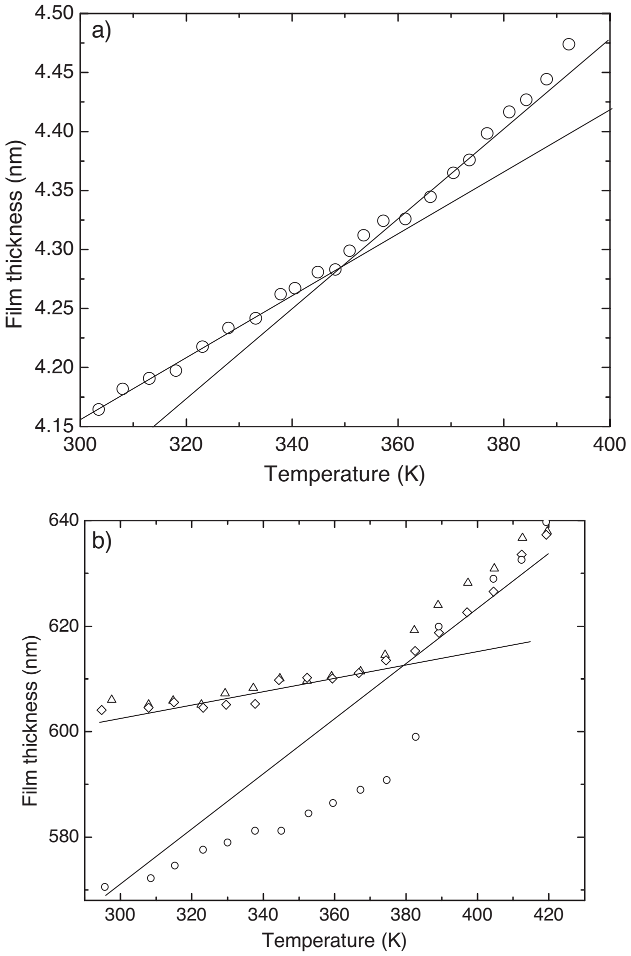

Figure 19. The first measurements of the thickness dependence of the glass transition in ultrathin PS films as reported by Keddie *et al* [97]. (a) Film thickness measurements at approximately 5 K increments in temperature. (b) Incremental thickness measurements for a sample that was not equilibrated above the bulk T_g prior to experiments. After [97] with permission.

by Bernazzani and co-workers [277, 278] on freeze dried polystyrene show that the annealing process used to recover the normal T_g takes over 60 h at 150 °C (i.e., $T_g + 50$ °C). Hence, current annealing treatments at lower values of $T + T_g$ and for shorter times may not be sufficient to 'equilibrate' the thin films.

Also, we note here that recent results reported from our laboratory by Alcoutlabi *et al* [279, 280] and Zheng and McKenna [281, 282] have shown that a glass formed by a temperature jump is very different from that formed after a concentration jump. In that work, it was found that the concentration-formed glass is more stable than the temperature-formed glass in spite of the former having a higher excess volume: the time required to reach equilibrium for the concentration-formed glass is much longer than that for the normal T-formed glass [279, 281]. While the freeze drying and concentration-formed glasses are not exactly the same as spin coated films, it is clear from such studies that rapid removal of solvent from polymer glasses has complicated effects on the behaviour of such materials. Hence, work on thin films, while

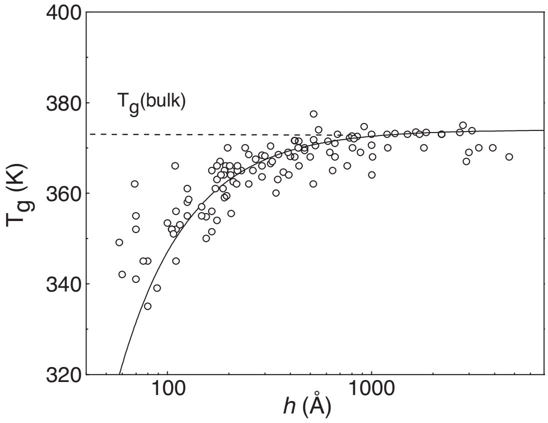

Figure 20. Measured values for the glass transition temperature of thin supported polystyrene films. The data were reported using different experimental techniques (see the text). After Forrest and Dalnoki-Veress [194] with permission.

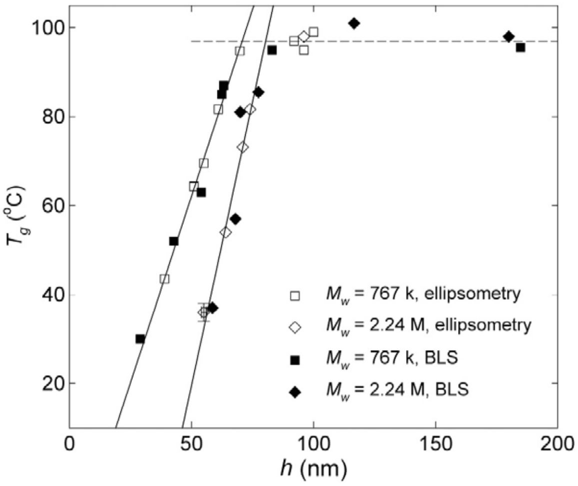

Figure 21. The glass transition T_g versus film thickness for free standing PS films with two different molecular weights. The experiments were carried out using Brillouin light scattering and ellipsometry. After Dalnoki-Veress *et al* [18] with permission.

extremely important to our understanding of behaviour at the nanoscale, has the potential for pitfalls due to the film creation process. These effects have been little investigated in a systematic way for ultrathin films.

3.2. Pseudo-thermodynamic and thermodynamic measurements on thin polymer films

In pseudo-thermodynamic measurements, the film properties have been investigated with two surfaces, one free surface and one constrained surface or both surfaces constrained. In figure 20 we show literature data reported by Forrest and Dalnoki-Veress [193] on the glass transition for supported thin polymer films (polystyrene) as a function of the film thickness. The results are those obtained by many research groups using different techniques [17, 97, 93, 226]. The figure shows a decrease of the glass transition as the thickness of the PS film increases. Figure 21 shows the results reported by Dutcher and co-workers [18] for the T_g of free standing films of PS using ellipsometry and Brillouin light scattering where a dramatic decrease in the glass transition of polystyrene was observed. The details of the results shown in figures 20 and 21 as well as the experimental techniques used to perform the experiments are discussed below. In the following section we discuss the results reported using the pseudo-thermodynamic and thermodynamic measurements on both supported and free standing thin polymer films. What we mean here by free standing films is that the films are not constrained (i.e., between two physical hard walls) and, thus, there are no interactions between a substrate and the film. We do note that the 'free' surface of such films is a thermodynamically 'hard' wall in the sense that the polymer is repelled by the free surface.

3.2.1. Ellipsometry, reflectivity and positron annihilation measurements of T_g for films constrained to substrates. Ellipsometry is among the first techniques that were used to investigate the dependence of the glass transition temperature on the thickness of polymer films [96, 97]. In this technique, the quantity measured is the ellipticity induced upon the reflection of polarized light from a bare or film-covered surface. The glass transition of the film is determined by measuring the temperature dependence of the refractive index or thickness of the film.

There are many reports describing measurement of the glass transition in supported thin polymer films. Using ellipsometry, Keddie *et al* [97] performed the first measurement of T_g for thin polystyrene films constrained to substrates. In that work, a reduced T_g, compared to the bulk one, was reported [97]. Keddie *et al* [19, 226], Dutcher and co-workers [17] and Kawana and Jones [197, 198] have performed measurements on the change in T_g for thin polymer films as a function of the thickness in this way. We have shown in figures 19(a) and (b) typical data obtained by ellipsometry for supported PS films [97]. The measurements were performed after annealing the film above the bulk glass transition for 1 h and then the cooling and reheating steps were performed at constant rate. Keddie *et al* [97] suggested that the decrease in T_g for $h < 40$ nm was caused by the existence of a liquid-like layer at the polymer–air interface accompanied by, also, effects of the interaction with the substrate. The authors did not observe a molecular weight dependence of the depression of T_g in supported PS films. Keddie *et al* [19] also reported results for supported thin PMMA films where an increase and decrease in the glass transition were observed. The authors suggested that the change in the glass transition as the thickness decreases in PMMA films arises due to the nature of the constraining substrate and its interaction with the polymer. For PMMA on silicon wafers with the native oxide layer left in place, the measured T_g value was observed to increase with decreasing film thickness whereas a decrease in T_g was observed for PMMA on a gold-coated silicon surface. Keddie *et al* [19] suggested that not only can the interaction between the polymer and the substrate affect the T_g measurements but also the treatment of the substrate can have an important role in the T_g behaviour in supported thin polymer films.

Prucker *et al* [233] reported results for thin PMMA films supported on a hydrophobic substrate (treated substrate) using an optical waveguide spectroscopy technique. The results showed a lowered T_g as the film thickness decreases [233]. Results reported by Kawana and Jones [197, 198] for supported PS films using ellipsometry showed results similar to those observed previously by Keddie *et al* [19]. Similar ellipsometric measurements reported by Zin and co-workers have also shown reductions in T_g for thin poly(methyl styrene) and polysulfone [234] as well as for thin PS/PMMA and poly(2-vinyl pyridine-co-styrene) films supported on substrates [235]. Ellipsometric measurements performed by de Pablo and co-workers on supported thin poly(4-hydroxystyrene) films [218] show an increase or decrease in T_g relative to the bulk that depends on the type of the substrate and the surface energy of the substrate. In these studies, the effect occurs only for film thicknesses of less than 50 nm. Experimental results reported by Grohens and co-workers [112, 225] for supported isotactic and syndiotactic PMMA films showed an important effect of the molecular architecture on the glass transition in thin films. The T_g for the spin coated isotactic PMMA was found to increase for thicknesses lower than 100 nm whereas a depression of the T_g was reported for the syndiotactic PMMA under the same conditions. The authors concluded that the modification of chain packing in the confined state is responsible for the change in T_g reported in their work [112, 225]. Roth and Dutcher reported results from the ellipsometric measurements of the glass transition for thin atactic PMMA supported on two different substrates: a native oxide layer of silicon (Si) and gold-covered Si [195]. The authors found that for films supported on either substrate, the glass transition decreases with decreasing film thickness which is not consistent with the results reported by Keddie *et al* on the same material [19].

Forrest *et al* [17] reported results from ellipsometric measurements on supported thin PS films with two molecular weights: 767×10^3 and 2240×10^3 g mol^{-1}. In that work, the sample was heated in air to 30 K above the bulk glass transition and held for 12–20 h to erase prior histories of the material. After this equilibration period, the temperature was lowered at 1 K min^{-1} while recording the measured ellipsometric properties. The results showed a decrease in T_g with decreasing film thickness while no molecular weight dependence was observed [17]. The interaction between the substrate and the polymer was interpreted as being the cause of the decrease in T_g. Recent measurements of the glass transition in block copolymers on substrates using spectroscopic ellipsometry also show different results depending on the interaction with the substrate [227]. The copolymers used by Pham and Green [227] were PS and tetramethylbisphenol-A polycarbonate (TMPC). The glass transition of TMPC was found to increase with decreasing film thickness; this was due to the strong interaction with the substrate. In the case of PS/TMPC with 50% and 70% of TMPC, the glass transition decreased with decreasing film thickness. The authors used a model based on a free volume theory [237] to explain the decrease in T_g observed in the supported PS/TMPC films.

Using a local thermal analysis technique, de Pablo and co-workers studied the change in the glass transition for thin PS and PMMA films on polar and non-polar substrates [101]. The results reported in that work were in agreement with those observed by Keddie *et al* for the same materials using ellipsometry [19, 97].

Another method with which to measure the film thickness is the x-ray reflectivity approach. The reflectivity measurements can be used to probe the thermal expansion and thus measure the glass transition temperature in thin films [95]. The film thickness determination is not convoluted with the film density through the index of refraction. Therefore, the x-ray reflectivity technique gives better determination of the film thickness than that determined by ellipsometry. Orts *et al* [95] were among the first to use x-ray reflectivity to measure the thermal expansion in thin polymer films. The samples were polystyrenes supported on silicon. The sample was first annealed for 1 h at 90 °C and then the x-ray reflectivity scan started at 30 °C. In that work, contractions of the thin films below the glass transition (negative coefficient of thermal expansion) were observed and an indication of a decrease in T_g relative to the bulk one was qualitatively reported. X-ray reflectivity experiments performed later by the same group [20] for monodisperse polystyrene on hydrogen terminated silicon surfaces showed a dramatic increase in the glass transition of the films. According to the authors, these results indicated that the substrate has a major effect on the change in T_g for supported films where the experiments were carried out under vacuum. In figure 22 we show the thermal expansion (thickness versus temperature) of the supported PS films for different thicknesses as reported by Wallace *et al* using the x-ray reflectivity technique [20]. The solid lines in each curve represent the linear thermal expansion of the bulk material and the dotted lines represent the

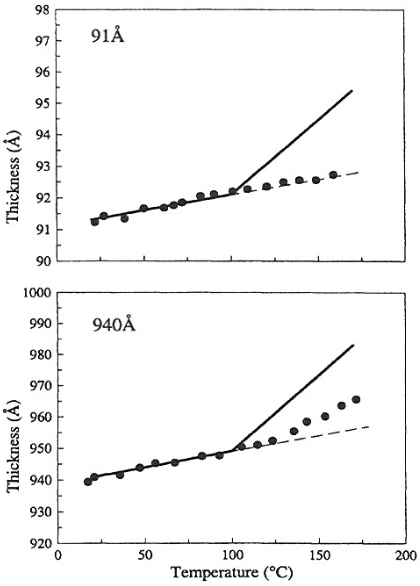

Figure 22. Temperature versus thickness plots for four different initial film PS thicknesses. The solid lines correspond to predictions made solely from extrapolation from bulk behaviour. The break in the solid lines corresponds to the bulk glass transition temperature of 100 °C. Uncertainty is expressed by the scatter in the data points. After Wallace *et al* [20] with permission.

thermal expansion of the thin films where now a glass transition is well defined. The figure shows that the thermal expansion of thin PS films in the glassy state is independent of the film thickness, whereas for that of the rubbery state, the thermal expansion is found to decrease with decreasing film thickness. In addition, figure 22 shows that the glass transition temperature in the supported PS films for all thicknesses greater than 9.1 nm appears to be greater than the bulk value of approximately 100 °C. Although the observation by Wallace *et al* [20] of loss in T_g in the 9.1 nm supported PS film is interesting, their observation and interpretation of an increased T_g relative to the bulk value for the 47.9 nm and greater thickness films are questionable. Clear examination of figure 22 suggests that, in fact, there may be a temperature measurement or other issue in these experiments because the T_g is virtually independent of the film thickness from 47.9 to 198.8 nm and is 20–25 °C higher than the bulk T_g normally reported for PS. Because 200 nm is well above the thickness where the bulk T_g is normally recorded in supported polystyrene films (see figure 20), it appears that these data are in error and were misinterpreted. Forrest and Dalnoki-Veress have remarked on this as well [194].

In addition to the above techniques used to investigate the confinement effects on the glass transition for polymers confined to thin films, positron annihilation lifetime spectroscopy (PALS) has been used to study the thermal expansion coefficients and T_g for thin polymer films [99, 100]. This technique has been described elsewhere [88, 100]. The PALS technique was used by DiMaggio *et al* to measure the glass transition in supported thin PS [99]. The results showed a decrease in the glass transition with decreasing film thickness, which is consistent with results reported using other techniques [17, 97, 93, 226]. The results also showed that the thermal expansion coefficient of the PS films in the glassy state was independent of the film thickness and that in the liquid state was found to decrease with decreasing film thicknesses [99]. This is consistent with the x-ray reflectivity data reported by Wallace *et al* [20] but not in agreement with the ellipsometric results observed by Keddie *et al* [97]. Also, positron annihilation lifetime spectroscopy (PALS) has been used to probe the near surface region of thin PS films [100]. In that work, a surface glass transition was found to be the same as the bulk glass transition of PS [100]. Another PALS study by Jean *et al* [229] did find a significant surface effect. The surface T_g values were measured as a function of the surface depth probed and found to decrease from the bulk value for a probe depth larger than 40 nm to a value 57 K less than the bulk T_g when a surface region of 5 nm was probed. The disagreement between the two results is not understood.

In addition to the pseudo-thermodynamic methods used to study the glass transition in thin polymer films, a novel thermodynamic approach was recently used to measure T_g for thin films. Efremov *et al* [106] developed a differential scanning nanocalorimeter to investigate size effects on the thermodynamic properties of supported ultrathin films. In that technique, very high heating rates from 20 to 200 K ms^{-1} and a cooling rate of 1–2 K ms^{-1} were used to allow the nanocalorimeter to operate under near adiabatic conditions. Efremov *et al* [239] used three thin polymer films of PS, PMMA and poly(2-vinyl pyridine) PVP of different molecular weights. The heat capacities $C_P(T)$ of the films were measured upon reheating at a heating rate of 30–40 K ms^{-1}. The authors observed a clear glass transition for films with thicknesses from 1 to 3 nm [239]. In that work, no significant change in the glass transition for PS, PMMA and PVP for thicknesses from 200 nm down to 3 nm was reported. In addition, no significant effect of molecular weight on T_g was observed [239]. However, the results for all polymers studied showed both broadening and loss of transition contrast effects with decreasing film thicknesses. The authors suggested that the absence of confinement or size effects on T_g for the films could be related to the high heating and cooling rates used in the experiments [239]. We add that recent work by Forrest on constrained polystyrene films suggests that rate effects may be important [283]. The observations are surprising, however, as the effect of rate is dramatically different from that for bulk materials.

3.2.2. Pseudo-thermodynamic measurements of T_g in free standing films. In addition to the pseudo-thermodynamic and thermodynamic measurements of T_g discussed above, pseudo-thermodynamic measurements have been widely employed to study confinement effects in free standing films. Ellipsometric measurements performed by Sharp and Forrest [203] have recently shown that the glass transition of thin, free standing films of PMMA is only depressed by 10 K for thicknesses in the region of 40 nm. This is different from what is observed for free standing PS films where a reduction of 40 K in T_g was reported for similar thickness films [18]. Hence, details of molecular chemistry and the molecular architecture can have a strong influence on the T_g depression in thin polymer films.

Unlike supported films, there is evidence of a strong molecular weight effect on the glass transition of free standing thin PS films [17, 196, 201]. Significant effects have been reported for molecular weights from approximately 5×10^5 to over 2×10^6 g mol^{-1} in PS films [201]. For example, the glass transition for thin PS films having thicknesses $h \leqslant R_{EE}$ (R_{EE} being the end-to-end distance of the polymer molecule) was found to decrease dramatically with decreasing film thickness and also molecular weight. This is seen in figure 21 where increases in the slope of T_g versus h and in the initial film thickness, h_0, with increasing M_w are observed. On the other hand, the T_g depression observed in supported thin PS films did not show a significant dependence of the T_g reduction on molecular weight [17]. Also, in free standing polymer films, this effect depends on the molecular structure of the polymer. For example, for free standing films of both PS and PMMA having the same molecular weights, decreases in T_g were reported. However, the magnitude of the T_g depression and the slope of T_g versus h were higher for PS than for PMMA [196].

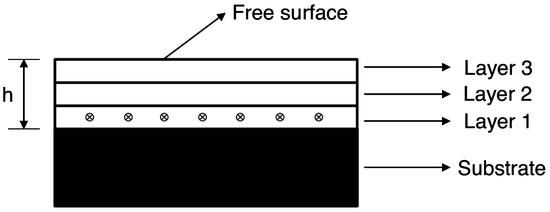

Figure 23. A schematic representation of the multilayer film used by Ellison and Torkelson [102–104] in fluorescence spectroscopy experiments. h is the film thickness; the dye molecules can be inserted in any layer between the free surface and the substrate.

Dalnoki-Veress *et al* [18] reported results for thin free standing PS films using transmission ellipsometry. In that work, a dramatic decrease in the glass transition as the film thickness decreased was reported. The authors observed a molecular weight dependence of the T_g reduction and this demonstrated that chain confinement effects are important for understanding the observed behaviour [18]. In the case of lower molecular weights, it was suggested that the finite size effects are dominant in determining the cause of the change in T_g [18], but that molecular weight or chain effects become dominant at high molecular weights.

Another technique used to study the behaviour of free standing films is Brillouin light scattering (BLS) investigation. In BLS experiments, the measured quantity is the frequency shift of light, which is inelastically scattered from thermally excited acoustic phonons. Dutcher and co-workers [16] reported the first measurements of the glass transition in free standing thin polymer films using the BLS technique. The results reported in that work showed a large reduction in T_g compared to that reported for supported PS films. For example, the measured T_g value for a 29 nm thick film was reduced by more than 65 K relative to the bulk one. In addition, a molecular weight dependence of T_g in thin PS films was observed. This technique was also used by Dutcher and co-workers to study the high frequency (elastic) properties of polystyrene [89] and of polystyrene/polyisoprene multilayered thin films [90]. The results showed that the Brillouin frequency response of thin polymer layers is similar to that of the bulk materials [90]. The authors concluded that the high frequency elasticity remains unchanged even when the polymer is confined to ultrathin films [90]. The BLS technique can also be used for supported films but the laser heating of the substrate makes this technique difficult to use for reliable T_g measurements [17, 88].

3.2.3. T_g gradient in thin polymer films. The above results on thin polymer films have often been interpreted in terms of layer models. This is equivalent to a gradient in T_g through the films where the local T_g varies with the distance from the free surface. The first direct measurements of a T_g gradient in thin films come from Ellison and Torkelson [102–104] who used fluorescence measurements to investigate the T_g gradient in PS systems. The authors [102–104] applied a fluorescent probe method [284] to multilayer films incorporating thin layers in which dye-labelled molecules are placed at known positions in the film. Figure 23 shows a schematic representation of the multilayer films.

In this technique, fluorescence intensity is measured as a function of density and the measurement probes a pseudo-thermodynamic aspect of the T_g behaviour [102–104]. In figure 24, we show the temperature dependence of the fluorescence intensity of pyrene-labelled PS. The intersection of straight lines of the glassy and liquid states of the pyrene fluorescence intensity is interpreted as the glass transition of the PS films. The figure shows that the glass transition temperature of supported PS films decreases from 370 to 346 K as the film thickness

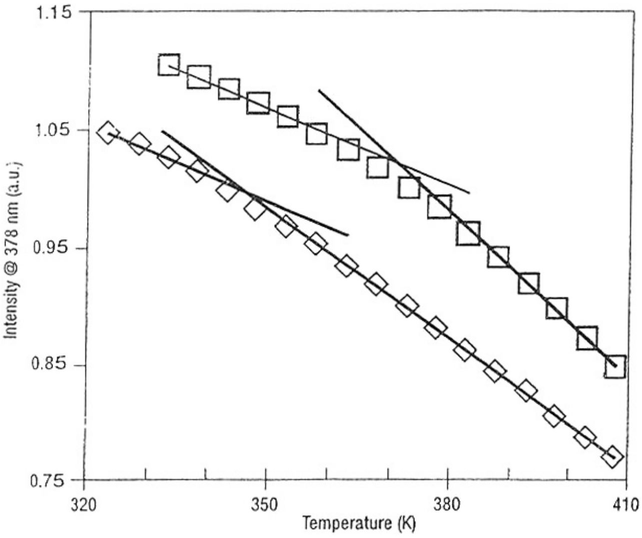

Figure 24. The temperature dependence of the fluorescence for pyrene-labelled PS single-layer films: 545 nm thick (squares) and 17 nm thick (diamonds). After Ellison and Torkelson [103] with permission.

decreases from 545 to 17 nm [103]. The study of Ellison and Torkelson addressed the effect of confinement on the distribution of T_g (gradient in T_g) with distance from the free surface. The authors demonstrated that the free surface and substrate confinement are both important: T_g decreases near a free surface and this decrease can extend over a distance of 10–14 nm from the free surface, but the magnitude of the reduction depends on the overall thickness of the film [102, 104]. In very thin films, the reduction in T_g near the free surface is less than that observed in thicker films. This was the first measurement of the distribution of a glass transition across thin PS films, which indicates the existence of a gradient in T_g for the thin films.

3.3. Dynamic measurements on thin polymer films

While there are multiple techniques for studying the pseudo-thermodynamic glass transition in thin films, only a few experimental studies have been reported on the relaxation dynamics in thin polymer films [107–112, 243–256]. This is because of the difficulty of measuring the relaxation dynamics of the small amounts of material in a thin film (typically $<10\ \mu$g).

The first direct dynamic measurement in thin polymer films was reported by Torkelson and co-workers on the relaxation dynamics for the special case of isobutyl methacrylate copolymerized with chromophore probe molecules [113]. In that work, the relaxation experiments were carried out above and below the bulk glass transition of the copolymer using second-harmonic generation (SHG) [113]. This technique measures the second-order susceptibility directly in the time domain and the relaxation response in the thin films was obtained over nine logarithmic decades in time. After the spin coating process, the films were dried under vacuum above the bulk T_g for 12 h. The film thicknesses of the copolymer films were between 7 and 1000 nm. The relation between the average relaxation times τ_{avg} and the temperature was similar for all films, indicating that the T_g value was unchanged. However, the authors observed that the relaxation mechanism for ultrathin films was different from that of the bulk material [113]. For example, for the experiments performed between

80 and 120 °C and using the KWW function to fit the dynamic data, it was observed that the average β_{KWW} value for thick films (>190 nm) was 0.13 higher than that for thin films (<90 nm); e.g. for the experiments performed between 80 and 120 °C, the β_{KWW} values of 520 nm thick film were between 0.55 and 0.7. For film thicknesses of 135 and 190 nm, the β values lay between these two with $\beta_{\mathrm{KWW}}(190\ \mathrm{nm}) \geqslant \beta_{\mathrm{KWW}}(135\ \mathrm{nm})$, indicating a transition from ultrathin film behaviour with a very broad relaxation distribution to thin films having bulk polymer properties [113].

Forrest *et al* [246] have studied the relaxation dynamics in thin free standing films using photon correlation spectroscopy (PCS) and quartz crystal microbalance (QCM) techniques. In the PCS technique, the intensity autocorrelation function of light is measured. The glass transition temperature for the free standing PS films used in the experiments was determined as the temperature at which the films had a relaxation time of 100 s and was found to decrease by 70 K from the bulk value due to an increase in the segmental mobility for the PCS measurements on a 22 nm thick film. Because the KWW β values were found to be the same as those for bulk PS, this indicates a shift in the entire relaxation function to shorter times as film thickness decreases [246]. This result is not consistent with a gradient in the glass transition. Forrest *et al* [246] also reported results from quartz crystal microbalance measurements of the adhesion of small particles to thin PS films. These results, which reflect the polymer film dynamics, indicated a reduced T_g as the PS film thickness decreased, but not nearly as strongly as did the PCS measurements.

Fukao and Miyamoto [107] performed dielectric measurements on supported thin PS films. The temperature T_α, corresponding to the peak in the dielectric loss of the α process, was determined as a function of the film thickness. The results are shown in figure 25 where the peak frequency $f_{\max}$, which corresponds to the inverse of the relaxation time τ_α for the α process, is plotted as a function of the inverse temperature [107]. It is seen in the figure that the values of τ_α for the films with thickness from 33 to 194 nm fall on the same curve, which is described by the VFT equation. When the film thickness decreased to 14 nm, the relaxation time τ_α became shorter than for thicker films, which indicates a decrease in T_α. The relaxation function for the α process was obtained using the observed frequency dependence of the peak profile of the dielectric loss. The KWW β parameter was found to decrease as the film thickness decreases, which indicates that the distribution of relaxation times for the α process broadens with decreasing film thickness [107].

In addition to the isothermal dielectric measurements, Fukao and Miyamoto performed experiments on thin PS films at constant frequency and measured the dielectric loss as a function of temperature during the cooling process (vitrification) [107]. For a PS film thickness of 9 nm, a second relaxation process, α_1, was observed at lower temperatures. This process disappeared for a film thickness of 105 nm. In addition, the α_1 process was more pronounced at higher frequencies than that observed at a lower frequency of 100 Hz. We note here that the experiments performed by Fukao and Miyamoto under isochronal conditions (vitrification and devitrification) are similar to the TSDC experiments performed by Pissis *et al* [85, 86, 163] to investigate the size effects on small molecules in nanopores.

Fukao and Miyamoto [108] also reported on the dielectric behaviour of thin PS films having molecular weights of 2.8×10^5 and 6.7×10^6. They found that T_g decreased with decreasing film thickness. The glass transition T_g and the Vogel temperature T_0 were found to depend on the molecular weight of the thin film. In that work, Fukao and Miyamoto analysed their data in terms of the fragility concept developed by Angell [73]. The change in the relaxation times with PS film thicknesses of two different molecular weights is shown in figures 26(a) and (b). The figure shows the behaviour of different thin PS films in terms of relaxation time as a function of T_g/T (the fragility plot). It can be seen in figure 26 that, for the PS films of

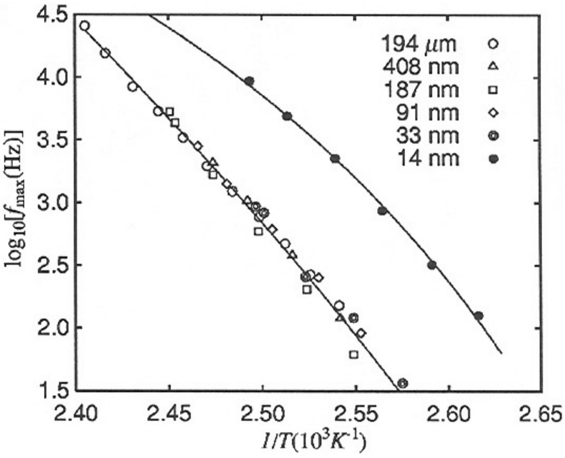

Figure 25. Peak frequency of dielectric loss due to the α relaxation process as a function of the inverse of temperature for thin films with various thicknesses. After Fukao *et al* [107] with permission.

different molecular weights, the relaxation times at the same values of T_g/T become longer as the thickness decreases. However, as shown in figure 27 the Vogel temperature T_0 (and hence T_g) decreases as the film thickness decreases. In figure 28, the activation energy parameter (i.e. Vogel parameter) of the films is represented by the symbol U instead of B (see equation (2)) and is seen to increase (in figure 28 $1/U$ is plotted) with decreasing film thickness, i.e., the thin PS films become more fragile as the thickness decreases. In addition, the VFT parameters, B and T_0 [153–155], vary with film thickness; the Vogel temperature T_0 decreases with decreasing film thickness whereas the B parameter increases with decreasing film thickness [108]. According to the authors, this means that the temperature dependence of the average relaxation times has an increasingly Arrhenius dependence as the thickness decreases. We remark here that Kremer and co-workers [182] showed in their dielectric experiments on small molecules confined in nanopores that the temperature dependence of the relaxation times of the α process was described by the Arrhenius law for ethylene glycol confined in zeolites with pore size less than 0.5 nm. Also, in the Richert and co-workers work, different VFT behaviours were observed for the confined PPG in nanopores [143, 171].

The dielectric properties for thin syndiotactic poly(methyl methacrylate) (s-PMMA) and PVAc films have also been investigated in the frequency range from 0.1 to 1 MHz at temperatures between 263 and 423 K [109]. For both the s-PMMA and PVAc, a broadening of the distribution of the relaxation times was observed and this broadening was more pronounced for the α process than for the β process. The broadening increases with decreasing film thickness indicating a different dynamics for confined thin films to that for the bulk material [109].

Kremer and co-workers [111] performed dielectric measurements for thin films of isotactic (i-PMMA) of two molecular weights sandwiched between aluminium electrodes. We remark here that the commercial PMMA used in research and industry is a mostly syndiotactic PMMA, which has a higher T_g than isotactic PMMA. Also, the glass transition of the thin i-PMMA films was determined by temperature-dependent ellipsometric measurements of the thickness of films prepared on silica. The dynamic results showed a decrease in the glass transition for thin i-PMMA films and a broadening of the relaxation time distribution. Also, a decrease of the dielectric strength with decreasing film thickness was reported [111]. In

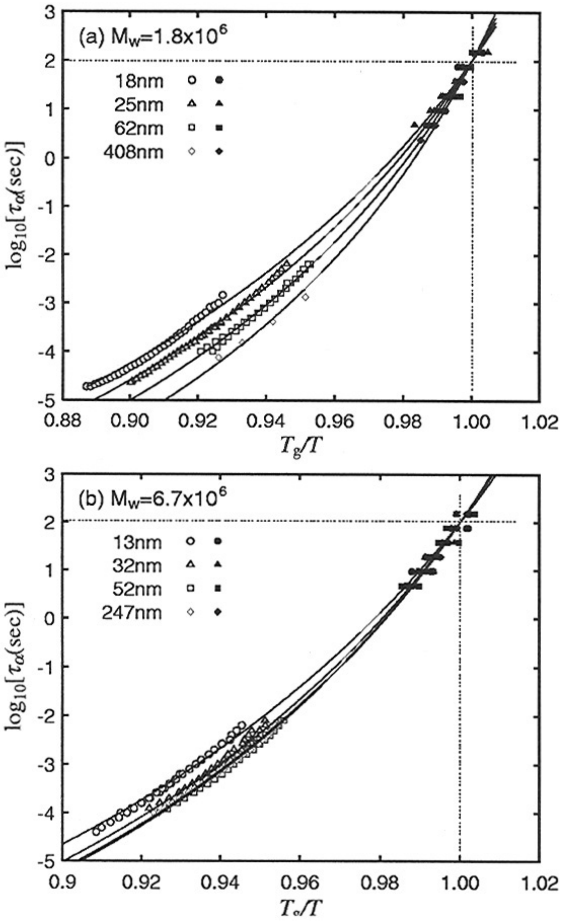

Figure 26. Relaxation times versus the inverse of the reduced temperature T_g/T (fragility plot) for different thicknesses of thin PS films of two different molecular weights. After Fukao and Miyamoto [108] with permission.

contrast, the ellipsometric measurements for the same material showed an increase in the glass transition with decreasing film thickness (e.g., T_g increases by 70 K for film thickness of 20 nm) [111]. The contradictory results reported on T_g for i-PMMA films were attributed to the interaction between the films and the substrate: while the polymer is embedded in aluminium for dielectric measurements, it forms interfaces with the substrate and air/interface in the case of the ellipsometric measurements [111].

In addition to being used to study confinement effects on the α relaxation process for thin films, dielectric spectroscopy has also been used to study the secondary β relaxation [109–111, 255]. Fukao *et al* [109] found that the dynamics of the β relaxation in a-PMMA became faster with decreasing film thicknesses. The authors suggested that there is a strong correlation between the α and β processes despite the fact that these relaxations are located at different temperatures and different frequencies [109]. Dutcher and co-workers [255] observed in the case of thin isotactic PMMA that there was a strong correlation between the relaxation times for both α and β processes. It was also found that the β relaxation of i-PMMA became faster for thicknesses below 10 nm. However, in the Kremer and co-workers work, the β relaxation

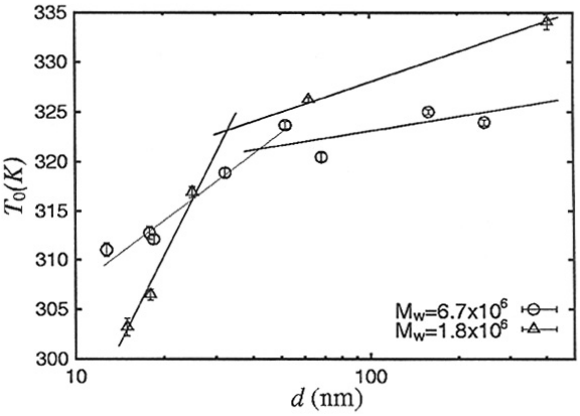

Figure 27. The thickness dependence of the Vogel temperature T_0 for thin films of a-PS of two different molecular weights. After Fukao and Miyamoto [108] with permission.

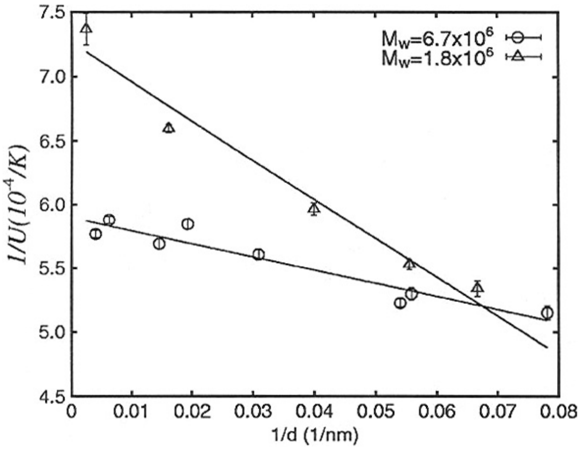

Figure 28. The dependence of $1/U$ or $(U = B)$ the activation energy parameter in the VFT expression in equation (2) on film thickness for thin PS films. After Fukao and Miyamoto [108] with permission.

for PMMA was found to be independent of the film thickness whereas the dynamics of the α relaxation became faster with decreasing film thickness [111].

3.4. Mechanical measurements on thin polymer films

In addition to the pseudo-thermodynamic and dynamic measurements reported for the glass transition and relaxation dynamics in thin polymer films, mechanical measurements of the thermoviscoelastic response have been performed to investigate confinement effects on the T_g in thin polymer films [117–121]. The experiments have been performed using dewetting dynamics methods [117–120] and by atomic force microscopy (AFM) [121].

Reiter reported the first experiments on thin PS films using dewetting dynamics. The method provides indirect dynamic measurements of the glass transition temperature of thin polymer films [117–119]. This technique also provides some insight into the interactions between the substrate and the thin film. In order for dewetting of the thin polymer film to occur, the mobility of the film must be high enough, i.e. the dewetting does not occur in the glassy state but above the glass transition temperature. Hence, the dewetting process indicates that the molecules are above the T_g for the polymer where the viscosity may be a function of the film thickness. In that work, the dewetting of PS films supported on a glass substrate was investigated as a function of the film thickness and temperature [117–119]. The thicknesses of the PS films used were less than the end-to-end distance (R_{EE}) of the molecules. The results showed a decrease in the glass transition with a decrease in film thickness. Reiter suggested that the shift in T_g was due to the decrease in density of the thin films. In order to confirm this, direct measurements of the density in thin films, as a function of film thickness, need to be performed.

Remark here that if the density were the cause of the T_g reduction observed in thin polymer films, then a high specific volume or density changes of the materials would occur [25, 26]. We note here that for polystyrene, the change in the bulk T_g with hydrostatic pressure is approximately 0.29 K MPa^{-1} [285]. For example, the hydrostatic pressure corresponding to the change of 65 K observed in free standing thin PS films is approximately 250 MPa, which requires a volume change or density change of 13% (i.e., this would be 25 MPa or 1.3% volume change for 6.5 °C change in temperature). Wallace and co-workers [257] have performed reflectivity experiments to measure the density for thin PS films supported on silicon substrates. The film thicknesses were between 6.5 and 79 nm. In that work, no significant change in the density with changing film thicknesses was observed [257]. For all samples, the densities were close to the bulk density where the relative uncertainty in the density measurement was of the order of 1%–4%.

Another approach for studying the rheological and mechanical properties in thin polymer films is the nanobubble inflation technique used recently by O'Connell and McKenna [121]. Absolute (as opposed to relative) values of the biaxial creep compliance can be measured by this technique by applying a relatively low pressure across a free standing thin polymer film that has been deposited on a cylindrical through-channel in a silicon nitride wafer. The bubble size is monitored as a function of time with an AFM. O'Connell and McKenna measured the response of films of poly(vinyl acetate) (PVAc) having thicknesses as small as 27.5 nm and over temperatures spanning the glass transition of the bulk material. The results were compared with those reported by Plazek for PVAc bulk materials [286] and a reduction in T_g no greater than 3 °C at the film thickness of 27.5 nm was observed. These results are significantly different from those described previously for thin polystyrene films where a decrease of 60 K in T_g was observed at similar thicknesses [201]. This suggests that chemical structure may play an important role in the effects of size and confinement on the glass transition and associated dynamics. Interestingly, O'Connell and McKenna [121] also reported a dramatic stiffening of the films in the rubbery plateau (entanglement) response that is not at present understood.

3.5. Indirect measurements of dynamics in thin polymer films

Indirect probes of the dynamics in thin polymer films are hole growth [116, 193, 287] and lateral force microscopy [105]. In these experiments, the chain mobilities of thin polymer films are probed to provide insights into the change in glass transition of the film.

3.5.1. Hole growth and probe microscopy measurements. The hole growth approach has been employed to investigate the molecular mobility in thin polymer films [116, 193, 287]. In this technique, upon heating a thin film to above the bulk glass transition temperature, holes start to form and grow when mobility is sufficient for the entire chain to move perpendicular to the plane of the film [195]. Hence, the measurement of the mobility in a thin polymer film is a direct probe of the thermal stability of the film. The thermal instability in supported films can cause the dewetting of the film [117–119], whereas in free standing films, rupture or hole growth can occur [116, 193, 288, 289]. Using optical microscopy, Dalnoki-Veress *et al* reported on the formation and growth of holes in free standing thin PS films [193]. The experiments were carried out at 115 °C (18 °C above the bulk T_g) for film thicknesses between 97 and 372 nm. In that work, the hole radius R was found to increase exponentially with time while the growth rate of the holes increased with increasing film thickness. In addition, the film viscosity decreased with increasing shear strain rate, i.e., shear thinning occurred. The experiments performed by Dalnoki-Veress *et al* [193] did not give a clear indication of the change in T_g in free standing PS films, though it provided a probe of the viscous behaviour in the non-linear high strain rate regime. More recently, Roth *et al* have reported results on hole formation for free standing PS films [287]. The experiments were carried out at different temperatures (below and above T_g) and different film thicknesses using a differential pressure apparatus to investigate confinement effects on the glass temperature in free standing films [287]. In that work, the characteristic growth time τ for two film thicknesses, 68 and 91 nm, was measured as a function of temperature between 97 and 105 °C. The free standing PS film of thickness 91 nm had the bulk T_g whereas film having a thickness of 68 nm showed a T_g reduction of 30 °C [287]. In addition, the results reported in the Roth *et al* work showed that the characteristic growth time τ was found to decrease monotonically with increasing temperature. For example, for film thickness of 68 nm, the results at 100 °C showed a factor of 3.8 decrease in τ compared to what was observed for the 91 nm thick PS films. The authors interpreted their results in terms of shear thinning where the viscosity η of the film decreases with increasing shear strain rate $d\gamma/dt$ (i.e. the relationship between η and $d\gamma/dt$ is described by a power law) [287].

Another probe technique used to study the viscoelastic behaviour in thin polymer films is scanning probe microscopy (SPM). In this technique, the friction and the adhesion properties are studied as a function of temperature, frequency and load force on the SPM tip [290]. Using lateral (shear) force microscopy (SFM), Sokolov and co-workers have studied confinement effects on the glass transition in supported and free standing thin polymer films [105]. In that work, no change in T_g was observed for free standing PS films and the glass temperature for supported thin PS films was found to be independent of film thicknesses that are higher than 20 nm [105]. However, the PS films supported on silicon substrate showed a slight increase in T_g of 5 K for a lower thickness ($h = 17$ nm). In the SPM technique, the mechanical interaction between the tip and the viscoelastic surface can have an impact on the interpretation of the results reported on the mobility near surfaces. In addition, the results are not readily interpreted because of contact mechanics [105] issues and caution needs to be exercised with such complicated mechanical measurements.

As seen above, the results reported on thin polymer films showed an agreement about the T_g depression especially in the case of polystyrene supported on silicon or silica substrates reported by Keddie *et al* [19, 97] and by Fukao and co-workers [107–110]. Also, recent reviews [194, 195] have found considerable agreement among many studies of this system (PS), supporting the empirical relation [97]

$$T_g(h) = T_g(\text{bulk}) \left[1 - \left(\frac{A}{h} \right)^{\delta} \right] \tag{4}$$

where h is film thickness, A is a characteristic length (3.2 nm), $d = 1.8$ and $T_g(\text{bulk}) = 374$ K. In addition, many authors [87, 91, 99, 107, 194, 197, 20, 237, 291–293] have studied the T_g depression in thin polymer films using two- or three-layer models [99]. The two-layer model suggests that the free surface layer has enhanced mobility and reduced T_g relative to the rest of the film, which has bulk T_g [107, 194, 197, 200]. The three-layer model has a substrate interface layer that is added to the two-layer model. The third layer may be considered as a dead layer, showing no T_g over the temperature range of interest [99], or may have a higher T_g compared to the bulk which is the case for thin PS film with attractive interactions with the substrate [200]. These models can fit well the data with T_gs that decrease monotonically with decreasing thickness. The three-layer model can describe behaviour in supported thin polymer films where an increase in T_g with decreasing thickness is observed. However, these models do not readily lead to a physical interpretation of the cause of the change in T_g for thin polymer films despite the fact that these models can fit the data well in an empirical sense.

3.6. Surface glass transition

We terminate our examination of T_g in thin films with a brief discussion of surface glass transition effects. It is important to develop a full understanding of the effects of surfaces, particularly free surfaces, on molecular mobility or the apparent glass transition temperature. The reason for this is twofold. First, the observation of reduced T_g in thin polystyrene films is frequently attributed to the effects of the free surface [102–104, 194, 195, 197, 200]. Second, similar to the reports for the changing T_g for thin films and confined liquids, the reports in the literature concerning the behaviour of free surfaces are mixed [102–104, 204–207, 242, 290, 294–317]. For example, Russell and co-workers performed relaxation experiments on polystyrene near a free surface using near edge x-ray absorption fine structure (NEXAFS) spectroscopy [205]. At temperatures below the bulk T_g, the authors did not observe an increase in mobility near the free surface [205]. In a subsequent work, Russell and co-workers, using surface topography measurements by AFM [242], examined the effects of the free surface on the relaxation behaviour for PS films of thickness $>10\ \mu$m. The authors observed a partial relaxation for the free surface at temperatures far below the bulk T_g of PS [242] but complete relaxation only occurred above the bulk T_g.

An example of the difficulty of the determination of the surface T_g can be found in the results and interpretation of experiments in which nanospheres embedding into polystyrene surfaces were studied. In these experiments, the depth of embedment was followed as a function of time and for temperatures from above to below the bulk glass transition. Teichroeb and Forrest [204] interpreted the sphere embedment behaviour as indicative of a surface liquid layer on the PS film. However, a viscoelastic contact mechanics analysis of the same data performed by Hutcheson and McKenna [317] provided a strong reason to conclude that the surface rheological properties were identical to the bulk ones, i.e., there is no significant reduction in the glass transition at the surface.

AFM measurements by Tsui *et al* [295] and surface mechanical measurements by Sokolov and co-workers [105] are consistent with the NEXAFS results of Russell and co-workers [205]. In both works, the surface T_g or mobility was found to be similar to the bulk property. On the other hand, measurements performed by Tanaka and co-workers [294, 316], using lateral force microscopy (LFM) and scanning viscoelasticity microscopy (SVM), showed an enhanced mobility at the free surface of PS films of low molecular weights. Dhinojwala and co-workers [300, 301] performed measurements using an optical birefringence technique and also found an enhanced mobility at the surface that was interpreted as the cause of reduced T_g in the thin films. Finally, results obtained by Tsang *et al* [303, 304], using reflectance difference spectroscopy, showed the existence of an additional (near surface) relaxation at 10 K below T_g. It is clear then that when studying the surface glass transition and mobility near a free surface, the different techniques employed provide contradictory results [204–207, 242, 290, 294–317]. As an additional comment, measurements of the surface mobility can be difficult to compare directly with bulk behaviour ones. For example, orientation of the surface by rubbing may have occurred by yielding of the polymer. Yet, it is known that even in the bulk state, large deformations increase the molecular mobility [318–325]. Hence, simply observing a mobility increase in an oriented surface may not reflect a change in T_g for the surface. In any event, surface T_g reduction is as mixed in understanding as is the reduction of T_g in thin films. How or whether these are related remains the subject of continuing research.

3.7. Discussion of the behaviour of thin polymer films

As seen above, the glass transition in thin polymer films can show different behaviours depending on material and specific experimental technique. The results generally show a dependence of the glass transition on the film thickness below 50–80 nm. The sign of the shift in T_g depends on the interaction between the surface and the substrate. In the case of constrained films where there is a strong interaction between the polymer and the substrate, an increase in T_g with decreasing film thickness was reported for different polymers [19, 226]. In the case of free standing films a decrease in T_g was observed for different polymers [17, 18]. Of particular interest has been the observation that in the case of free standing PS films, a dramatic decrease in T_g can occur. This is not the case for free standing thin films of PMMA where a decrease of only 10 K in T_g was reported for 40 nm films [203] or for PVAc [121] where no change was seen. Furthermore, a significant molecular weight dependence on T_g was also observed for the PS free standing films.

In some cases a loss in the glass transition is observed when films are thin enough [20]. In general, it has been found that the magnitude of the depression of T_g depends on the material studied and can be much less than what has been found for PS using ellipsometry and Brillouin light scattering methods. Apparently, details of molecular chemistry and architecture have a strong influence on the T_g and corresponding dynamics of thin polymer films [122].

An important set of results concerning effects of the material and method used to study T_g for thin polymer films comes from work by Grohens and co-workers [112, 225]. They carried out ellipsometric measurements on s-PMMA and i-PMMA, supported on substrates. The goal of the experiments was first to investigate chemical structure effects on T_g for thin films and second to compare the results with those obtained on the same materials using dielectric measurements performed by Fuako *et al* [107] and by Kremer and co-workers [111]. Figure 29 represents the dynamic and the pseudo-thermodynamic measurements reported on both s-PMMA and i-PMMA [107, 111]. The ellipsometric and dielectric results depicted in figure 29 show that T_g for thin i-PMMA films decreases with decreasing film thickness. In the case of i-PMMA, the ellipsometric results [112] show a large increases in T_g (70 K) for thicknesses lower than 50 nm whereas the dielectric results [111] show a decrease in T_g with decreasing film thickness. This figure also indicates that the tacticity of PMMA samples has a large effect on the shift observed in the glass transition of the thin films. Moreover, the rheological measurements on free standing thin PVAc films reported by O'Connell and McKenna [121] showed no significant decrease in T_g. This is contrary to the high reduction in T_g observed in free standing PS films using other techniques [18, 201].

What is the cause of the decrease in the glass transition observed in thin polymer films? Is it an intrinsic size effect? Is it due to confinement effects or density (sample preparation) effects, surface or interface effects, or another mechanism? On the basis of the results reported on thin polymer films, we have seen that the confinement can increase the mobility in thin polymer films—similar to what is observed for glass forming small molecules in confined geometries. However, it is observed that confinement effects occur at significantly larger system sizes and are much larger than for small molecules.

As discussed above, possible contributions to the reduced T_g in ultrathin films occur in sample preparation. In earlier work, McKenna suggested that the observed reduced T_g of

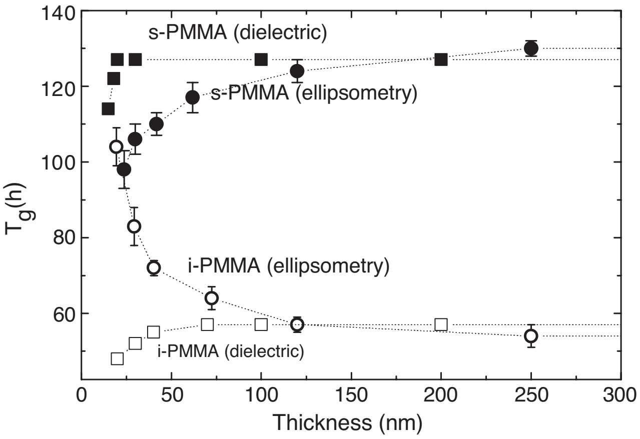

Figure 29. Evolution of $T_g(h)$ as a function of thickness for stereoregular PMMA (35 kg mol^{-1}) investigated by variable temperature ellipsometry (●, ○) and dielectric spectroscopy (■, □). Full and open symbols represent s-PMMA and i-PMMA, respectively. (■ and □ are from [106] and [108] respectively.) After Grohens *et al* [225] with permission.

thin polymer films might be affected by the spin coating process often used to prepare the films [191]. For example, the spin coating process may induce high molecular weight thin polymer films with lower entanglement concentrations than in the bulk [277, 278]. As discussed above, the experiments on thin polymer films are often carried out after annealing the sample above the bulk T_g (T_g + 30 K) for times between 10 and 20 h. This annealing may not be enough for the chains to reach their equilibrium values, especially for high molecular weight polymers [122, 277, 278]. In addition, the spin coating process can cause orientation and elongation of the molecules in the plane of the resulting thin polymer film [273, 274]. On the other hand, the observation of a negative thermal expansion coefficient of thin polymer films, presumably due to chain entropy effects [95, 326], is a clear indication of how complicated the situation for thin polymer films may be.

However, even here the results discussed above are unclear. If there is a large increase in mobility at the surface, as suggested by the multilayer models of T_g in thin films, it is unclear why a thin layer seems to have such a strong effect in, e.g., thin PS films and not in PMMA or PVAc films. In addition, as discussed previously, even the presence of the liquid layer in PS is not universally agreed upon. Ellison and Torkelson's gradient results [102–104] are perhaps the best indicator of such an effect, but direct surface measurements are either controversial [204] or seen to show no effect [317].

4. Computer simulations and modelling of behaviour in confined geometries

In addition to the large amount of work reported on experimental measurements of the glass transition in confined geometries, there has also been considerable effort in theory and computer simulation for both small molecules in nanopores [24, 146, 327–344] and thin polymer films [22, 23, 345–384]. The work that has been done on modelling of nanocomposites has also indicated that there is an effect of confinement or size on the behaviour of these materials [385–395]. The modelling work has been developed both to study the structure and dynamics of confined glassy liquids as well as to explain experimental data for dynamics in confinement. The study of confinement effects on the properties of glass formers by computer simulation or modelling must address several difficulties. The first difficulty is the lack of well defined geometry for the most commonly used nanoporous materials. The second difficulty arises from the combination of several effects (surface, finite size, wall effect, disorder, low dimensionality), which complicate the interpretation. Furthermore, because the computer simulations are almost invariably carried out at high temperature, one may not be addressing glass transition phenomena. This may be particularly true if the T_c of mode coupling theory reflects a true change in dynamics [396–398].

The aim of computer simulations of confined small molecules or polymer thin films is to provide results at the nanoscale that give insights into material behaviour and not to simply reproduce the material behaviour observed experimentally. Generally, the simulations are performed by two methods: molecular dynamics (MD) and Monte Carlo (MC) techniques. However, there are some restrictions that limit the simulations; among these are the size of the confined liquid, the length of the confined chain in polymers and the rate of quenching from higher to lower temperatures. In general, simulating the dynamics of glassy liquids is very challenging because the timescale for motion becomes extremely long (100 s) as the temperature is lowered toward the glass transition; the timescale or the time window represented by the simulations is very short (10^{-8} s). For these reasons, a direct comparison between experimental results and those obtained from computer simulations remains very limited. However, results obtained from computer simulations on the static and dynamic properties of small molecules in confined geometries can provide some insights for the experimentalists [24, 146].

The simulations have focused on the static and dynamic properties of collections of small molecules confined in cylindrical tubes (nanopores) and of short polymer chains confined between walls (slits). These simulations have focused on the effects of density, changing chain length in thin films, wall separation (distance from pore centre), wall potential, wall roughness and temperature. Scheidler *et al* used MD simulations [24] to investigate the relaxation dynamics of a liquid confined in a narrow pore. The authors found that a smooth wall led to a layering of the confined liquid, i.e., its structure was very different from that in the bulk. To avoid this problem, a solid wall having a liquid-like structure similar to that of the confined liquid was chosen. With this choice of wall, the static properties of the confined system (density profile) remained unchanged [345], so only the confinement effect on the dynamics was taken into account. The authors found that the presence of a wall led to strong slowing-down of the dynamics (rough surface) and by measuring the dynamics of the particles as a function of their distance from the wall, a strong increase in the relaxation times was observed as the wall was approached [24]. The results showed a gradient in the dynamic properties of the liquids in nanopores. The properties of the confined liquids in the centre of the pore were the same as those of the bulk whereas a slowing down of the dynamics was observed as the particles approached the wall [24].

In a later paper, Binder and co-workers [146] performed MD simulations to study the dynamics of supercooled liquids close to smooth walls as well as close to rough walls. In that work, very interesting results were reported: in the case of strong interaction with the wall an increase of the relaxation times was observed whereas a decrease in relaxation times was reported for smooth surfaces. Figure 30 shows the results reported by the authors as the relaxation times versus the distance from the wall in the two cases of strong and weak interactions. As the distance from the wall increases, the behaviour of the confined liquid is the same as in the bulk. The figure also shows the gradient in properties of the confined liquid (gradient in T_g). Two important remarks have to be emphasized here. First, in the case where there is an interaction between the particles and the rough surface, the glass transition increases close to the wall whereas T_g bulk is observed far from the wall. Second, a decrease in the glass

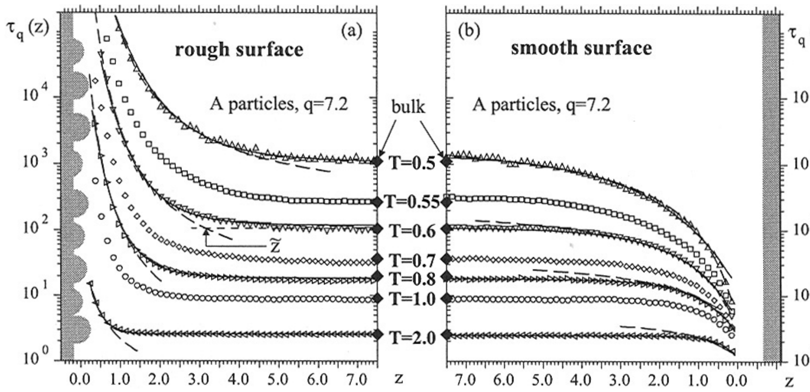

Figure 30. Relaxation time as a function of particle distance from the wall for (a) rough and (b) smooth surfaces at different temperatures. The large diamonds are the bulk values and the long dashed curves and the solid ones show fits obtained by the simulations performed in the Binder and co-workers work [146]. After Binder and co-workers [146] with permission.

transition is observed close to the smooth wall and a bulk glass transition is observed when the distance increases from the wall into the pore centre. It is obvious that a gradient in the glass transition as a function of the distance from the wall is observed. These results are consistent with the experimental results reported on the thermodynamic glass transition from DSC [75], dielectric measurements [77–79, 143, 144, 171], NMR studies [145] and the Torkelson results reported on the glass transition gradient using fluorescence methods [103, 104]. However, we note that the authors did not observe an increase and decrease in T_g for the confined liquid. This is discussed previously and is shown in table 1.

Regarding the prediction of material behaviour in ultrathin polymer films, Mansfield and Theodorou were among the first to study the static and dynamic properties of free standing polypropylene films using molecular dynamics [381]. In that work, the simulations were performed at a temperature lower than the experimental value of T_g. Mansfield and Theodorou found that the mobility was increased for chains that are located a distance from the free surfaces comparable to the end-to-end distance of the molecules (R_{EE}). Baschnagel and co-workers [23, 347, 358] used Monte Carlo (MC) techniques to predict the dynamic properties of polymer chains confined between hard neutral walls. In that work, the polymer chains were observed to be oriented and elongated parallel to the wall. These effects were more pronounced at lower temperatures when the film thickness decreased to of the order of R_{EE} [23, 347, 358]. The orientation can have an important effect on the dynamic behaviour of thin polymer films. Anisotropy in the dynamic properties of confined molecules (and polymer melts) has also been observed in simulations performed at higher temperature [350, 381–383]. Recent MD simulations of thin films by Baschnagel and co-workers have focused on several issues. First, the modelling of free surfaces using a ‘softer’ wall potential ($\sim z^{-9}$, where z is the distance from the wall) than that within the film ($\sim z^{-12}$) [22] resulted in an acceleration of the dynamics next to the wall. Second, the authors studied the decrease with wall separation (film thickness D) of Ngai’s coupling temperature T_c, [396–398] instead of T_g and the Vogel temperature T_0. Both $T_c(D)$ and $T_0(D)$ were found to decrease with the film thickness and T_g was found to decrease with decreasing film thickness [22, 361]. Kim and Yamamoto performed molecular dynamics simulations to examine system finite size effects on the dynamics of supercooled liquids [341]. A significant finite size effect was found in the relaxation at lower temperatures and the cooperative particle motions were strongly suppressed in smaller systems for temperatures below T_c at which the correlation length, ξ, becomes comparable to the system size. The size effects observed in that work were regarded as a natural consequence of the dynamical heterogeneity appearing in supercooled liquids [341]. De Pablo and co-workers [291] used a hard sphere MD technique to simulate both supported and free standing polymer films. An apparent glass transition temperature was identified after a fast cooling sequence by monitoring the film thickness as a function of temperature and also by extrapolating the temperature dependence of the mobility to low temperatures. In that work, an increase in T_g and lower dynamics of the chain close to the wall were observed for an attractive interaction with the wall, whereas a decrease in T_g and enhanced dynamics were observed for a repulsive interaction with the wall and also for free standing films [291]. However, the molecular weight dependence of the T_g depression, observed experimentally for free standing thin polymer films, has not yet been observed in molecular dynamics or Monte Carlo simulations. Hence, the investigations of the effects of molecular weight on the glass transition in free standing films can be considered as a big challenge for the computer simulations. For more details on the simulation work published on the T_g change at the nanometre size scale, we refer the reader to [22–24, 146, 327–382]. A large amount of work has been published in this area and is beyond the scope of this review.

Molecular simulations were extensively used to study interface effects on the mechanical behaviour of nanocomposites filled with nanoparticles [392]. For example, using Monte Carlo simulations to predict the mechanical behaviour in nanocomposites seems useful as regards certain questions concerning the thermodynamics of mixing of nanoparticles and polymer matrices [337, 391]. Picu and Ozmusul performed Monte Carlo simulations in which a filler size effect on the total behaviour of the nanocomposite was observed [392]. In the case where there were no energetic interactions between the polymer matrix and the filler, the overall composite moduli are smaller than those of conventional composites. However, the existence of a strong attractive interaction between the filler and the polymer matrix led to a size effect that was found to be rather weak. In this case, the nanocomposites were slightly stiffer than the equivalent conventional composite [392]. Glotzer and co-workers [390] performed molecular dynamics simulations of an idealized polymer melt surrounding a nanoscopic filler particle and showed that the glass transition temperature of the melt can be shifted to either higher or lower temperatures by changing the interactions between polymer and filler. In that work, a gradual change of the polymer dynamics approaching the filler surface caused the change in the glass transition [390]. Extensive modelling and computer simulation work has been published on the behaviour of nanocomposites and carbon nanotube composites; the details of this topic are beyond of the scope of this work and we refer the reader to [385–395].

5. Theory and models

In addition to the computer simulations cited above, a substantial number of theoretical models have been developed for studying the change in the glass transition of glass forming materials in confined geometries [188, 237, 243, 333, 292, 293, 354–356, 360, 373–375, 378]. Most of these models have been developed in an effort to understand the behaviour in free standing and supported films where different results were reported [16, 18, 105, 120, 193, 201]. In addition, a few theoretical models have been proposed for studying the change in T_g for glass forming small molecules confined in nanopores [188, 293, 399]. Note that prior theoretical efforts have been made to understand the dynamical theories of the liquid–glass transition [400, 401] and the role of free surface on the behaviour of polymers in small particles on droplets [399, 403].

The modelling in thin polymer films focuses on enhanced mobility at the free surface and on the propagation of the increased mobility deeper into the films. However, no one of these theoretical models can account for all the data obtained on thin polymer films (e.g., the dependence of T_g on M_w). For example, Ngai has applied the coupling model [396–398] to thin polymer films [243, 355]. The author proposed two mechanisms to explain the T_g reduction in thin polymer films. The first mechanism operates when the thickness of the film (h) is not higher than the cooperative length scale at T_g for the bulk material. The other suggested mechanism, operative only for high molecular weight thin polymer films, is the induced orientation of the polymer chains parallel to the surfaces when h becomes comparable to R_{EE} for the polymer chains [243, 355]. De Gennes has developed a model based on the reptation and free volume theories to predict the depression of T_g for thin polymer films [292]. The model predicts only 10 K depression of T_g, which is not in agreement with the observation of Forrest and co-workers for free standing PS films [16, 18]. Inspired by the percolation model developed by Hunt [373], Long and Lequeux [237] have recently developed a percolation model incorporating spatial heterogeneity [252, 254] to study the change in T_g observed experimentally in thin polymer films. The model is based on the idea that the bulk glass transition is controlled by the percolation of small domains of slow dynamics. This model also allows the explanation of the heterogeneous nature of the dynamics in the glass transition region. In the case of 2D thin films, the percolation of these small domains at lower temperature is responsible for the decrease in T_g.

On the other hand, Truskett and co-workers have developed an energy landscape based mean field theory for thin films confined between parallel substrates [403, 404]. Using the potential energy landscape approach to investigate the effects of the size of the film and its interactions with the substrate on the equilibrium phase diagram and the glass transition, this model has shown quantitative agreement with the size effects on the glass transition in thin polymer films that have been observed experimentally. In addition, the prediction of the energy landscape model was in agreement with the McCoy and Curro free volume model [293, 354] that is discussed below.

In addition to the models developed to study the behaviour in thin polymer films, several theoretical models have been proposed to address the change in T_g for glass forming small molecules confined in nanopores [188, 293, 354, 399]. Hunt [373] developed a percolation model to characterize the transport properties of strongly disordered liquids. Hunt suggested that below the mode coupling temperature, T_c, the transport properties are fundamentally percolative in character, i.e., inhomogeneous rather than homogeneous [373]. In addition, Hunt established an equation for calculating the change in T_g for small molecules confined in nanopores. He showed that an average of a glass transition over a number of large small domains must correspond to an average barrier height and, therefore, the average glass transition was found to decrease with confinement in nanopores [373]. Sappelt and Jackle [188] have developed a model based on ideas of second-order phase transitions to account for the finite size effect on T_g. This model predicts a reduction and broadening of T_g from size constraints on the ‘correlation length’ defined for the glass. McCoy and Curro [293, 354] proposed a model based on the free volume theory [70–72, 369–372] to predict the glass transition in confined geometries (nanopores). In that model, the shift in T_g for polymers in confined geometries is largely attributed to the inhomogeneous density profile of the liquid [293, 354]. It was assumed that the glass temperature in the inhomogeneous state can be approximated by the T_g for a corresponding homogeneous, bulk polymer, but at a density equal to the average density of the inhomogeneous system. Simple models based on this hypothesis give results that are in agreement with experimental measurements of the glass transition for confined liquids. For example, x-ray reflectivity experiments performed by Yu *et al* [230] have demonstrated that layering over a few molecular diameters exists near the surface in thin liquid films. The theoretical prediction of the model was in agreement with experimental results reported by

Jackson and McKenna on confined liquids [1]. The authors also predicted a decrease in T_g for the confined liquid when the interaction of the molecules with the wall is weak (the wall attraction is weak).

Couchman and Karasz, on the other hand, examined the role of free surfaces in the structure of polymers and discussed the effect of particle size and geometry on the glass transition for a matrix containing an assembly of amorphous domains of macromolecules [399]. The authors treated the non-equilibrium glass transition as a true thermodynamic second-order transition. An increase in T_g as the particle size decreases was predicted. In addition, the authors compared this prediction with that reported by Bares [374] who used a free volume treatment to examine size effects on the glass transition (namely the effect of mixing at the surface of microphase domains embedded in a matrix with a lower glass transition [399]). In that work, for a styrene–isoprene–styrene block copolymer a reduced T_g of 5 K for a 10 nm diameter particle was observed [374].

As discussed above, as implemented by McCoy and Curro [293, 354], the free volume model can explain the results obtained for thin polymer films whereas this is not the case when we try to use the configurational entropy model to explain the data on thin polymer films (polymers are complicated structures, whereas small molecules are simple structures). However, the results reported by Wallace and co-workers on the measurements of film density do not show a decrease in density of the film [258]. Also, the Zorn, Alba-Simionesco, Frick [28, 147, 176, 177] neutron scattering work shows a modest decrease in density as well as an increase in T_g for toluene in nanopores. Hence, the results are not consistent from this perspective.

Each of the theoretical approaches used to explain the change of the glass transition or associated dynamics in confined geometries [237, 243, 293, 356, 373, 399] has its successes but here we do not choose one approach over the others for several reasons.

For example, there are multiple views (concepts) of the glass transition. Among these are, as mentioned above, the thermodynamic view often based on configurational entropy-type models [68, 69]; the free volume-type models are generally seen as kinetic [25, 70–72]; and the cooperativity length concept has been successfully used to describe the temperature dependence of molecular mobilities [158]. Considering the simple argument that entropy decreases upon confinement, one expects from the entropy-type models [68, 69] that the glass transition temperature at the nanometre size scale should increase compared to the bulk T_g. Within the cooperativity framework, the cooperativity length ξ increases with decreasing temperature. Hence, and as proposed by Jackle and co-workers, a shift in T_g to higher temperatures is expected for materials in confined geometries [188, 378]. Others have considered that cooperativity length considerations should lead to a decrease in T_g as size goes down [78, 176].

The various glass transition models, including the configurational entropy [68, 69], the kinetic [70–72] and thermodynamic [405, 406] aspects of the free volume model, the cooperativity length concepts that are related to configurational entropy [158], the more modern consideration of cooperativity length [188, 378] and the percolation model [237, 373], give conflicting expectations for the effect of size or confinement on T_g. Hence, it remains a challenge to the theoreticians to resolve the modelling issue for the glass transition at the nanolength scale and, perhaps, provide a means of reconciling the range of experimental results reported.

6. Summary and conclusions

In this article, we have reviewed confinement and size effects on the properties of small molecules and polymers. We first focused on the first-order thermodynamic melting transition where we showed that, although the Gibbs–Thomson model is widely used to explain the depression of the melting point, T_m, at the nanometre size scale, in fact this model is deficient and further work needs to be done to fully capture size effects on melting behaviour.

The major focus of the review was the behaviour of glass forming liquids and polymers at the nanometre size scale. We discussed the experimental and modelling work that considers changes in T_g for both small molecules confined in nanopores and for thin polymer films. Most of the experimental results show that the glass transition at the nanometre size scale is different from that of the bulk material, though the sign, magnitude and cause are still under discussion. In addition, molecular simulation and modelling work shows similar trends.

Regarding the glass transition for glass forming materials confined in nanopores, we discussed the thermodynamic, pseudo-thermodynamic and dynamic measurements reported in the literature. It is clear that there is a surface effect on the observed changes in the glass transition or its associated dynamics. Less clear is whether or not there is an intrinsic size effect on the T_g at the nanometre size scale. While one of the present authors (GBM) has provided work [122] that supports this position and there are other works in the literature by, e.g., Kremer and co-workers [77–79] and Alba Simionesco and co-workers [28, 147] that also suggest that there is an intrinsic size effect, there is also a considerable amount of work that suggests that the effects of confinement are primarily due to the details of the interactions between the surface of the confining medium and the confined liquid or polymer [24, 143, 144, 146, 171].

For thin polymer films, there is evidence that the interaction between the substrate and the film can play a crucial role in determining the sign of the shift in T_g. In the case of supported thin polymer films, when the interactions are strong, an increase in T_g is observed whereas a depression in T_g occurs for weak interactions. The results discussed for supported thin polymer films have shown that T_g does not depend on the molecular weight of the material. In addition, the fluorescence measurements have shown interesting results on the T_g reduction of thin PS films [102–104]. These experiments have shown a reduced T_g near a free surface, which extends to many layers into the film within 10–14 nm. This has addressed an important issue of confinement effects on the gradient in T_g with distance from the free surface observed in thin PS films [102, 104].

In free standing films, the results have shown a dramatic depression in T_g for PS where the T_g was found to depend on the molecular weight. However, we have seen that different material behaviour was observed using different techniques. This is particularly seen when the magnitudes of the T_g depression in Brillouin light scattering and ellipsometry experiments were compared with the magnitudes observed in hole growth and lateral force microscopy experiments on the same material (PS).

Many fundamental questions concerning the origins of the dependence of the glass transition on the film thickness in ultrathin polymer films remain unsolved. For example, as the temperature varies in ellipsometric experiments, do we measure a true glass transition of the films or do other effects such as an entropic contribution to the film response modify the T_g determined? How do we define a glass transition temperature of a system that is out of equilibrium even above the normal T_g and is also anisotropic due to molecular orientation? Also, how should such a glass transition, if defined properly, be compared with its counterpart for the bulk material? It is known that there is a difference between a calorimetric glass transition T_g and a dynamic T_g as observed in relaxation measurements [25]. It is important that we have to distinguish between the two types of transition when interpreting the results.

The details of molecular chemistry and architecture seem to have a large impact on material behaviour at the nanometre length scale and the reasons for this are not clear. In addition, enthalpic factors (such as interfacial interactions which may increase with temperature) and also entropic influences (such as chain orientations that in extreme cases might lead to negative coefficients of thermal expansion) can significantly contribute to the observed T_g for thin polymer films [93, 242, 273, 274]. Finally, specific interactions have also been reported to be important [348]. The computer simulations by Binder and co-workers suggest that the confining wall's physical or atomic smoothness might also be important [346–348].

It is clear now that there is evidence of a reduced T_g at the nanometre size scale. What is not clear though is whether the T_g reduction is due to an intrinsic size effect, confinement effects, sample preparation or a combination of these effects. Further investigation needs to consider these effects. We emphasize that the field is largely empirically driven. There are many experiments and we feel that most of them are correct and repeatable, but they show a multitude of results. It remains a challenge to build a widely accepted theoretical model that accounts for the total panoply of experimental and computational results.

Acknowledgments

We gratefully acknowledge the financial support of the National Science Foundation under grant no. DMR-0304640. We also thank Lameck Banda and Jian Wang from the Chemical Engineering Department at Texas Tech University for their help in preparing some of the figures in this paper.

References

[1] Jackson C L and McKenna G B 1991 The glass transition of organic liquids confined to pores *J. Non-Cryst. Solids* **131–133** 221

[2] Takahashi A and Yamashita Y 1975 *Copolymers Polyblends and Composites* (*Advances in Chemistry Series* vol 142) ed N A J Platzer (Washington, DC: American Chemical Society) pp 267–87

[3] Wang B and Krause S 1987 Properties of dimethylsiloxane microphases in phase-separated dimethylsiloxane block copolymers *Macromolecules* **20** 2201–8

[4] Tyagi D, Hedrick J L, Webster D C, McGrath J E and Wilkes G L 1988 Structure property relationships in perfectly alternating segmented polysulphone-poly(dimethylsiloxane) co-polymers *Polymer* **29** 833–44

[5] Guar U and Wunderlich B 1980 Study of microphase separation in block co-polymers of styrene and alpha-methylstyrene in the glass transition region using quantitative thermal analysis *Macromolecules* **13** 1618–25

[6] Liu L, Jiang B and Zhou E 1996 Study of semicrystalline–amorphous diblock copolymers. 1. Microphase separation, glass transition and crystallization of tetrahydrofuran methyl methacrylate diblock copolymers *Polymer* **37** 3937

[7] Lee S G, Jae J H, Choi K Y and Rhee J M 1998 Glass transition behavior of polypropylene/polystyrene/styrene–ethylene–propylene block copolymer blends *Polym. Bull.* **40** 765–71

[8] Chapman B R, Hamersky M W, Milhaupt J M, Kostelecky C, Lodge T P, von Meerwall E D and Smith S D 1998 Structure and dynamics of disordered tetrablock copolymers: composition and temperature dependence of local friction *Macromolecules* **31** 4562–73

[9] Aharoni S M 1998 Increased glass transition temperature in motionally constrained semicrystalline polymers *Polym. Adv. Tech.* **9** 169–201

[10] Laredo E, Grimau M, Muller A, Bello A and Suarez N 1998 Influence of aging and crystallinity on the molecular motions in bisphenol-A polycarbonate *J. Polym. Sci.* B **34** 2863–79

[11] Dobbertin J, Hensel A and Schick C 1996 Dielectric spectroscopy and calorimetry in the glass transition region of semicrystalline poly(ethylene terephthalate) *J. Therm. Anal.* **47** 1027–40

[12] Cheng S Z D, Wu Z Q and Wunderlich B 1987 Glass transition and melting behavior of poly(thio-1, 4-phenylene) *Macromolecules* **20** 2802–10

[13] Dubochet J, Adrian M, Teixeria Alba C M, Kadiyala R K, MacFarlane D R and Angell C A 1984 Glass-forming microemulsions—vitrification of simple liquids and electron-microscope probing of droplet-packing modes *J. Phys. Chem.* **88** 6727–32

[14] Angell C A, Kadiyala R K and MacFarlane D R 1984 Glass-forming microemulsions *J. Phys. Chem.* **88** 4593–6

[15] MacFarlane D R and Angell C A 1982 An emulsion technique for the study of marginal glass-formation in molecular liquids *J. Phys. Chem.* **86** 1927–30

[16] Forrest J A, Dalnoki-Veress K, Stevens J R and Dutcher J R 1996 Effect of free surfaces on the glass transition temperature of thin polymer films *Phys. Rev. Lett.* **77** 2002–5

[17] Forrest J A, Dalnoki-Veress K and Dutcher J R 1997 Interface and chain confinement effects on the glass transition temperature of thin polymer films *Phys. Rev.* E **56** 5705–16

[18] Dalnoki-Veress K, Forrest J A, Murray C, Gigault C and Dutcher J R 2001 Molecular weight dependence of reductions in the glass transition temperature of thin freely standing polymer films *Phys. Rev.* E **63** 031801

[19] Keddie J L, Jones R A L and Cory R A 1994 Interface and surface effects on the glass transition temperature in thin polymer films *Faraday Discuss.* **98** 219–30

[20] Wallace W E, Van Zanten J H and Wu W L 1995 Influence of an impenetrable interface on a polymer glass-transition temperature *Phys. Rev.* E **52** R3329–33

[21] Jain T S and de Pablo J J 2002 Monte Carlo simulation of free-standing polymer films near the glass transition temperature *Macromolecules* **35** 2167–76

[22] Varnik F, Baschnagel J and Binder K 2002 Reduction of the glass transition temperature in polymer films: a molecular-dynamics study *Phys. Rev.* E **65** 021507

[23] Mischler C, Baschnagel J and Binder K 2001 Polymer films in the normal-liquid and supercooled state: a review of recent Monte Carlo simulation results *Adv. Colloid Interface Sci.* **94** 197–227

[24] Scheidler P, Kob W and Binder K 2000 The relaxation dynamics of a simple glass former confined in a pore *Europhys. Lett.* **52** 277–83

[25] McKenna G B 1989 Glass formation and glassy behavior *Comprehensive Polymer Science* (vol 2 *Polymer Properties*) ed C Booth and C Price (Oxford: Pergamon) pp 311–62

[26] Jackson C L and McKenna G B 1990 The melting behavior of organic materials confined in porous solids *J. Chem. Phys.* **93** 9002–11

[27] Jackson C L and McKenna G B 1996 Vitrification and crystallization of organic liquids confined to nanoscale pores *Chem. Mater.* **8** 2128–37

[28] Alba-Simionesco C, Dosseh G, Dumont E, Frick B, Geil B, Morineau D, Teboul V and Xia Y 2003 Confinement of molecular liquids: consequences on thermodynamic, static and dynamical properties of benzene and toluene *Eur. Phys. J.* E **12** 19–28

[29] Wallacher D, Ackermann R, Huber R, Enderle M and Knorr K 2001 Diffraction study of solid oxygen embedded in porous glasses *Phys. Rev.* B **64** 184203

[30] Knorr K, Wallacher D, Huber P, Soprunyuk V and Ackermann R 2003 Are solidified fillings of mesopores basically bulk-like except for the geometric confinement? *Eur. Phys. J.* E **12** 51–6

[31] Schober H, Itoh H, Klapproth A, Chihaia V and Kuhs W F 2003 Guest–host coupling and anharmonicity in clathrate hydrates *Eur. Phys. J.* E **12** 41–9

[32] Hung F R, Dudziak G, Sliwinska-Bartkowiak M and Gubbins K E 2004 Freezing/melting behaviour within carbon nanotubes *Mol. Phys.* **102** 223–34

[33] Morishige K and Iwasaki H 2003 X-ray study of freezing and melting of water confined within SBA-15 *Langmuir* **19** 2808–11

[34] Buffat P H and Borel J-P 1976 Size effect on the melting temperature of gold particles *Phys. Rev.* A **13** 1050–2947

[35] Couchman P R and Jesser W A 1977 Thermodynamic theory of size dependence of melting temperature in metals *Nature* **269** 481–3

[36] Bassett D C and Davitt R 1974 On crystallization phenomena in polytetrafluoroethylene *Polymer* **15** 721–8

[37] Gibbs J W 1928 *Collected Works* (New York: Yale University Press)

[38] Thomson W 1871 On the equilibrium of vapour at a curved surface of liquid *Phil. Mag.* **42** 448–52

[39] Defay R, Prigogine I, Bellemans A and Everett D H 1966 *Surface Tension and Adsorption* (New York: Wiley)

[40] Castro T and Reifenberger R 1990 Size-dependent melting temperature of individual nanometer-sized metallic clusters *Phys. Rev.* B **42** 8548–56

[41] Lai S L, Guo J Y, Petrova V, Ramanath G and Allen L H 1996 Size-dependent melting properties of small tin particles: nanocalorimetric measurements *Phys. Rev. Lett.* **77** 99–102

[42] Bachels T and Guntherodt H 2000 Melting of isolated tin nanoparticles *Phys. Rev. Lett.* **85** 1250–3

[43] Dippel M, Maier A, Gimple V, Wider H, Evenson W E, Rasera R L and Schatz G 2001 Size-dependent melting of self-assembled indium nanostructures *Phys. Rev. Lett.* **87** 095505

[44] Coombes C J 1972 Melting of small particles of lead and indium *J. Phys. F: Met. Phys.* **2** 441–9

[45] Zhang M, Efremov M Y, Schiettekatte F, Olson E A, Kwan A T, Lai S L, Wisleder T, Greene J E and Allen L H 2000 Size-dependent melting point depression of nanostructures: nanocalorimetric measurements *Phys. Rev.* B **62** 10548–57

[46] Peters K F, Cohen J B and Chung Y 1998 Melting of Pb nanocrystals *Phys. Rev.* B **57** 13430–8

[47] Peters K F, Chung Y and Cohen J B 1997 Surface melting on small particles *Appl. Phys. Lett.* **71** 2391–3

[48] Lai S L, Carlsson J R A and Allen L H 1998 Melting point depression of Al clusters generated during the early stages of film growth: nanocalorimetry measurements *Appl. Phys. Lett.* **72** 1098–100

[49] Zhang Z, Li J C and Jiang Q 1999 Finite size effect on melting enthalpy and melting entropy of nanocrystals *Physica* B **270** 249–54

[50] Zhang Z, Li J C and Jiang Q 2000 Modelling for size-dependent and dimension-dependent melting of nanocrystals *J. Phys. D: Appl. Phys.* **33** 2653–6

[51] Nanda K K, Sahu S N and Behera S N 2002 Liquid-drop model for the size-dependent melting of low-dimensional systems *Phys. Rev.* A **66** 013208

[52] Bergese P, Colombo I, Gervasoni D and Depero L E 2004 Melting of nanostructured drugs embedded into a polymeric matrix *J. Phys. Chem.* **108** 15488–93

[53] Dosseh G, Xia Y and Alba-Simionesco C 2003 Cyclohexane and benzene confined in MCM-41 and SBA-15: confinement effects on freezing and melting *J. Phys. Chem.* B **107** 6445–53

[54] Watanabe A, Iiyama T and Kaneko K 1999 Melting temperature elevation of benzene confined in graphitic micropores *Chem. Phys. Lett.* **305** 71–4

[55] Radhakrishnan R, Gubbins K E and Sliwinska-Bartkowiak M 2000 Effect of the fluid–wall interaction on freezing of confined fluids: toward the development of a global phase diagram *J. Chem. Phys.* **112** 11048–57

[56] Watanabe A, Kaneko K, Iiyama T, Radhakrishnan R and Gubbins K E 1999 A remarkable elevation of freezing temperature of CCl4 in graphitic micropores *J. Phys. Chem.* B **103** 7061–3

[57] Radhakrishnan R, Gubbins K E, Watanabe A and Kaneko K 1999 Freezing of simple fluids in microporous activated carbon fibers: comparison of simulation and experiment *J. Chem. Phys.* **111** 9058–67

[58] Decressain R, Cochon E, Mansare T and Gors C 1996 Nuclear magnetic resonance of confined MBBA *Magn. Reson. Imaging* **14** 929–30

[59] Decressain R, Cochin E and Carpentier L 2000 Dynamics NMR investigations of a glassy crystal confined in porous materials *J. Physique* IV **10** 299–303

[60] Decressain R, Mansare T and Cochin E 2003 Dynamics and phase behaviour of materials in confined geometry *Phase Transit.* **76** 807–13

[61] Christenson H K 2001 Confinement effects on freezing and melting *J. Phys.: Condens. Matter* **13** R95–133

[62] Sun J and Simon S L 2004 The melting behavior of aluminum nanoparticles, in preparation

[63] Hill T L 1964 *Thermodynamics of Small Systems* (New York: Benjamin)

[64] Chamberlin R V 2003 Critical behavior from Landau theory in nanothermodynamic equilibrium *Phys. Lett.* A **315** 313–8

[65] Hill T L and Chamberlin R V 2002 Critical behavior from Landau theory in nanothermodynamic equilibrium *Nano Lett.* **2** 609–13

[66] Toscano F, Vallejos R O and Tsallis C 2004 Random matrix ensembles from nonextensive entropy *Phys. Rev.* E **69** 066131

[67] Zhang J, Liu G and Jonas J 1992 Effects of confinement on the glass transition temperature of molecular liquids *J. Phys. Chem.* **96** 3478–80

[68] Gibbs J H and DiMarzio 1958 Nature of the glass transition and the glassy state *J. Chem. Phys.* **28** 373–83

[69] DiMarzio E A and Gibbs J H 1958 Chain stiffness and the lattice theory of polymer phases *J. Chem. Phys.* **28** 807–13

[70] Simha R and Somcynsky T 1971 On the statistical thermodynamics of spherical and chain molecule fluids *Macromolecules* **2** 342–50

[71] Robertson R E, Simha R and Curro J G 1985 Effects of pressure on volume-recovery experiments *Macromolecules* **18** 2239–46

[72] LaGasse Curro J G and Simha R 1982 Diffusion-model for volume recovery in glasses *Macromolecules* **15** 1621–6

[73] Angell C A 1991 Relaxation in liquids polymers and plastic crystals—strong fragile patterns and problems *J. Non-Cryst. Solids* 1 **131** 13–31

[74] Angell C A, Ngai K L, McKenna G B, McMillan P F and Martin S W 2000 Relaxation in glass forming liquids and amorphous solids *J. Appl. Phys.* **88** 3113–57

[75] Park J Y and McKenna G B 1999 Size and confinement effects on the glass transition behavior of polystyrene/*o*-terphenyl polymer solutions *Phys. Rev.* B **61** 6667–76

[76] Barut G, Pissis P, Plester R and Nimtz G 1998 Glass transition in liquids: two versus three-dimensional confinement *Phys. Rev. Lett.* **80** 3543–6

[77] Arndt M, Stannarius R, Gorbatschow W and Kremer F 1996 Dielectric investigations of the dynamic glass transition in nanopores *Phys. Rev.* E **54** 5377–90

[78] Arndt M, Stannarius R, Groothus H, Hempel H and Kremer F 1997 Length scale of cooperativity in the dynamic glass transition *Phys. Rev. Lett.* **79** 2077–80

[79] Gorbatschow W, Arndt M, Stannarius R and Kremer F 1996 Dynamics of H-bonded liquids confined to nanopores *Europhys. Lett.* **35** 719–924

[80] Liu G, Mackowiak M, Li Y and Jonas J 1991 Rotational diffusion of liquid toluene in confined geometry *J. Chem. Phys.* **94** 239–42

[81] Streck C, Mel'nichenko Yu B and Richert R 1996 Dynamics of solvation in supercooled liquids confined to the pores of sol–gel glasses *Phys. Rev.* B **53** 5341

[82] Wendt H and Richert R 1999 Cooperativity and heterogeneity of the dynamics in nano-confined liquids *J. Phys.: Condens. Matter* **11** A199–206

[83] Wendt H and Richert R 2000 Relaxations in confinement as probed by solvation dynamics *J. Physique* IV **10** 67–72

[84] Richert R and Yang M 2003 Solvation dynamics of molecular glass-forming liquids in confinement *J. Phys.: Condens. Matter* **15** S1041–50

[85] Pissis P, Daoukaki D, Apekis L and Christodoulides C 1994 The glass transition in confined liquids *J. Phys.: Condens. Matter* **6** L325–8

[86] Pissis P, Kyritsis A, Barut G, Pelster R and Nimtz G 1998 Glass transition in 2- and 3-dimensionally confined liquids *J. Non-Cryst. Solids* **235** 444–9

[87] Dalnoki-Veress K, Forrest J A, de Gennes P G and Dutcher J R 2000 Glass transition reductions in thin freely-standing polymer films: a scaling analysis of chain confinement effects *J. Physique* IV **10** 221–6

[88] Forrest J A and Jones R A L 1999 Polymer surfaces *Interfaces and Thin Films* ed A Karim and S Kumar (Singapore: World Scientific)

[89] Forrest J A, Dalnoki-Veress K and Dutcher J R 1998 Brillouin light scattering studies of the mechanical properties of thin freely standing polystyrene films *Phys. Rev.* E **58** 6109–14

[90] Forrest J A, Rowai A C, Dalnoki-Veress K, Stevens J R and Dutcher J R 1996 Brillouin light scattering studies of the mechanical properties of polystyrene/polyisoprene multilayered thin films *J. Polym. Sci.* B **44** 3009–16

[91] Van Zanten J H, Wallace W E and Wu W l 1996 Effect of strongly favorable substrate interactions on the thermal properties of ultrathin polymer films *Phys. Rev.* E **53** R2053–6

[92] Cecchetto E, de Zouza N R and Jerome B 2000 Glass transition of ultrathin films probed by x-ray reflectivity *J. Physique* IV **10** 247–50

[93] Tsui O K C, Russell T P and Hawker C J 2001 Effect of interfacial interactions on the glass transition of polymer thin films *Macromolecules* **34** 5535–9

[94] Pochan D J, Lin E K, Satija S, Cheng S Z D and Wu W L 1999 Thermal expansion and glass-transition behavior of thin films with and without a free surface via neutron reflectivity *Dynamic in Small Confining Systems IV* vol 543, ed J M Drake (Warrendale, PA: Material Research Society) p 163

[95] Orts W J, Van Zanten J H, Wu W L and Satija S K 1993 Observation of temperature dependent thicknesses in ultrathin polystyrene films on silicon *Phys. Rev. Lett.* **71** 867–70

[96] Beaucage G, Composto R and Stein R S 1993 Ellipsometric study of the glass transition and thermal expansion coefficients of thin polymer films *J. Polym. Sci. Polym. Phys. Edn* **31** 319–26

[97] Keddie J L, Jones R A L and Cory R A 1994 Size-dependent depression of the glass transition temperature in polymer films *Europhys. Lett.* **27** 59–64

[98] Pham J Q, Mitchell C A, Bahr J L, Tour J M, Krishanamoorti R and Green P F 2003 Glass transition of polymer/single-walled carbon nanotube composite films *J. Polym. Sci.* B **41** 3339–45

[99] DeMaggio G B, Frieze W E, Gidley D W, Zhu M, Hristov H A and Yee A F 1997 Interface and surface effects on the glass transition in thin polystyrene films *Phys. Rev. Lett.* **78** 1524–7

[100] Xie L, DeMaggio G B, Frieze D W, Devries J, Gidley D W, Hristov H A and Yee A F 1995 Positronium formation as a probe of polymer surfaces and thin-films *Phys. Rev. Lett.* **74** 4947–50

[101] Fryer D S, Nealey P F and de Pablo J J 2000 Thermal probe measurements of the glass transition temperature for ultrathin polymer films as a function of thickness *Macromolecules* **33** 6439–47

[102] Ellison C J and Torkelson J M 2002 Sensing the glass transition in thin and ultrathin polymer films via fluorescence probes and labels *J. Polym. Sci.* B **40** 2745–58

[103] Ellison C J and Torkelson J M 2003 The distribution of glass-transition temperatures in nanoscopically confined glass formers *Nat. Mater.* **2** 695–700

[104] Ellison C J, Kim S D, Hall D B and Torkelson J M 2002 Confinement and processing effects on glass transition temperature and physical aging in ultrathin polymer films *Eur. Phys. J.* E **8** 155–66

[105] Ge S, Pu Y, Zhang W, Rafailovich M, Sokolov J, Buenviaje C, Buckmaster R and Overney R M 2000 Shear modulation force microscopy study of near surface glass transition temperatures *Phys. Rev. Lett.* **85** 2340–3

[106] Efremov M Y, Warren J T, Olson E A, Zhang M, Kwan A T and Allen L H 2002 Thin-film differential scanning calorimetry: a new probe for assignment of the glass transition of ultrathin polymer films *Macromolecules* **35** 1481–3

[107] Fukao K and Miyamoto Y 2000 Glass transitions and dynamics in thin polymer films: dielectric relaxation of thin films of polystyrene *Phys. Rev.* E **61** 1743–54

[108] Fukao K and Miyamoto Y 2001 Slow dynamics near glass transitions in thin polymer films *Phys. Rev.* E **64** 011803

[109] Fukao K, Uno S, Miyamoto Y, Hoshino A and Miyaji H 2001 Dynamics of alpha and beta processes in thin polymer films: poly(vinyl acetate) and poly(methyl methacrylate) *Phys. Rev.* E **64** 051807

[110] Fukao K 2003 Dynamics in thin polymer films by dielectric spectroscopy *Eur. Phys. J.* E **12** 119–25

[111] Hatmann L, Gorbatschow W, Hauwede J and Kremer F 2002 Molecular dynamics in thin films of isotactic poly(methyl methacrylate) *Eur. Phys. J.* E **8** 145–54

[112] Grohens Y, Hamon L, Carriere P, Holl Y and Schultz J 2000 Tacticity and surface chemistry effects on the glass transition temperature of thin supported PMMA films *Mater. Res. Soc. Symp.* **629** FF171–7

[113] Hall D B, Hooker J C and Torkelson J M 1997 Ultrathin polymer films near the glass transition: effect on the distribution of alpha-relaxation times as measured by second harmonic generation *Macromolecules* **30** 667–9

[114] Yuan C G, Meng O Y and Koberstein J T 1999 Effects of low-energy end groups on the dewetting dynamics of poly(styrene) films on poly(methyl methacrylate) substrates *Macromolecules* **32** 2329–33

[115] White C, Wu W L, Pu Y X, Rafailovich M and Sokolov J 2003 Probe segregation and T_g determination of a supported ultra-thin polystyrene film studied by X-ray and neutron reflectivity and SIMS *Polym. Eng. Sci.* **43** 1241–9

[116] Dutcher J R, Dalnoki-Veress K, Nickel B G and Roth C B 2000 Instabilities in thin polymer films: from pattern formation to rupture *Macromol. Symp.* **159** 143–50

[117] Reiter G 1993 Mobility of polymers in films-thinner than their unperturbed size *Eur. Phys. Lett.* **23** 579–84

[118] Reiter G 1994 Dewetting as a probe of polymer mobility in thin films *Macromolecules* **27** 3046–52

[119] Reiter G 2002 Are changes in morphology clear indicators for the glass transition in thin polymer films? Tentative ideas *Eur. Phys. J.* E **8** 251–5

[120] Green P F and Ganesan V 2003 Dewetting of polymeric films: unresolved issues *Eur. Phys. J.* E **12** 449–54

[121] O'Connell P and McKenna G B 2004 Rheological measurements of the thermoviscoelastic response of ultrathin polymer films *Science* at press

[122] McKenna G B 2003 Status of our understanding of dynamics in confinement: perspectives from confit *Eur. Phys. J.* E **12** 191–4

[123] Haller W 1965 Chromatography on glass of controlled pore size *Nature* **206** 693–6

[124] Haller W 1983 Application of controlled pore glass in solid phase biochemistry *Solid Phase Biochemistry* ed W H Scouten (New York: Wiley) chapter 11

[125] Bellissent-Funel M C, Lal J and Bosio L 1993 Structural study of water confined in porous glass by neutron scattering *J. Chem. Phys.* **98** 4246–52

[126] Wang Y, Snow W M and Sokol P E 1995 The structure of deuterium in Vycor *J. Low Temp. Phys.* **101** 929–49

[127] Schaefer D W and Keefer K D 1986 Structure of random porous materials: silica aerogel *Phys. Rev. Lett.* **65** 2199–202

[128] Devreux F, Boilot J P, Chaput F and Sapoval B 1990 NMR determination of the fractal dimension in silica aerogels *Phys. Rev. Lett.* **65** 614–7

[129] Kovacs A R 1958 La contraction isotherme du volume des polymères amorphes *J. Polym. Sci.* **30** 131–47

[130] McKinney J E and Goldstein M 1974 Pressure–volume–temperature relations for liquid and glassy poly(vinyl acetate) *J. Res. Natl Bur. Stand.* A **78** 331–53

[131] Ferry J D 1980 *Viscoelastic Properties of Polymers* 3rd edn (New York: Wiley)

[132] Moynihan C T *et al* 1976 Structural relaxation in vitreous materials *Ann. New York Acad. Sci.* **279** 15

[133] Kovacs A J, Aklonis J J, Hutchinson J M and Ramos A R 1979 Isobaric volume and enthalpy recovery of glasses. II. A transparent multiparameter theory *J. Polym. Sci. Polym. Phys. Edn* **17** 1097–162

[134] Scherer G W 1986 *Relaxation in Glass and Composites* (New York: Wiley)

[135] Angell C A and Qing Z 1989 Glass in stretched state formed by negative-pressure vitrification—trapping in and relaxing out *Phys. Rev.* B **39** 8784–7

[136] Atake T and Angell C A 1979 Pressure dependence of the glass transition temperature in molecular liquids and plastic crystals *J. Phys. Chem.* **83** 3218–23

[137] Alcoutlabi M, Simon S L and McKenna G B 2003 Analysis of the development of isotropic residual stresses in a bismaleimide/spiro orthocarbonate thermosetting resin for composite materials *J. Appl. Polym. Sci.* **88** 227–44

[138] Simon S L, Park J Y and and McKenna G B 2002 Enthalpy recovery of a glass-forming liquid constrained in a nanoporous matrix: negative pressure effects *Eur. Phys. J.* E **8** 209–16

[139] Tool A Q 1946 Relation between inelastic deformability and thermal expansion of glass in its annealing range *J. Am. Ceram. Soc.* **29** 240–6

[140] Narayanaswamy O S 1971 A model of structural relaxation in glass *J. Am. Ceram. Soc.* **54** 491–8

[141] Moynihan C T, Macedo P B, Montrose C J, Gupta P K, DeBolt M A, Dill J F, Dorn B E, Drake P W, Esteal A J, Elterman P B, Moeller R H, Sasabe H and Wilder J A 1976 Thermodynamic and transport properties of liquids near the glass transition temperature. Structural relaxation in vitreous materials *Ann. New York Acad. Sci.* **279** 15–35

[142] Colucci D M, McKenna G B, Filliben J I, Lee A, Curliss D B, Bowman K B and Russell J D 1997 Isochoric and isobaric glass formation: similarities and differences *J. Polym. Sci.* B **35** 1561–73

[143] Schuller J, Mel'nichenko Yu B, Richert R and Ficher E W 1994 Dielectric studies of the glass transition in porous media *Phys. Rev. Lett.* **73** 2224–7

[144] Schuller J, Richert R and Ficsher E W 1995 Dielectric relaxation of liquids at the surface of a porous glass *Phys. Rev.* B **52** 15232–8

[145] Liu G, Li Y and Jonas J 1989 Reorientational dynamics of molecular liquids in confined geometries *J. Phys. Chem.* **90** 5881–2

[146] Scheidler P, Kob W and Binder K 2002 Cooperative motion and growing length scales in supercooled confined liquids *Europhys. Lett.* **59** 701–7

[147] Morineau D, Xia Y D and Alba-Simionesco C 2002 Finite-size and surface effects on the glass transition of liquid toluene confined in cylindrical mesopores *J. Chem. Phys.* **117** 8966–72

[148] Schonhals A, Goering H, Schick C, Frick B and Zorn R 2003 Glassy dynamics of polymers confined to nanoporous glasses revealed by relaxational and scattering experiments *Eur. Phys. J.* E **12** 173–8

[149] Schonhals A, Goering H and Schick C 2002 Segmental and chain dynamics of polymers: from the bulk to the confined state *J. Non-Cryst. Solids* **305** 140–9

[150] Morineau D and Alba-Simionesco C 1998 Hydrogen-bond-induced clustering in the fragile glass-forming liquid m-toluidine: experiments and simulations *J. Chem. Phys.* **109** 8494–503

[151] Morineau D and Alba-Simionesco C 2003 Liquids in confined geometry: how to connect changes in the structure factor to modifications of local order *J. Chem. Phys.* **118** 9389–400

[152] Nemilov S V 1995 *Thermodynamic and Kinetic Aspects of the Vitreous State* (Ann Arbor, MI: CRC Press)

[153] Vogel H 1921 The law of the relation between the viscosity of liquids and temperature *Z. Phys.* **22** 645–6

[154] Fulcher G S 1925 Analysis of recent measurements of the viscosity of glasses *J. Am. Ceram. Soc.* **8** 339–55

[155] Tammann G and Hesse W 1926 The dependence of viscosity upon temperature of supercooled liquids *Z. Anorg. Allg. Chem.* **156** 245–57

[156] Angell C A 1984 *Relaxations in Complex Systems* ed K L Ngai and G B Wright (Springfield, VA: US Department of Commerce) p 3

[157] Ito K, Moynihan C T and Angell C A 1999 Thermodynamic determination of fragility in liquids and a fragile-to-strong liquid transition in water *Nature* **398** 492–5

[158] Adam G and Gibbs J H 1965 The temperature dependence of cooperative relaxation in glass-forming liquids *J. Chem. Phys.* **43** 139–46

[159] Donth E 1993 Characteristic length of glass transition—impossibility of a sharp critical kinetic temperature T_C greater than T_G *Phys. Scr.* T **49** 223–6

[160] Donth E 2001 *The Glass Transition: Relaxation Dynamics in Liquids and Disordered Materials* (*Springer Series in Material Sciences* vol 48) (Berlin: Springer)

[161] Kohlrausch R 1854 Theorie des Elektrischen Ruckstandes in der Leidner Flasche *Pogg. Ann. Phys. Chem.* **XCI** 179–214

[162] Williams G and Watts D C 1970 Non-symmetrical dielectric relaxation behaviour arising from a simple empirical decay function *Trans. Faraday Soc.* **66** 80–5

[163] Pissis P, Kyritsis A, Daoukaki D, Barut G, Pelster R and Nimtz G 1998 Dielectric studies of glass transition in confined propylene glycol *J. Phys.: Condens. Matter* **10** 6205–27

[164] Maddox M and Gubbins K E 1997 A molecular simulation study of freezing/melting phenomena for Lennard-Jones methane in cylindrical nanoscale pores *J. Chem. Phys.* **107** 9659–67

[165] Loughnane B J, Farrer R A, Scodinu A and Fourkas J T 1999 Dynamics of a wetting liquid in nanopores: an optical Kerr effect study of the dynamics of acetonitrile confined in sol–gel glasses *J. Chem. Phys.* **111** 5116–23

[166] Petychakis L, Floudas G and Fleischer G 1997 Chain dynamics of polyisoprene confined in porous media. A dielectric spectroscopy study *Europhys. Lett.* **44** 685–90

[167] Wubbenhorst M, Klap G J, Jansen J C, Van Bekkum H and Van Turnhout J 1999 Glass transition of one-dimensional molecular chains of p-nitroaniline confined in AlPO $4 - 5$ nanopores revealed by dielectric spectroscopy *J. Chem. Phys.* **111** 5637–40

[168] Stannarius R, Kremer F and Arndt M 1995 Dynamic exchange effects in broad-band dielectric-spectroscopy *Phys. Rev. Lett.* **75** 4698–701

[169] Schonhals A and Stauga R 1998 Broadband dielectric study of anomalous diffusion in a poly(propylene glycol) melt confined to nanopores *J. Chem. Phys.* **108** 5130–6

[170] Schonhals A and Stauga R 1998 Dielectric normal mode relaxation of poly(propylene glycol) melts in confining geometries *J. Non-Cryst. Solids* **235** 450–6

[171] Melnichenko Y B, Schuller J, Richert R, Ewen B and Loong C K 1995 Dynamics of hydrogen-bonded liquids confined to mesopores—A dielectric and neutron spectroscopy study *J. Chem. Phys.* **103** 2016–4

[172] Kalogeras I M, Vassilikou-Dova A and Neagu E R 2001 Dielectric characterization of poly(methyl methacrylate) geometrically confined into mesoporous SiO_2 glasses *Mater. Res. Innovat.* **4** 322–33

[173] Patkowski A, Ruths T and Fischer E W 2003 Dynamics of supercooled liquids confined to the pores of sol–gel glass: a dynamic light scattering study *Phys. Rev.* E **67** 021501

[174] Haralampus N, Argiriadi P, Gilchriest A, Ashmore E, Scordalakes C, Martin W, Kranbuehl D and Verdier P 1998 Dielectric measurements and computer simulation of the effect of confinement on the glass transition temperature *J. Non-Cryst. Solids* **235** 428–34

[175] Crupi V, Maisano G, Majolino D, Miliardo P and Venuti V 1998 Dynamic evidence of chemical and physical traps in H-bonded confined liquids *J. Chem. Phys.* **109** 7394–404

[176] Zorn R, Richter D, Hartmann L, Kremer F and Frick B 2000 Inelastic neutron scattering experiments on the fast dynamics of a glass forming liquid in mesoscopic confinements *J. Physique* IV **10** Pr7-83-86–6

[177] Zorn R, Hartmann L, Frick B, Richter D and Kremer F 2002 Inelastic neutron scattering experiments on the dynamics of a glass-forming material in mesoscopic confinement *J. Non-Cryst. Solids* **307** 547–54

[178] Pelster R 1999 Dielectric spectroscopy of confinement effects in polar materials *Phys. Rev.* B **59** 9214

[179] Bergman R, Mattsson J, Svanberg C, Schwartz G A and Swenson J 2003 Confinement effects on the excess wing in the dielectric loss of glass-formers *Eur. Phys. Lett.* **64** 675–81

[180] Zhang Q and Archer L A 2003 Effect of surface confinement on chain relaxation of entangled *cis*-polyisoprene *Langmuir* **19** 8094–101

[181] Kalampounias A G, Kirillov S A, Steffen W and Yannopoulos S N 2003 Raman spectra and microscopic dynamics of bulk and confined salol *J. Mol. Struct.* **651** 475–83

[182] Kremer F, Huwe A, Arndt M, Behrens P and Schwieger W 1999 How many molecules form a liquid? *J. Phys.: Condens. Matter* **11** A175–88

[183] Petychakis L, Floudas G and Fleischer G 1997 Chain dynamics of polyisoprene confined in porous media. A dielectric spectroscopy study *Europhys. Lett.* **40** 685–90

[184] Lusceac S A *et al* 2004 Type a versus type B glass formers: NMR relaxation in bulk and confining geometry *J. Phys. Chem.* B **108** 16601–5

[185] Torquato S 2002 *Random Heterogeneous Materials Microstructure and Macroscopic Properties* (New York: Springer)

[186] Pissis P, Anagnostopoulou-Konsta A, Apekis L, Daoukaki D and Christodoulides C 1991 Dielectric effects of water in water-containing systems *J. Non-Cryst. Solids* **131** 1174–81

[187] Daoukaki D, Barut G, Pelster R, Nimtz G, Kyritsis A and Pissis P 1998 Dielectric relaxation at the glass transition of confined *N*-methyl-epsilon-caprolactam *Phys. Rev.* B **58** 5336–45

[188] Sappelt D and Jackle J 1993 The cooperativity length in models for the glass transition *J. Phys. A: Math. Gen.* **26** 7325–41

[189] Jerome B, Cocchetto E, de Souza N R and Demirel A L 2000 Relaxation dynamics in confined glasses *J. Physique* IV **10** Pr7-227–32

[190] McKenna G B 2000 Size and confinement effects in glass forming liquids: perspectives on bulk and nano-scale behaviours *J. Physique* IV **10** 53–7

[191] McKenna G B 2000 International workshop on dynamics in confinement: a personal summary *J. Physique* IV **10** 343–6

[192] Wang L M, He F and Richert R 2004 Intramicellar glass transition and liquid dynamics in soft confinement *Phys. Rev. Lett.* **92** 095701

[193] Dalnoki-Veress K, Nickel B G, Roth C and Dutcher J R 1999 Hole formation and growth in freely standing polystyrene films *Phys. Rev.* E **59** 2153–6

[194] Forrest J A and Dalnoki-Veress K 2001 The glass transition in thin polymer films *Adv. Colloid Interface Sci.* **94** 167–96

[195] Roth C B and Dutcher J R 2004 Mobility on different length scales in thin polymer films *Soft Materials: Structure and Dynamics* ed J R Dutcher and A G Marangoni (New York: Dekker)

[196] Roth C B and Dutcher J R 2003 Glass transition temperature of freely-standing films of atactic poly(methyl methacrylate) *Eur. Phys. J.* E **12** S103–7

[197] Kawana S and Jones R A L 2001 Character of the glass transition in thin supported polymer films *Phys. Rev.* E **63** 021501

[198] Kawana S and Jones R A L 2003 Effect of physical ageing in thin glassy polymer films *Eur. Phys. J.* E **10** 223

[199] Sun L, Dutcher J R, Giovannin L, Nizzoli F, Stevens J R and Ord J L 1994 Elastic and elasto-optic properties of thin-films of poly(styrene) spin-coated onto Si(001) *J. Appl. Phys.* **75** 7482–8

[200] Forrest J A and Mattsson J 2000 Reductions of the glass transition temperature in thin polymer films: probing the length scale of cooperative dynamics *Phys. Rev.* E **61** R53–6

[201] Mattsson J, Forrest J A and Borjesson L 2000 Quantifying glass transition behavior in ultrathin free-standing polymer films *Phys. Rev.* E **62** 5187–200

[202] Sharp J S and Forrest J A 2003 Free surfaces cause reductions in the glass transition temperature of thin polystyrene films *Phys. Rev. Lett.* **91** 235701

[203] Sharp J S and Forrest J A 2003 Thickness dependence of the dynamics in thin films of isotactic poly(methylmethacrylate) *Eur. Phys.* E **12** S97–S101

[204] Teichroeb J H and Forrest J A 2003 Direct imaging of nanoparticle embedding to probe viscoelasticity of polymer surfaces *Phys. Rev. Lett.* **91** 016104

[205] Liu Y, Russell T P, Samant M G, Stohr J, Brown H R, Cossy-Favre A and Diaz J 1997 Surface relaxations in polymers *Macromolecules* **30** 7768–71

[206] Pu Y, Rafailovich M H, Sokolov J, Gersappe D, Peterson T, Wu W L and Schwarz S A 2001 Mobility of polymer chains confined at a free surface *Phys. Rev. Lett.* **87** 206101

[207] Winesett D A, Ade H, Sokolov J, Rafailovich M H and Zhu S 2000 Substrate dependence of morphology in thin film polymer blends of polystyrene and poly(methyl methacrylate) *Polym. Int.* **49** 458–62

[208] Xavier J H, Pu Y, Li C, Rafailovich M H and Sokolov J 2004 Transition of linear to exponential hole growth modes in thin free-standing polymer films *Macromolecules* **37** 1470–5

[209] Tseng K C, Turro N J and Durning C J 2000 Molecular mobility in polymer thin films *Phys. Rev.* E **61** 1800–11

[210] Jiang Q, Shi H X and Li J C 1999 Finite size effect on glass transition temperatures *Thin Solid Films* **354** 283–6

[211] Jerome B and Commandeur J 1997 Dynamics of glasses below the glass transition *Nature* **386** 589–92

[212] Jerome B 1999 Dynamics of glass-forming materials confined in thin films *J. Phys.: Condens. Matter* **11** A189–97

[213] Cho Y K, Watanabe H and Granick S 1999 Dielectric response of polymer films confined between mica surfaces *J. Chem. Phys.* **110** 9688–96

[214] Bauer C, Bohmer R, Moreno-Flores S, Richert R, Sillescu H and Neher D 2000 Capacitive scanning dilatometry and frequency-dependent thermal expansion of polymer films *Phys. Rev.* E **61** 1755–64

[215] Zhao J-H, Kiene M, Hu C and Ho P S 2000 Thermal stress and glass transition of ultrathin polystyrene films *Appl. Phys. Lett.* **77** 2843–5

[216] Sakai Y, Ikehara T, Nishi T, Nakajima K and Hara M 2000 Nanorheology measurement on a single polymer chain *Appl. Phys. Lett.* **81** 724–6

[217] Masson J L and Green P F 2002 Hole formation in thin polymer films: a two-stage process *Phys. Rev. Lett.* **88** 205504

[218] Tate R S, Fryer D S, Pasqualini S, Montague M F, de Pablo J J and Nealey P F 2001 Extraordinary elevation of the glass transition temperature of thin polymer films grafted to silicon oxide substrates *J. Chem. Phys.* **115** 9982–90

[219] Dinelli F, Buenviaje C and Ovrney M 2000 Glass transitions of thin polymeric films: speed and load dependence in lateral force microscopy *J. Chem. Phys.* **113** 2043–8

[220] Cristofolini L, Arisi S and Fontana M P 2000 Glass transition and relaxation following photo perturbation in thin polymeric films *Phys. Rev. Lett.* **85** 4912–5

[221] Weber R, Zimmermann K-M, Tolan M, Stettner J and Press W 2001 X-ray reflectivity study on the surface and bulk glass transition of polystyrene *Phys. Rev.* E **64** 061508

[222] Beaucage G, Banach M J and Vaia R A 2000 Relaxation of polymer thin films in isothermal temperature-jump measurements *J. Polym. Sci.* B **38** 2929–36

[223] Soles C L, Douglas J F, Wu W L and Dimeo R M 2002 Incoherent neutron scattering and the dynamics of confined polycarbonate films *Phys. Rev. Lett.* **88** 037401

[224] Gorbunov A A and Skvortsov A M 1995 Statistical properties of confined molecules *Adv. Colloid Interface Sci.* **62** 31–108

[225] Grohens Y, Hamon L, Reiter G, Soldera A and Holl 2002 Some relevant parameters affecting the glass transition of supported ultra-thin polymer films *Eur. Phys. J.* E **8** 217–24

[226] Keddie J L and Jones R A L 1995 Glass transition behavior in ultra-thin polystyrene films *ISR. Chem. Soc.* **35** 21–6

[227] Pham J Q and Green P F 2002 The glass transition of thin film polymer/polymer blends: interfacial interactions and confinement *J. Chem. Phys.* **116** 5801–6

[228] Green P F and Limary R 2001 Block copolymer thin films: pattern formation and phase behavior *Adv. Colloid Interface Sci.* **94** 53–81

[229] Jean Y C, Zhang R, Cao H, Yuan J-P and Huang C-M 1997 Glass transition of polystyrene near the surface studied by slow-positron-annihilation spectroscopy P *Phys. Rev.* B **56** R8459–62

[230] Yu C-J, Richter A G, Datta A, Durbin M K and Dutta P 1999 Observation of molecular layering in thin liquid films using x-ray reflectivity *Phys. Rev. Lett.* **82** 2326–9

[231] Grohens Y, Sacristan J, Hamon L, Reinecke H, Mijangos C and Guenet J M 2001 Glass transition of ultra-thin films of modified PVC *Polymer* **42** 6419–23

[232] Grohens Y, Hamon L, Spevacek J and Holl Y 2003 The gel-like structure of polymer in thin films: an explanation of the thickness dependent glass transition? *Macromol. Symp.* **203** 155–64

[233] Prucker O, Christian S, Bock H, Ruhe J, Frank C W and Knoll W 1998 On the glass transition in ultrathin polymer films of different molecular architecture *Macromol. Chem. Phys.* **199** 1435–44

[234] Kim J H, Jang J and Zin W C 2000 Estimation of the thickness dependence of the glass transition temperature in various thin polymer films *Langmuir* **16** 4064–7

[235] Kim J H, Jang J and Zin W C 2001 Thickness dependence of the glass transition temperature in thin polymer films *Langmuir* **17** 2703–10

[236] Kim J H, Jang J, Lee D Y and Zin W C 2002 Thickness and composition dependence of the glass transition temperature in thin homogeneous polymer blend films *Macromolecules* **35** 311–3

[237] Long D and Lequeux F 2001 Heterogeneous dynamics at the glass transition in van der Waals liquids, in the bulk and in thin films *Eur. Phys. J.* E **4** 371–87

[238] Park C H, Kim J H, Ree M, Sohn B-H, Jung J C and Zin W C 2004 Thickness and composition dependence of the glass transition temperature in thin random copolymer films *Polymer* **45** 4507–13

[239] Efremov M Yu, Olson E A, Zhange M, Zhang Z and Allen L H 2003 Glass transition in ultrathin polymer films: calorimetric study *Phys. Rev. Lett.* **91** 085703

[240] Efremov M Y, Warren J T, Olson E A, Zhang M, Zhang Z and Allen L H 2004 Probing glass transition of ultrathin polymer films at a timescale of seconds using fast differential scanning calorimetry *Macromolecules* **37** 4607–16

[241] Efremov M Y, Olson E A, Zhang M, Lai S L, Schiettekatte F, Zhang Z S and Allen L H 2004 Thin-film differential scanning nanocalorimetry: heat capacity analysis *Thermo. Acta* **412** 13–23

[242] Kerle T, Lin Z Q, Kim H C and Russell T P 2001 Mobility of polymers at the air/polymer interface *Macromolecules* **34** 3484–92

[243] Ngai K L 2002 Mobility in thin polymer films ranging from local segmental motion, Rouse modes to whole chain motion: a coupling model consideration *Eur. Phys. J.* E **8** 225–35

[244] Johannsmann D 2002 The glass transition and contact mechanical experiments on polymer surfaces *Eur. Phys. J.* E **8** 257–9

[245] Forrest J A 2002 A decade of dynamics in thin films of polystyrene: where are we now? *Eur. Phys. J.* E **8** 261–6

[246] Forrest J A, Svanberg C, Revesz K, Rodahl M, Torell L M and Kasemo B 1998 Relaxation dynamics in ultrathin polymer films *Phys. Rev.* E **58** 1226–9

[247] Lee Y-C, Bretz K C, Wise F W and Sachse W 1996 Picosecond acoustic measurements of longitudinal wave velocity of submicron polymer films *Appl. Phys. Lett.* **69** 1692–4

[248] Jaworek T, Neher D, Wegner G, Wieringa R H and Schouten A J 1998 Electromechanical properties of an ultrathin layer of directionally aligned helical polypeptides *Science* **279** 57–60

[249] Serghei A and Kremer F 2003 Confinement-induced relaxation process in thin films of *cis*-polyisoprene *Phys. Rev. Lett.* **91** 165702

[250] Schwodiauer R, Neugschwandtner G S, Bauer-Gogonea S and Rosenmayer T 2000 Dielectric and electret properties of nanoemulsion spin-on polytetrafluoroethylene films *Appl. Phys. Lett.* **76** 2612–4

[251] Masson J L and Green P F 2002 Viscosity of entangled polystyrene thin film melts: film thickness dependence *Phys. Rev.* E **65** 031806

[252] Cicerone M T, Blackburn F R and Ediger M D 1995 How do molecules move near T_g molecular rotation of 6 probes in o-terphenyl across 14 decades in time *J. Chem. Phys.* **102** 471–9

[253] Kracke B and Damaschke B 2000 Measurement of nanohardness and nanoelasticity of thin gold films with scanning force microscope *Appl. Phys. Lett.* **77** 361–3

[254] Thurau C T and Ediger M D 2002 Influence of spatially heterogeneous dynamics on physical aging of polystyrene *J. Phys. Chem.* **116** 9089–99

[255] Wubbenhorst M, Murray C A and Dutcher J R 2003 Dielectric relaxations in ultrathin isotactic PMMA films and PS-PMMA-PS trilayer films *Eur. Phys. J.* E **12** S109–12

[256] Grohens Y, Papaleo R M and Hamon L 2003 Ion crater healing and variable temperature ellipsometry as complementary probes for the glass transition in thin polymer films *Eur. Phys. J.* E **12** S81–5

[257] Wallace W E, Tan N C B, Wu W L and Satija S 1998 Mass density of polystyrene thin films measured by twin neutron reflectivity *J. Chem. Phys.* **108** 3798–804

[258] Kaya H and Jerome B 2003 Unstable thin films: new questions *Eur. Phys. J.* E **12** 383–6

[259] Thiele U, Jonas A M, Sharma A, Kaya H, Jerome B and Jonas A M 2003 Spinodal-like dewetting of thermodynamically-stable thin polymer films—Discussion *Eur. Phys. J.* E **12** 395–6

[260] Ziherl P, Zumer S, Kaya H, Jerome B and Thiele U 2003 Many paths to dewetting of thin films: anatomy and physiology of surface instability—Discussion *Eur. Phys. J.* E **12** 408

[261] Steiner U, Thiele U, Sharma A, Green P, Kaya H and Jerome B 2003 Open questions and promising new fields in dewetting—Discussion *Eur. Phys. J.* E **12** 415–6

[262] Kaya H, Jerome B, Sharma A and Thiele U 2003 Stability and rupture of aqueous wetting films *Eur. Phys. J.* E **12** 435

[263] Kaya H, Jerome B, Sharma A and Thiele U 2003 Stability and rupture of aqueous wetting films—Discussion *Eur. Phys. J.* E **12** 448

[264] Sharp J S and Forrest J A 2003 Dielectric and ellipsometric studies of the dynamics in thin films of isotactic poly(methylmethacrylate) with one free surface *Phys. Rev.* E **67** 031805

[265] Serghei A, Hartmann L, Pouret P, Leger L and Kremer F 2004 Molecular dynamics in thin (grafted) polymer layers *Colloid Polym. Sci.* **282** 946–54

[266] Kalogeras I M and Neagu E R 2004 Interplay of surface and confinement effects on the molecular relaxation dynamics of nanoconfined poly(methyl methacrylate) chains *Eur. Phys. J.* E **14** 193–204

[267] Alcoutlabi M, Alberola N D and Merle G 1999 L'effet du confinement sur les properties thermodynamique et viscoelastique des polymers, unpublished data

[268] Fryer D S, Peters R D, Kim E J, Tomaszewski J E, de Pablo J J and Nealey P F 2001 Dependence of the glass transition temperature of polymer films on interfacial energy and thickness *Macromolecules* **34** 5627–34

[269] Jiang Q and Lang X Y 2004 Glass transition of low-dimensional polystyrene *Macromolecules* **25** 825–8

[270] Singh L, Ludovice P J and Henderson C L 2004 Influence of molecular weight and film thickness on the glass transition temperature and coefficient of thermal expansion of supported ultrathin polymer films *Thin Solid Films* **449** 231–41

[271] Priestly R D, Broadbelt L J and Torkelson J M 2005 Physical aging of ultrathin polymer films above and below the bulk glass transition temperature: effects of attractive versus neutral polymer–substrate interactions measured by fluorescence *Macromolecules* **38** 654–7

[272] White C C, Migler K B and Wu W L 2001 Measuring T_g in ultra-thin polymer films with an excimer fluorescence technique *Polym. Eng. Sci.* **41** 1497–505

[273] Jones R L, Kumar S K, Ho D L, Briber R M and Russell T P 1999 Chain conformation in ultrathin polymer films *Nature* **400** 146–9

[274] Jones R L, Kumar S K, Ho D L, Briber R M and Russell T P 2001 Chain conformation in ultrathin polymer films using small-angle neutron scattering *Macromolecules* **34** 559–67

[275] McKenna G B 2003 Mechanical rejuvenation in polymer glasses: fact or fallacy? *J. Phys.: Condens. Matter* **15** S737–63

[276] Angell C A, Poole P H and Shao J 1994 Glass-forming liquids, anomalous liquids and polyamorphism in liquids and biopolymers *Nuovo Cimento* D **16** 993–1025

[277] Bernazzani P, Simon S L, Plazek D J and Ngai K L 2002 Effects of entanglement concentration on T_g and local segmental motions *Eur. Phys. J.* E **8** 201–7

[278] Simon S L, Bernazzani P and McKenna G B 2003 Effects of freeze-drying on the glass temperature of cyclic polystyrenes *Polymer* **44** 8025–32

[279] Alcoutlabi M, Briatico-Vangosa F and McKenna G B 2002 Effect of chemical activity jumps on the viscoelastic behavior of an epoxy resin: physical aging response in carbon dioxide pressure jumps *J. Polym. Sci.* B **40** 2050–64

[280] Alcoutlabi M, Banda L and McKenna G B 2004 A comparison of concentration-glasses and temperature-hyperquenched glasses: CO_2-formed glass versus temperature-formed glass *Polymer* **45** 5629–34

[281] Zheng Y and McKenna G B 2003 Structural recovery in a model epoxy: comparison of responses after temperature and relative humidity jumps *Macromolecules* **36** 2387–96

[282] Zheng Y, Priestley R D and McKenna G B 2004 Physical aging of an epoxy subsequent to relative humidity jumps through the class concentration *J. Polym. Sci.* B **42** 2107–21

[283] Forrest J A 2004 *Paper given at March 2004 American Physical Society Mtg* (not in abstracts)

[284] Lakowicz J R 1999 *Principles of Fluorescence Spectroscopy* 2nd edn (New York: Kluwer–Academic/Plenum)

[285] Zoller P and Walsh D J 1995 *Standard Pressure–Volume–Temperature Data for Polymers* (Lancaster, PA: Technomic) p 171

[286] Plazek D J 1980 The temperature dependence of the viscoelastic behavior of poly(vinyl acetate) *Polym. J.* **12** 43–53

[287] Roth C B, Nickel B G, Dutcher J R and Dalnoki-Veress K 2003 Differential pressure experiment to probe hole growth in freely standing polymer films *Rev. Sci. Instrum.* **74** 2796–804

[288] Debregeas G, Martin P and Brochard-Wyart F 1995 Viscous bursting of suspended films *Phys. Rev. Lett.* **75** 3886–9

[289] Debregeas G, de Gennes P G and Brochard-Wyart F 1998 The life and death of ‘bare’ viscous bubbles *Science* **279** 1704–7

[290] Kajiyama T, Tanaka K, Satomi N and Takahara A 1998 Surface relaxation process of monodisperse polystyrene film based on lateral force microscopic measurements *Macromolecules* **31** 5150–1

[291] Torres J A, Nealey P F and de Pablo J J 2000 Molecular simulation of ultrathin polymeric films near the glass transition *Phys. Rev. Lett.* **85** 3221–4

[292] de Gennes P G 2000 Glass transition in thin polymer films *Eur. Phys. J.* E **2** 201–3

[293] McCoy J D and Curro J G 2002 Conjectures on the glass transition of polymers in confined geometries *J. Chem. Phys.* **116** 9154–7

[294] Tanaka K, Takahara A and Kajiyama T 2000 Rheological analysis of surface relaxation process of monodisperse polystyrene films *Macromolecules* **33** 7588–93

[295] Tsui O K C, Wang X P, Ho J Y L, Ng T K and Xiao X D 2000 Studying surface glass-to-rubber transition using atomic force microscopic adhesion measurements *Macromolecules* **33** 4198–204

[296] Satomi N, Takahara A and Kajiyama T 1998 Determination of surface glass transition temperature of monodisperse of polystyrene based on temperature dependent scanning viscoelasticity microscopy *Macromolecules* **32** 4474–6

[297] Boiko Y M and Prud’homme R E 1997 Bonding at systematic polymer/polymer interfaces below the glass transition temperature *Macromolecules* **30** 3708–10

[298] Boiko Y M and Prud’homme R E 1998 Surface mobility and diffusion at interfaces of polystyrene in the vicinity of the glass transition *J. Polym. Sci.* B **36** 567–72

[299] Wallace W E, Fischer D A, Efimenko K, Wu W L and Genzer J 2001 Polymer chain relaxation: surface outpaces bulk *Macromolecules* **34** 5081–2

[300] Schwab A D, Agra D M G, Kim J H, Kumar S and Dhinojwala A 2000 Surface dynamics in rubbed polymer thin films probed with optical birefringence measurements *Macromolecules* **33** 4903–9

[301] Agra D M G, Schwab A D, Kim J H, Kumar S and Dhinojwala A 2000 Relaxation dynamics of rubbed polystyrene thin films *Eur. Phys. Lett.* **51** 655–60

[302] Schwab A D, Acharya B, Kumar S and Dhinojwala A 2002 Isothermal relaxation of rubbed polystyrene thin films probed with optical birefringence measurements *Mod. Phys. Lett.* **16** 415–21

[303] Tsang O C, Tsui O K C and Yang Z 2001 Temporal evolution of relaxation in rubbed polystyrene thin films *Phys. Rev.* E **63** 061603

[304] Tsang O C, Xie F C, Tsui O K C, Yang Z, Zhang J M, Shen D Y and Yang X Z 2001 Rubbing-induced molecular alignment and its relaxation in polystyrene thin films *J. Polym. Sci.* B **39** 2906–14

[305] Zhang X M, Tasaka S and Inagaki N 2000 Surface mechanical properties of low-molecular-weight polystyrene below its glass-transition temperatures *J. Polym. Sci.* B **38** 654–8

[306] Zhang X M, Tasaka S and Inagak N 2000 Studies on surface molecular motion of oligomeric polystyrene by differential scanning calorimetry *Polym. Adv. Tech.* **11** 40–7

[307] Hammerschmidt J A, Gladfelter W L and Haugstad G 1999 Probing polymer viscoelastic relaxations with temperature-controlled friction force microscopy *Macromolecules* **32** 3360–7

[308] Fischer H 2002 Thermal probe surface treatment of a bulk polymer: does a surface layer with a lower glass transition than the bulk exist? *Macromolecules* **35** 3592–5

[309] Rouse J H, Twaddle P L and Ferguson G S 1999 Frustrated reconstruction at the surface of a glassy polymer *Macromolecules* **32** 1665–71

[310] Mumbauer P D, Carey D H and Ferguson G S 1995 Organic chemistry at polymer surfaces to promote adhesion to gold and copper—surface modified polybutadiene having functional groups containing sulfur *Chem. Mater.* **7** 1303–14

[311] Bliznyuk V N, Assender H E and Briggs G A D 2002 Surface glass transition temperature of amorphous polymers. A new insight with SFM *Macromolecules* **35** 6613–22

[312] Tanaka K, Jiang X Q, Nakamura K, Takahara A, Kajiyama T, Ishizone T, Hirao A and Nakahama S 1998 Effect of chain end chemistry on surface molecular motion of polystyrene films *Macromolecules* **31** 5148–9

[313] Buck E, Petersen K, Hund M, Krausch G and Johannsmann D 2004 Decay kinetics of nanoscale corrugation gratings on polymer surface: evidence for polymer flow below the glass temperature *Macromolecules* **37** 8647–52

[314] Hamdorf M and Johannsmann D 2000 Surface-rheological measurements on glass forming polymers based on the surface tension driven decay of imprinted corrugation gratings *J. Chem. Phys.* **112** 4262–70

[315] Petersen K and Johannsmann D 2002 Measurements on the surface glass transition of PMMA from the decay of imprinted surface corrugation gratings: the influence of molecular weight *J. Non-Cryst. Solids* **307** 532–7

[316] Kajiyama T, Tanaka K and Takahara A 1998 Study of the surface glass transition behaviour of amorphous polymer film by scanning-force microscopy and surface spectroscopy *Polymer* **39** 4665–73

[317] Hutcheson S A and McKenna G B 2004 Nanosphere embedding into polymer surfaces: a viscoelastic contact mechanics analysis *Phys. Rev. Lett.* at press

[318] Knauss W G and Emri I 1987 Volume change and the nonlinearly thermo-viscoelastic constitution of polymers *Polym. Eng. Sci.* **27** 86–100

[319] Hasan O A, Boyce M C, Li X S and Berko S 1993 An investigation of the yield and post-yield behavior and corresponding structure of poly(methylmethacrylate) *J. Polym. Sci.* B **31** 185–97

[320] Hasan O A and Boyce M C 1993 Energy storage during inelastic deformation of glassy polymers *Polymer* **34** 5085–92

[321] Tervoort T A, Klompen E T J and Govaert L E 1996 A multi-mode approach to finite three-dimensional, nonlinear viscoelastic behavior of polymer glasses *J. Rheol.* **40** 779–97

[322] Govaert L E, Timmemans P H M and Brekelamns W A M 2000 The influence of intrinsic strain softening localization in polycarbonate: modeling and experimental validation *Trans. ASME, J. Eng. Mater. Technol.* **1222** 177–85

[323] Tervoort T A and Govaert L E 2000 Strain hardening behavior of polycarbonate in the glassy state *J. Rheol.* **44** 1263–77

[324] O'Connell P A and McKenna G B 1997 Large deformation response of polycarbonate: time–temperature, time–aging time and time–strain superposition *Polym. Eng. Sci.* **37** 1485–95

[325] O'Connell P A and McKenna G B 2002 The non-linear viscoelastic response of polycarbonate in torsion: an investigation of time–temperature and time–strain superposition *Mech. Time-Dep. Mater.* **6** 207–29

[326] Mukherjee M, Bhattacharya M, Sanyal M K, Geue T, Grenzer J and Pietsch U 2002 Reversible negative thermal expansion of polymer films *Phys. Rev.* E **6** 061801

[327] Fehr T and Lowen H 1995 Glass transition in confined geometry *Phys. Rev.* E **52** 4016–25

[328] Kob W 1999 Computer simulations of supercooled liquids and glasses *J. Phys.: Condens. Matter* **11** R85–115

[329] Hobach J, Kob W, Binder K and Angell C A 1996 Finite size effects in simulations of glass dynamics *Phys. Rev.* E **54** R5897–900

[330] Binder K, Baschnagel J, Benemann C and Paul W 1999 Monte Carlo and molecular dynamics simulation of the glass transition of polymers *J. Phys.: Condens. Matter* **11** A47–55

[331] Kob W and Anderson H C 1995 Testing mode-coupling theory for a supercooled binary Lennard-Jones mixture I: the van Hove correlation function *Phys. Rev.* E **51** 4626–41

[332] Kob W and Anderson H C 1995 Testing mode-coupling theory for a supercooled binary Lennard-Jones mixture: II. Intermediate scattering function and dynamic susceptibility *Phys. Rev.* E **52** 4134–53

[333] Jackle J 2000 Expected influence of spatial confinement on glass transitions *J. Physique* IV **10** Pr7-3-7

[334] Ngai K L 1999 Modification of the Adam–Gibbs model of glass transition for consistency with experimental data *J. Phys. Chem.* B **103** 5895–902

[335] Neyertz S, Brown D, Colombini D and Alberola N D 2000 Volume dependence of molecular flexibility in poly(ethylene oxide) under negative pressure *Macromolecules* **33** 1361–9

[336] Gallo P, Pellarin R and Rovere M 2002 Mode coupling relaxation scenario in a confined glass former *Europhys. Lett.* **57** 212–8

[337] Jendrejack R M, Schwartz D C, Graham M D and de Pablo J J 2003 Effect of confinement on DNA dynamics in microfluidic devices *J. Chem. Phys.* **119** 1165–73

[338] Nemeth Z T and Lowen H 1999 Freezing and glass transition of hard spheres in cavities *Phys. Rev.* E **59** 6824–9

[339] Kuppa V and Manias E 2003 Dynamics of poly(ethylene oxide) in nanoscale confinements: a computer simulations perspective *J. Chem. Phys.* **118** 3421–9

[340] Jendrejack R M, Dimalanta E T, Schwartz D C, Graham M D and de Pablo J J 2003 DNA dynamics in a microchannel *Phys. Rev. Lett.* **91** 038102

[341] Kim K and Yamamoto 2000 Apparent finite-size effects in the dynamics of supercooled liquids *Phys. Rev.* E **61** R41–4

[342] Moreno A J, Colmenero J, Algeria A, Alba-Simionesco C, Dosseh G, Morineau D and Frick B 2003 Methyl group dynamics in a confined glass *Eur. Phys. J.* E **12** S44–6

[343] Yamamoto R and Onuki A 1998 Dynamics of highly supercooled liquids: heterogeneity, rheology, and diffusion *Phys. Rev.* E **58** 3515–29

[344] Gupta S A, Cochran H D and Cummings P T 1997 Shear behavior of squalane and tetracosane under extreme confinement.1. Model, simulation method, and interfacial slip *J. Chem. Phys.* **107** 10316–26

Gupta S A, Cochran H D and Cummings P T 1997 Shear behavior of squalane and tetracosane under extreme confinement.2. Confined film structure *J. Chem. Phys.* **107** 10327–34

[345] Scheidler P, Kob W and Binder K 2000 Static and dynamical properties of a supercooled liquid confined in a pore *J. Physique* IV **10** Pr7-33-36

[346] Baschnagel J, Mischler C and Binder K 1996 Dynamics of glassy polymer melts in confined geometry: a Monte Carlo simulation *J. Physique* **6** 1271–94

[347] Binder K, Mischler C and Baschnagel J 1996 Simulation studies on the dynamics of polymers at interfaces *Annu. Rev. Mater. Sci.* 2 **6** 107–34

[348] Baschnagel J, Mischler C and Binder K 2000 Dynamics of confined polymer melts: recent Monte Carlo simulation results *J. Physique* IV **10** 1–14

[349] Sivaniah E, Sferrazza M and Jones R A L 1999 Chain confinement effects on interdiffusion in polymer multilayers *Phys. Rev.* E **59** 885–8

[350] Druker P and Mattice W 1999 Mobility of the surface and interior of thin films composed of amorphous polyethylene *Macromolecules* **32** 194–8

[351] Bauer C and Dietrich S 2000 Shapes contact angles, and line tensions of droplets on cylinders *Phys. Rev.* E **62** 2428–38

[352] Dinelli F, Biswas S K, Briggs G A D and Kolosov O V 2000 Measurements of stiff-material compliance on the nanoscale using ultrasonic force microscopy *Phys. Rev.* B **61** 13995–4006

[353] Varnik F, Baschnagel J and Binder K 2000 Molecular dynamics of supercooled polymer films *J. Physique* IV **10** Pr7-239-242

[354] McCoy J D, Texeira M A and Curro J G 2001 Polymeric contributions to entropic surface forces *J. Chem. Phys.* **114** 4289–95

[355] Ngai K L 2003 The effects of changes of intermolecular coupling on glass transition dynamics in polymer thin films and glass-formers confined in nanometer pores *Eur. Phys. J.* E **12** 93–100

[356] Ngai K L 2002 Relaxation in nanometre-size polymers and glass formers: application of the coupling model to some current problems *Phil. Mag.* B **82** 291–303

[357] Varnik F, Baschnagel J and Binder K 2002 Glassy dynamics in thin polymer films: recent MD results *J. Non-Cryst. Solids.* **307** 524–31

[358] Mischler C, Baschnagel J, Dasgupta S and Binder K 2002 Structure and dynamics of thin polymer films: a case study with the bond-fluctuation model *Polymer* **43** 467–76

[359] Eurich F, Maass P and Baschnagel J 2002 Gaussian ellipsoid model for confined polymer systems *J. Chem. Phys.* **117** 4564–77

[360] Frischknecht A L, Curro J G and Frink L J D 2002 Density functional theory for inhomogeneous polymer systems. II. Application to block copolymer thin films *J. Chem. Phys.* **117** 10398–411

[361] Varnik F, Baschnagel J and Binder K 2002 Static and dynamic properties of supercooled thin polymer films *Eur. Phys. J.* E **8** 175–92

[362] Saulnier F, Rapael E and de Gennes P-G 2002 Dewetting of thin polymer films near the glass transition *Phys. Rev. Lett.* **88** 196101

[363] Saulnier F, Rapael E and de Gennes P-G 2002 Dewetting of thin-film polymers *Phys. Rev.* E **66** 061607

[364] Scheidler P, Kob W, Binder K and Parisi G 2002 Growing length scales in a supercooled liquid close to an interface *Phil. Mag.* B **82** 283–90

[365] Scheidler P, Kob W and Binder K 2003 The relaxation dynamics of a confined glassy simple liquid *Eur. Phys. J.* E **12** 5–9

[366] Sotta P and Long D 2003 The crossover from 2D to 3D percolation: theory and numerical simulations *Eur. Phys. J.* E **11** 375–87

[367] Varnik F, Baschnagel J, Binder K and Mareschal M 2003 Confinement effects on the slow dynamics of a supercooled polymer melt: Rouse modes and the incoherent scattering function *Eur. Phys. J.* E **12** 167–71

[368] Donth E 2003 Can dynamic neutron scattering help to understand a thermodynamic variant of an internal quantum-mechanical experiment in the angstrom range? *Eur. Phys. J.* E **12** 11–8

[369] Simha R and Somcynsky T 1969 Statistical thermodynamics of spherical and chain molecule fluids *Macromolecules* **2** 342–50

[370] Somcynsky T and Simha R 1971 Hole theory of liquids and glass transition *J. Appl. Phys.* **42** 4545–8

[371] Robertson R E, Simha R and Curro J G 1984 Free-volume and the kinetics of aging of polymer glasses *Macromolecules* **17** 911–9

[372] Simha R, Curro J G and Ribertson R E 1984 Molecular-dynamics of physical aging in the glassy state *Polym. Eng. Sci.* **24** 1071–8

[373] Hunt A 1994 Finite-size effects on the glass transition temperature *Solid State Commun.* **90** 527–32

[374] Bares J 1975 Glass transition of the polymer microphase *Macromolecules* **8** 244–6

[375] Jackle J 1986 Model of the glass transition *Rep. Prog. Phys.* **49** 171–231

[376] Defay R and Prigogine I 1966 *Surface Tension and Absorption* (New York: Wiley)

[377] McKenna G B, Jackson C L, O'Reilly and Sedita J S 1992 *Polym. Preprints* **33** 118–9

[378] Donati C and Jackle J 1996 The characteristic length of cooperativity derived from dynamic size effects in a lattice gas *J. Phys.: Condens. Matter* **8** 2733–40

[379] Donati C, Douglas J F, Kob W, Plimpton S J, Poole P H and Glotzer S C 1998 Stringlike cooperative motion in a supercooled liquid *Phys. Rev. Lett.* **80** 2338–41

[380] Mansfield K F and Theodorou D N 1991 Molecular-dynamics simulation of a glassy polymer surface *Macromolecules* **24** 6283–94

[381] Mansfield K F and Theodorou D N 1989 Interfacial structure and dynamics of macromolecular liquids—a Monte-Carlo simulation approach *Macromolecules* **22** 3143–52

[382] Matsuda T, Smith G D, Winkler R G and Yoon D Y 1995 Stochastic dynamics simulations of N-alkane melts confined between solid-surfaces—influence of surface-properties and composition with Scheutjens–Fleer theory *Macromolecules* **28** 165–73

[383] Smith G D, Bedrov D and Borodin O 2003 Structural relaxation and dynamic heterogeneity in a polymer melt at attractive surfaces *Phys. Rev. Lett.* **90** 226103

[384] Soles C L, Douglas J F and Wu W-L 2004 Dynamics of thin polymer films: recent insights from incoherent neutron scattering *J. Polym. Sci.* B **42** 3218–34

[385] Starr F W, Schroder T B and Glotzer S C 2001 Effects of a nanoscopic filler on the structure and dynamics of a simulated polymer melt and the relationship to ultrathin films *Phys. Rev.* E **64** 021802

[386] Starr F W, Schroder T B and Glotzer S C 2002 Molecular dynamics simulation of a polymer melt with a nanoscopic particle *Macromolecules* **35** 4481–92

[387] Vacatello M 2002 Chain dimensions in filled polymers: an intriguing problem *Macromolecules* **35** 8191–3

[388] Borrdin O, Smith G D, Bandyopadhyaya R and Byutner O 2003 Molecular dynamics study of the influence of solid interfaces on poly(ethylene oxide) structure and dynamics *Macromolecules* **36** 7873–83

[389] Vacatello M 2003 Phantom chain simulations of polymer–nanofiller systems *Macromolecules* **36** 3411–6

[390] Starr F W, Douglas J F and Glotzer S C 2003 Origin of particle clustering in a simulated polymer nanocomposite and its impact on rheology *J. Chem. Phys.* **119** 1777–88

[391] Brown D, Mele P, Marceau S and Alberola N D 2003 A molecular dynamics study of a model nanoparticle embedded in a polymer matrix *Macromolecules* **36** 1395–406

[392] Picu R C and Ozmusul M S 2003 Structure of linear polymeric chains confined between impenetrable spherical walls *J. Chem. Phys.* **118** 11239–2348

[393] Smith G D, Bedrov D and Borodin O 2003 Structural relaxation and dynamic heterogeneity in a polymer melt at attractive surfaces *Phys. Rev. Lett.* **90** 226103

[394] Wong S, Vaia R A, Giannelis E P and Zax D B 1996 Dynamics in a poly(ethylene oxide)-based nanocomposite polymer electrolyte probed by solid state NMR *Solid State Ion.* **86** 547–57

[395] Ash B J, Siegel R W and Schadler L S 2004 Glass-transition temperature behavior of alumina/PMMA nanocomposites *J. Polym. Sci.* B **42** 4371–83

[396] Ngai K L 1980 Universality of low-frequency fluctuation, dissipation and relaxation properties of condensed matter. II *Commun. Solid State Phys.* **9** 141–55

[397] Tsang K-Y and Ngai K L 1996 Relaxation in interacting arrays of oscillators *Phys. Rev.* E **54** R3067–70

[398] Tsang K-Y and Ngai K L 1997 Dynamics of relaxing systems subjected to nonlinear interactions *Phys. Rev.* E **56** R17–20

[399] Couchman P R and Karasz F E 1977 *J. Polym. Sci.* B **15** 1037

[400] Fredrickson G H 1988 Recent developments in dynamical theories of the liquid–glass transition *Annu. Rev. Phys. Chem.* **39** 149–80

[401] Ray P and Binder K 1994 Finite-size effect in the dynamics near the glass-transition *Europhys. Lett.* **27** 53–8

[402] Mayes A M 1994 Glass transition of amorphous polymer surfaces *Macromolecules* **27** 3114–5

[403] Truskett T M and Ganesan V 2003 Ideal glass transitions in thin films: an energy landscape perspective *J. Chem. Phys.* **119** 1897–900

[404] Mittal J, Shah P and Truskett T M 2004 Using energy landscapes to predict the properties of thin films *J. Phys. Chem.* B **108** 19769–79

[405] Cohen M H and Trunbull D 1958 Molecular transport in liquids and glasses *J. Chem. Phys.* **31** 1164–9

[406] Trunbull D and Cohen M H 1961 Free-volume model of the amorphous phase: glass transition *J. Chem. Phys.* **34** 120–5